FLUORESCENCE BASED SENSING FOR CRYSTALLIZATION AND FOR SOLUTION CHARACTERIZATION

By

Qiuxia Wang

A DISSERTATION

Submitted to
Michigan State University
in partial fulfillment of the requirements
for the degree of

DOCTORS OF PHILOSOPHY

Departments of Chemical Engineering and Chemistry

1998

ABSTRACT

FLUORESCENCE BASED SENSING FOR CRYSTALLIZATION AND FOR SOLUTION CHARACTERIZATION

By

Qiuxia Wang

Production of a specified crystal size distribution (CSD) is one of the primary goals of a crystallization process because CSD affects the cost of operation. Filtration and drying are often the limiting steps in chemical manufacturing processes and significant cost reductions can be realized by creating CSDs that have favorable filtration and drying properties. The CSD is determined by supersaturation of solution. Control of the CSD is realized by control of supersaturation which requires the accurate measurement of the supersaturation. No technique is available for the measurement of supersaturation of low solubility systems with solubility around 2wt%.

In this research, pyranine, 1-pyrene butyric acid and carminic acid were investigated as potential fluorescence probes to measure the supersaturation of low solubility systems, such as tryptophan. nicotinic acid, phenylalanine and benzoic acid, using steady state fluorescence. Pyranine was shown to be a very promising probe to be used as the sensor to measure supersaturation in solutions due to the smooth and nonlinear calibration curves which show a higher signal response at supersaturated region. In addition pyranine will not enter the crystal lattice. Pyranine is not listed as a food additive by FDA, so it can not be added directly into food and pharmaceutical production processes. Carminic acid (CA), a FDA approved food additive, was shown to be a good sensor for

phenylalanine solutions by following the fluorescence intensity change with the concentration of phenylalanine. With pyranine immobilized on a membrane, the PIR (Peak Intensity Ratio) changes with the concentration of solutes linearly. The fluorescence probe technique is a very promising technique to be used to monitor crystallization *in situ.*

The formation of nuclei is the beginning point of the crystallization. The nucleation of the solute must somehow depend upon the solute molecules in a supersaturated solution and also depend upon the various molecular interactions. Understanding the structure of supersaturated solutions can help us better design and control crystallization. Although lots of work has focused on this subject, no generally accepted theories are available, especially for low solubility systems, and there are no reports on supersaturated solution structure at all.

Fluorescence quenching requires the contact of fluorophores and quenchers, so the interaction of fluorophore and quenchers can provide information about the organization of solutes in solutions. Quenching curves show different trends of quenching in unsaturated and supersaturating regions which was taken as the evidence of the formation of aggregates of the solutes in supersaturated solutions. Different molecules show totally different quenching behaviors to pyranine in solution. The different quenching behaviors are the results of the different interactions of pyranine with solute molecules. The contact complex was suggested as the mechanism of the interaction between pyranine and solute molecules. The stronger quenching abilities of tryptophan and nicotinic acid are the results of formation of hydrogen bonding complex with pyranine duo to the amine in the rings. The different steady state quenching and lifetime quenching behavior of phenylalanine support strongly the contact complex assumption. The associates were suggested in tryptophan solutions and phenylalanine due to the downward quenching curves. It was shown only 73% of phenylalanine and tryptophan are accessible to fluorophores to quench the fluorescence. The excitation wavelength dependence of tryptophan maximum emission wavelength supports the exists of the associates in tryptophan solutions.

ACKNOWLEDGEMENTS

First, I would like to thank my mentor Kris A. Berglund for his encouragement, guidance and support. He helped me a lot personally and professionally. A body of work such as this would not be possible without his assistance. It has been a privilege to have had him as my preceptor. What I have learned from him is far beyond the appreciation of chemistry and chemical engineering, and what I learned will continue to influence me in my future.

I would like also to thank my committee members, Drs. Gary Blanchard, Greg Baker and Alec Scranton for their time and assistance.

I would also like to thank my colleagues in the research group for their caring and help. Everyone I have had the opportunity to interact with has meant something to me and helped in many different ways. Special thanks to Sanjay Yedur who I can always turn to whenever I need help in research and in my personal life. Also, special thanks to Dale LeCaptain who opened opportunities for me to experience American culture by inviting me to numerous social activities.

Many thanks are also due to my family for their love and my friends here in the USA and in China for their caring and support. They shared my frustrations and the happiness. All those unforgettable long hour talks on the phone helped me through the tough times and made me a happier person (of course the big phone bill annoyed my landlady sometimes). Out of many, Jingpin Jia, one of my great friends, helped me get settled here at MSU. I knew that whatever happened, I could count on her to be right there with her caring and support, that means a lot to me.

To all these people, thank you from the bottom of my heart.

TABLE OF CONTENTS

LIST OF TABLES

LIST OF FIGURES

Chapter 1

INTRODUCTION

1.1. Control of crystallization by control of supersaturation

Crystallization from solution is one of the most widely used unit operations in the food, pharmaceutical and chemical industries. It ranks second behind distillation in use as a separation process (1). Most bulk pharmaceutical and organic fine chemicals are marketed as crystalline products. That crystallization becomes such an important separation technique in industrial production is not a historical accident, but the consequence of some important factors. First, crystals are usually of extreme purity. Crystallization is cited as one of the best and least expensive method to produce pure solids from impure solutions. The purity of product is always an important aspect in industrial production, especially in food and pharmaceuticals. Second, crystallization improves the product's appearance, an important aspect of consumer acceptance. This is one sale factor. Third, one of the most important factors, the production of uniform crystals results in good flow, handling and packaging characteristics which facilitates subsequent finishing steps, such as filtering or drying (1, 16). When we talk about crystals making the finishing steps easier, we assume we have bigger crystals. If crystals are very tiny the finishing steps are harder. So production of a specified crystal size distribution (CSD) is one of the primary goals of a crystallization process. The CSD affects the cost of operation of down-stream units such as filtration equipment and dryers. These subsequent steps are often the limiting steps in chemical manufacturing processes and significant cost reductions can be realized by creating CSDs that have favorable filtration and drying properties.

Supersaturation, defined as the amount of solute in excess of the equilibrium solubility at a given temperature, has great influence in the resulting CSD (1,2). The effects of supersaturation on CSD reveal the influence of nucleation rate and growth rate. Supersaturation of the solution is the driving force for both crystal nucleation and growth but in different orders (1). In general, when supersaturation is high, nucleation rates will be high, resulting in formation of many nuclei and many tiny crystals. When the supersaturation is not very high, for example just a little bit over the solubility limit, the nucleation rate will not be very high, and the growth rate will become more dominant. Fewer nuclei formed in the solution will grow to become larger crystals, which is often the desired result in industry. Therefore, there is an industrial need to control the supersaturation of solution during crystallization processes which requires the measurement of supersaturation accurately.

Supersaturation is essential for any crystallization, so reaching supersaturation is always the first step of crystallization. Many crystallization processes start with a hot, saturated solution that is cooled and/or evaporated to create supersaturation. Different cooling processes of the solution will have an impact on the CSD because different cooling will give us different supersaturation profiles. Natural cooling will produce a supersaturation peak leading to high rates of nucleation and excessive fine crystals (1,3). Linear cooling results in larger crystals as compared with natural cooling. The largest crystals can be obtained by controlling the cooling rate (1,3), where the crystallizing system responds to a programmed cooling profile. The supersaturation versus corresponding time profiles for different cooling rates are given in Figure 1.1 (3). Programming cooling means we control the cooling curve just a little bit over the solubility curve which will achieve a low supersaturation. Low supersaturation results in low nucleation rates and the growth rate becomes a more dominant rate, thus producing larger crystals. The control of supersaturation is realized by controlling the cooling rate in a cooling crystallization. Evaporation rates and anti-solvent addition rates should be similarly controlled to produce

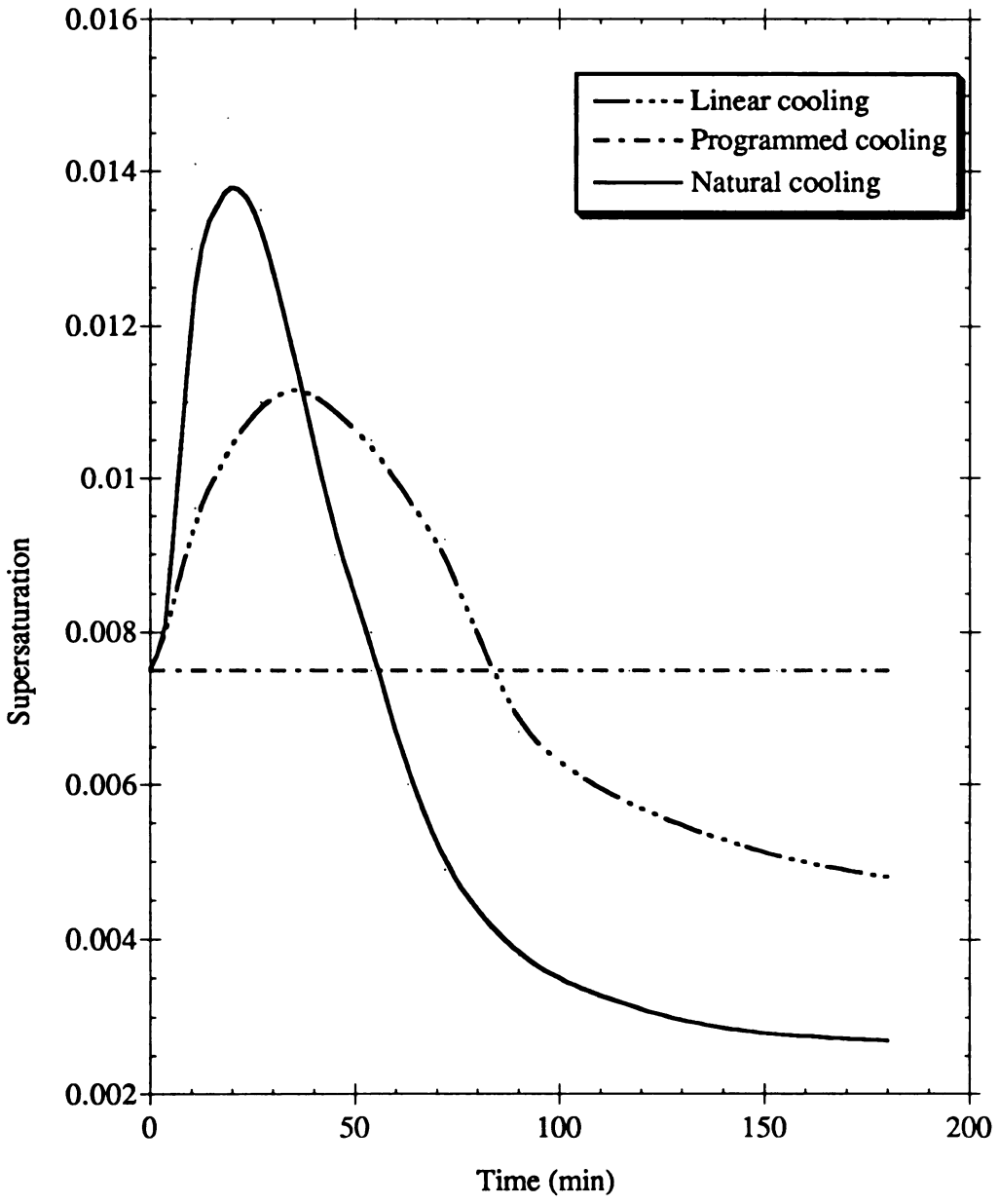

Figure 1.1. The supersaturation versus corresponding time profiles for different cooling rates (3).

the supersaturation profile as prescribed for controlling cooling to achieve larger CSDs in these processes.

The control of supersaturation of solution is critical to industrial crystallization. Any attempt to control an industrial crystallization process requires the *in situ* measurement and control of supersaturation. Therefore, the *in situ* measurement of supersaturation has been cited as one of the most important needs of the industry (1,15). One reason is that many industry crystallization processes are usually done in a batch mode. Control of batch industrial crystallization processes is more difficult than continuous processes due to the complexity and difficulty of the crystallization itself and also the different retention time needs for the required growth of crystals. Another consideration is batch to batch fluctuations, which can cause considerable variation in the crystallization resulting in final product divergence. Such variation is often unacceptable to the Food and Drug Administration (FDA). Reworking a batch that does not meet specifications incurs additional costs and opens the opportunity for additional contamination. All of these reasons show us that there is a need to implement control strategies that provide a quantitative output that can be used either by an operator or implemented in an automatic control scheme. Supersaturation has been shown to be a very sensitive factor in batch crystallization. Minor changes in operation sometimes result in the random fluctuations of supersaturation. What is desired in industry is to find an *in situ* technique which can be used to monitor supersaturation and to control the supersaturation just in the metastable zone by adjusting the rate of cooling and/or the rate of evaporation to maintain optimal conditions during the operation. An *in situ* monitoring system can eliminate the need to draw off sample aliquots, thus reducing the possibility of experimental error due to changes that occur in the solution due to its metastablity. Clearly, there is a need for the development of *in situ* measurements to follow the crystallization processes.

1.2. The fluorescent probe technique for measurement of supersaturation

In order to control supersaturation in the solution, we must first be able to measure the supersaturation accurately. If the concentration of a solution can be measured and the solubility is known, the supersaturation can be calculated. The measurement of supersaturation turns out to be dependent on the measurement of concentration of the solutions. Any techniques which can be used to measure the concentration can be used to measure supersaturation. The measurement of concentration can be realized by measuring properties of the system which are sensitive to solute concentration. Numerous analytical techniques for the measurement of supersaturation of solutes in solutions have been proposed such as conductometry, polarimetry, refractometry, viscometry, density calibrations, etc.(1,4). Solution density and refractive index are probably the two properties most commonly used to measure the supersaturation. In all cases, it always starts with making up a series of solutions of known concentration and measuring the physical properties of solutions to get the calibration curve. The primary difficulty in using these conventional analytical techniques is that the separation of the saturated or the supersaturated solution from the crystals is required prior to analysis. Supersaturated solutions are unstable and changes may occur during the separation and subsequent handling procedures. Special care must be taken to maintain process conditions, and to avoid adsorption of solute on any of the sampling and analytical equipment. This special care poses some difficulties for routine measurements in industrial practice. Therefore, we can not be sure the properties we measured are the properties of the system. For example, refractometry is one of the most common techniques to be used to measure supersaturation, the change of refractive index is very small with changes of concentration of the solution, which usually happens in the fourth or fifth decimal place. The sensitivity and accuracy of the measurements are not reliable. For low solubility systems with the concentration changes around 1%, the physical properties change, such as density and refractive index, will not be large. It will be very difficult or impossible to measure accurately physical

properties changes with the concentration of solutions by using these conventional techniques. To date there are no suitable techniques to measure the supersaturation in low solubility systems. These low solubility systems are very common in industry, so there are needs to find some suitable technique for the measurement of supersaturation of low solubility systems. Fluorescence spectroscopy, due to its high sensitivity, can be a potential technique to be used in study of low solubility systems.

Fluorescence spectroscopy is of extreme sensitivity and high specificity and has played a major role in the field of analysis, particularly in the determination of trace analysis in our environment, industries and bodies (13, 17-19). High sensitivity results from the difference in wavelengths between the exciting and fluorescence emission, which results in a signal contrasted with essentially zero background. A small signal can be measured directly .

It is always easier to measure a small signal than a small difference between two large signals as is done in absorption spectrophotometry. High specificity results from two separated spectra, excitation and emission spectra, and the possibility of measuring the lifetime of the fluorophore. Two compounds that are excited at the same wavelength, but emit at different wavelengths are readily differentiated without the use of chemical separation techniques. The same two compounds may fluoresce at the same wavelength but require different excitation wavelength (17).

Fluorescence spectroscopy is one of the most established techniques. It continues to be one of the most active research fields in science. This is evidenced by the exponentially increasing number of papers, monographs and reviews published each year and by the increasing sales of those companies selling fluorescence instruments. Fluorescence has some other advantages which other techniques can not compete with. In addition to the extreme sensitivity, fluorescence spectroscopy is experimentally simple, easy to control and generally inexpensive for operation. Very useful information can be obtained from this simple technique (13,17-19).

The basis for the use of fluorescence probes is that certain molecules display a selective affinity for a unique site on the molecule and the structure and dynamic properties of the host system are reflected in the fluorescence properties of the probe. Changes in the emission of the extrinsic probe molecule can be correlated to corresponding changes in the local solution environment. In a photochemical investigation, changes in emission of the fluorescing species gives information about the electronic state of fluorescing species (5). Fluorescence probes can be covalently linked or physically bound to specific sites in molecules such as proteins. The magnitude of the observed fluorescence signal provides information about energy transfer processes, the distances between reactive sites.

The fluorescence probe technique can be used in nonfluorescent systems. Although a host system does not fluoresce, a change in the host system will change the fluorescence of a probe. The change of probe fluorescence then reveals this change and gives us information about the host system. The concentration of the probe can be low enough, as low as 10^{-5}M, to preclude any effects other than that arising from the interaction of the probe molecule with its local environment. Additionally, this low concentration can minimize any potential effects on crystallization. Often the sensitivity of a probe to the solvent environment is enhanced in its excited state. Another advantage of using the fluorescence probe technique is the application of remote sensing. Remote sensing is often required in industrial production and the previously discussed convention measuring techniques are not easy to be used in remote sensing. The fluorescence probe technique can be made remote sensing by applying fiber optic technology.

The fluorescence probe technique has been shown to be effective for monitoring the supersaturation of high solubility systems (6, 7). This approach has been used to monitor the degree of supersaturation utilizing a peak intensity ratio (PIR) of pyranine in aqueous solutions of sucrose, glucose, fructose, and lactose (6). It has been demonstrated that pyranine can also be used as a fluorescent probe to measure supersaturation in citric acid

solutions and that the probe responds to the solvent microenvironment as well as changes in the pH of the solution (8).

1.3. The study of structure in supersaturated solutions by fluorescence quenching

It is well known that crystallization takes place with the formation of a stable crystal nucleus from a homogeneous supersaturated solution first, then these nuclei will grow to form crystals (1). The formation of nuclei is the beginning point of the crystallization. The nucleation of solute must somehow depend upon the structure of solute molecules in a supersaturated solution and also depend upon the various molecular interactions, such as solute-solute and solute-solvent interactions (1). Understanding the structure of a supersaturated solution can help us better design and control crystallization.

In aqueous solution, each ion is surrounded by dipole oriented water molecules due to the coulombic forces between ions and water molecules, which are called solvated ions. Water molecules who are closer to the ions are bonded to the ions much firmer than those water molecules which are far away from ions. Those far away molecules are bonded to ions non oriented and loose. The hydrated ions can be very big or small depending on the properties of the ions (1). The structure of the supersaturated solutions probably are more complex than undersaturated solutions.

Many techniques have been used to study the structure of supersaturated solutions, including Raman, FTIR, NMR, and X-ray diffraction (1). Researchers are trying to find the distinguishing features of supersaturated solutions by investigating the dependence of various physical properties on concentration. The discontinuity of any property versus concentration at the equilibrium saturation point has rarely been observed (1). Some theories, such as the cluster theory, have been provided about the structure of supersaturated solution (1,9) Solute cluster theory was reported by several researchers through observing the concentration gradients or different diffusion rate at high

concentration in high solubility systems (20-22). Previous work was focused on high solubility systems and theory was based on the study of high solubility systems whose solubility can be as high as 50wt%. No information about the organization of low solubility systems at supersaturated region has been given. A concentration gradient, which is the evidence for the formation of solute clusters, will not be noticeable in low solubility systems. Therefore, there is a need for suitable techniques to study low solubility systems.

Steady-state fluorescence spectroscopy represents a powerful optical spectroscopic technique for monitoring the dynamics of macromolecular interactions in solution (10-12). Steady state fluorescence spectroscopy using extrinsic trace fluorescent probe molecules is solvent sensitive. Specific information about the immediate molecular environment of the probe molecule, either free in solution or coupled to a macromolecule, can be obtained from changes in the peak intensities and wavelengths.

The fluorescence quenching technique is a very powerful tool for studying the dynamics of micellar system (13,18, 23). Quenching follows two mechanisms where one is viscosity-independent static quenching and the other is viscosity-dependent dynamic quenching. Dynamic quenching is a diffusion controlled process. Both of the quenching processes require the contact of the fluorophore and quenchers. Quenching is always interpreted as the contact complex formation between fluorophore and quenchers to some degree. Contact complexes are the results of Van der Waals molecular forces between probe molecule and quencher which are not very strong. Sometimes a stronger bonding such as hydrogen bonding may form between probe and quencher which will show stronger interaction and quenching ability. Static quenching is due to the ground state contact complex between fluorophore and quencher, which absorbs the incident excitation light and yield excited complex which is called as exciplex. In many cases ground state fluorophore and quencher can not form a strong contact complex, but when fluorophore is excited the change of dipole moment will make the formation of complex much easier.

Dynamic quenching involves the diffusion-controlled encounters of fluorophores and quenchers. The possible physical process of quenching can be shown by the schematic diagram in Figure 1.2 (13). M represents the fluorophore and Q represents quencher. (MQ)* represents the exciplex between M and Q. The triplet is described by 3. The quenching of M* can occur by processes ii(exciplex fluorescence), iii(exciplex internal conversion to ground state), v(energy transfer from $^1M^*$ to $^1Q^*$), vi(exciplex dissociation in ions or direct electron transfer) and vii(exciplex intersystem crossing to the triplet exciplex state). Process iv does not quench the fluorescence of M*. The fluorescence of the exciplex is not very common in the quenching process and the same exciplex internal conversion (process iii) to the ground state is not very common either due to the big large energy gap. With heavy atom quenchers, such as xenon, bromobenzene and various bromide and iodide heavy atom quenchers, the exciplex intersystem crossing to the triplet exciplex state is a very important mechanism of quenching. Direct electron transfer between $^1M^*$ and $^1Q^*$ is another common quenching mechanism which can be proved by transient absorption spectra (13). Quenching mechanisms can be fitted to different models. By interpreting quenching data we can deduce the behavior of quenchers in the solution, thus the information about solution. The investigation of the microscopic interactions between the solvent and solute by fluorescence quenching will result in a more directed and rational approach for understanding and control of crystallization.

1.4 Introduction of the systems for study

A significant amount of research has been done in our group by using the fluorescence probe method (6,8). It has been used to monitor the degree of supersaturation with a ratio of peak intensity of pyranine in aqueous solutions of sucrose, glucose, fructose, and lactose (6). It has been demonstrated that pyranine can be used as a fluorescent probe to measure supersaturation in citric acid solutions and that the probe responds to the solvent microenvironment as well as changes in the pH of the solution (8).

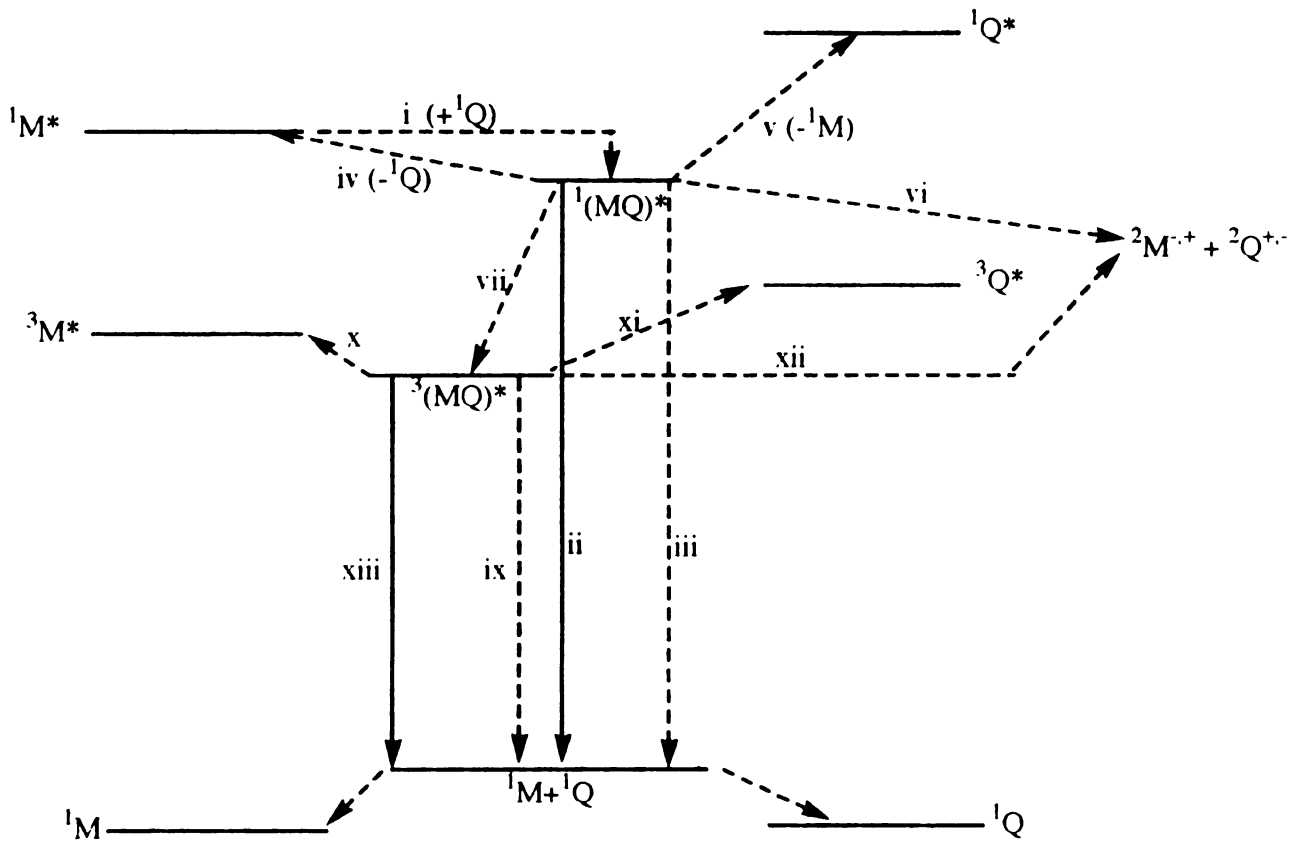

Figure 1.2. Schematic diagram of rate of processes in exciplex formation, dissociation and quenching. Solid lines, radiative processed; broken lines, radiationless processes. (i) formation of exciplex between fluorophore M and quencher Q (ii) fluorescence of exciplex (iii) internal conversion of exciplex (iv) dissociation of exciplex (v) energy transfer (vi) electron transfer (vii) intersystem crossing of exciplex

Previous studies have been done with very highly concentrated solutions, e.g. 50 wt %. For these studies the PIR is a measure of the ratio of water associated with the solute to that not associated with the solute (6,8). Pyranine responds to the available water in its immediate environment, but for dilute solution the behavior of solute should be different. In the current project tryptophan, nicotinic acid and phenylalanine will be studied. The solubility of tryptophan, nicotinic acid and phenylalanine are 1.136g, 1.67 g and 2.965g in 100ml water at 25°, respectively (Merck Index). Such low concentrations will probably not greatly affect the solvent behavior in the solution. The physical properties which are used to measure the supersaturation of high solubility systems will not change as much as in high solubility systems. This poses difficulty in measurement of supersaturation of low solubility systems by conventional methods. Another question is whether the structure of such dilute solution are the same as the highly concentrated solutions. Will the fluorescence probe method work for such dilute solution? This research is to understand the crystallization of low solubility systems by studying the supersaturation solution structure using the fluorescence quenching technique, and measuring supersaturation of solution in low solubility systems by fluorescence probe technique.

The reason that we choose L-tryptophan as our research system is that L-tryptophan is one of the essential amino acids which is not synthesized in the body. L- tryptophan is a major article of commerce. Additionally, the combination of aromatic and ionic groups makes L-tryptophan a good model system for complicated molecules. Tryptophan is an antidepressant drug used to improve the quality of people's sleep. It is a precursor for serotonin, an important neurotransmitter which can be produced during the deep sleep state (restorative phase of sleep during which the sleeping brain can restore the neurotransmitters and also muscles truly relax) (14). Serotonin may also reduce certain reactions and have a tranquilizing effect. L-tryptophan appears to be useful in the treatment of some depressive and anxiety disorders. It has been said that tryptophan reduces cravings for fatty foods, alcohol, among others.

Nicotinic acid is needed for proper circulation; healthy skin; functioning of the nerve and digestive system; Nicotinic acid helps to eliminate canker sores, reduces cholesterol and triglycerides, and improves the unpleasant symptoms of vertigo in Meniere's syndrome and is effective in the treatment of mental disorders (Information from internet).

Most bulk pharmaceutical and organic fine chemical are marketed as crystalline products, including tryptophan and nicotinic acid. But the crystallization of tryptophan is very hard to handle in industry because only fluffy crystals result. As we already know, this will add some problems to the filtration and/or drying processes and so will increase the cost of operation.

There is no suitable technique for measurement of the supersaturation of low solubility systems such as tryptophan and nicotinic acid solutions, which are very common in industrial crystallization. Clearly, there is a need for the development of a measurement technique to follow the crystallization process of low solubility systems and a suitable method to study the structure of supersaturation of solution of low solubility systems. It is the objective of this research project to develop sensors capable of measuring the supersaturation of tryptophan and nicotinic acid solutions then extend to general low solubility systems and study the structure of supersaturated solutions by using the fluorescence probe method.

1.5. Overview of this work

In chapter 2, pyranine in solution is used as a probe for measurement of supersaturation in tryptophan solution and nicotinic acid solutions. Results show that the PIR (Peak Intensity Ratio) of pyranine versus the concentration of tryptophan and nicotinic acid are smooth and nonlinear with a greater slope in the higher concentration region. PIR curves can be used as the calibration curve for measurement of the supersaturation of tryptophan and nicotinic acid solutions. The fluorescence of tryptophan crystallized in the

presence of pyranine from solution exhibited no pyranine, which indicates pyranine does not go into the crystal lattice. We can conclude that pyranine is a good probe and the fluorescence probe method is a promising technique for measurement of the supersaturation of low solubility systems.

In Chapter 3, pyranine is immobilized on a membrane as the probe to measure the supersaturation. Pyranine is not listed as a food additive by FDA and can not be added directly into food or pharmaceutical processes. Therefore it is necessary to immobilize pyranine onto a surface for use as a sensor. Pyranine is immobilized onto a membrane for this purpose. Results show that PIR versus concentration of solute is linear and can serve as the calibration curve for measurement of supersaturation. The fluorescence of the solution without probe membrane exhibit no pyranine emission, which confirms the stability of the sensor.

Chapter 4 is an investigation of other potential probes for supersaturation measurement. 1-Pyrenebutyric acid (PBA) and carbonic acid (CA) are studied. Carminic acid is an approved food additive by the FDA. If carminic acid can serve as a probe in this fluorescence probe technique, we can add carminic acid to of food and pharmaceutical processes. The fluorescence intensity of CA versus concentration of tryptophan and phenylalanine are smooth curves which can be used as calibration curves to measure supersaturation. Especially in phenylalanine solutions, intensity increases with the increase of phenylalanine concentration. Although the PIR of PBA versus the concentration of tryptophan and phenylalanine are smooth, PBA will enter the crystal lattice. So PBA can be used as the calibration curves to measure supersaturation. Tryptophan shows quenching to both CA and PBA, but not phenylalanine. Different quenching behaviors of tryptophan and phenylalanine to PBA and CA can give us information about different interactions of probe molecules with tryptophan and phenylalanine in solution.

The PIR versus solute concentration is the result of fluorescence quenching of pyranine by solutes. Different wavelengths have different quenching constants. The level

of supersaturation is an essential requirement for all crystallization operations. The formation of nuclei from supersaturation solutions is the beginning point of the crystallization. The nucleation of solute must somehow depend upon the solute molecules in a supersaturated solution and also depend upon the various molecular interactions, such as solute-solute and solute-solvent interactions. The interpretation of quenching behaviors can reveal information about the accessibility of solutes to probes then information about the organization of solutes in solution can be deduced from the interactions of solutes and probes. The fluorescence quenching studies of pyranine by tryptophan, nicotinic acid and phenylalanine are presented in detail in Chapter 5.

Chapter 6 deals with the fluorescence quenching study of pyranine by lifetime measurement. The emission lifetime of a probe molecule is highly sensitive to its environment. The measurement of lifetime can determine static and dynamic conformational information about macromolecules, make state assignments, and provide information on the diffusive processes such as collision quenching and proton transport. By using the lifetime Stern-Volmer quenching fitting, dynamic quenching and static quenching are very easily distinguished. Different quenching behaviors of tryptophan, nicotinic acid and phenylalanine to pyranine result from the organization in the various solutions.

Fluorescence of tryptophan shows excitation wavelength dependence at all excitation wavelengths which is uncommon. Fluorescence occurs from the lowest vibration state and the energy difference between the excited state and ground state will not change with the excitation. In general, the emission is not excitation dependent. Only when a fluorophore is in a polar and viscous environment where its mobility is restricted, the wavelength of maximum fluorescence will depend on the excitation wavelength. The maximum fluorescence emission will show red-shift when excited with extreme red edge wavelength. This phenomenon is well known as red edge excitation shift (REES). The fluorescence of tryptophan is studied in detail in chapter 7.

Excitation spectra of pyranine in water and in aqueous solutions of tryptophan, phenylalanine and nicotinic acid are presented in chapter 8. The excitation spectrum of pyranine shows fine vibronic structure around 460nm which is the result of the high dipole moment of solvated deprotonated form of pyranine which is represented by PyO^-. The introduction of even trace amount of solutes into solution change the excitation spectra dramatically. The introduction of solutes shifts the equilibrium between the protonated form of pyranine (PyOH) and the deprotonated form of pyranine (PyO^-) to the protonated form especially with nicotinic acid. The contact complex between pyranine and solute molecules is another reason for the change of the excitation spectra which matches the results we obtained from quenching data.

Chapter 9 gives a summary of the work and an overview of future work. The fluorescence quenching technique deserves more attention for solution study. Some molecules which have similar molecular structures as tryptophan, phenylalanine are suggested as target molecules to conduct the systematic study in order to understand the interactions better. New methods which can yield information about interactions may be developed to investigate solution structure. Time resolved fluorescence can be applied as a useful investigation tool. Fluorescence has been shown to be a very useful tool to measure supersaturation. How we apply this technique to the real measurement of the supersaturation in industrial crystallization is a consequence of industrial need. Flow injection analysis (FIA) is discussed as an possible application in industrial crystallization.

1.6. Reference

1. J. W. Mullin, *Crystallization*, Butterworth-Heinemann, Oxford, England (1993)

2. A. D. Randolph, and M. A. Larson, *Theory of Particulate processes*, Academic Press, New York, USA (1988)

3. A. G. Jones, and J. W. Mullin, *Chem. Eng. Sci.*, **29**,105 (1974)

4. H. K. Zimmerman, *Chemical Review*, **51**,25 (1952)

5. V. Ramamurthy, *Photochemistry in Organized & Constrained Media*, VCH (1991)

6. R. Chakraborty, and K. A. Berglund, *J. Crystal. Growth*, **125**, 81-96 (1992)

7. R. Chakraborty, and K. A. Berglund, *AICHE Symposium Series*, **284-7**, 114-123 (1991)

8. S. K. Yedur, and K. A. Berglund, *Applied Spectroscopy*, **50**(7), 866-870 (1996)

9. J. W. Mullin, and C. Leci, *AICHE Symp. Ser.*, **68**, 8 (1972)

10. H. Kondo, I. Miwa, and J. Dunamoto, *J. Phys. Chem.*, **86**, 4826-31 (1982)

11. E. Bardez, B. Goguillon, E. Keh, and B. Valeur, *J. Phys. Chem.*, **88**, 1909-13 (1984)

12. G. D. Correll, R. N. Cheeser III, F. Mome, and J. H. Fendler, *J. Am. Chem. Soc.*, **100:4**, 1254-1262 (1978)

13. J. B. Birks, *Photophysics of Aromatic Molecules*, New York, Wiley-Interscience (1970)

14. A. S. Gissen, *Vitamin Research Products Newsletter*, May/June (1993)

15 G. A. Hussman, M. A. Larson, and K. A. Berglund, *Industrial Crystallization '84* S. J. Jancic, and E. J. DeJong, Eds. Elsevier, Amstrdam (1984)

16. P. A. Belter, E. L. Cussler and Wei-shou Hu, *Bioseperations Downstream Processing for Biotechnology*, Johnm Wiley & Sons, , New York (1988)

17. G. G. Guilbault, *Practical Fluorescence*, M. Dekker, New York (1990)

18. J. R. Lakowicz, *Principles of Fluorescence Spectroscopy*, Plenum Press, New York and London (1983)

19. J. R. Lakowicz, *Topics in Fluorescence Spectroscopy*, Plenum Press, New York and London (1992)

20. J. W. Mullin, and C. L. Leci, *Phil. Mag.*, **19** (1969)

21. E. L. Cussler, *AIChE J.* **26**(1), 43 (1980)

22. L. S. Sorrel, and A. S. Myerson, *AIChE J.*, **28**(5), 772 (1982)

23. M. R. Eftink and C. A. Ghiron, *Biochemistry*, **15**(3), 672 (1976)

Chapter 2

SUPERSATURATION MEASUREMENTS OF LOW SOLUBILITY SYSTEMS USING A STEADY STATE FLUORESCENCE PROBE TECHNIQUE

2.1. Introduction

Supersaturation, which is defined as the amount of solute in excess of the equilibrium solubility, is the driving force for both crystal nucleation and growth. Different nucleation rates and growth rates will result in different crystal size distributions (CSDs), one of the most important parameters in industrial crystallization. Uniform CSD can make the finishing steps, such as filtration and drying faster and easier (1). Filtration and drying are usually limiting steps in chemical manufacturing processes and the determining factor for operation costs. Reduction of cost can be realized by a desired CSD. Since supersaturation is a determining factor of the final CSD of crystallization systems, the control of supersaturation is critical to industrial crystallization. Any attempt to control an industrial crystallization process requires the real time measurement and control of supersaturation. Therefore, the *in situ* measurement of supersaturation has been cited as one of the most important needs of the industry (1).

Numerous analytical techniques for the measurement of supersaturation of solutes in liquids have been proposed, including refractometry, interfertometry, viscometry and density calibrations (2). These techniques require the separation of the saturated or the supersaturated solution from the crystals prior to analysis. This separation from solution is difficult and the solution properties may change. All these techniques involve the

measurement of the physical properties which change with concentration. For low solubility systems, such as tryptophan and nicotinic acid, the concentration change is just around 1%, so the physical properties do not change very much with the concentration. This low concentration change will make conventional measurements inaccurate. Low solubility systems are common in industrial production; therefore, techniques for measurement of supersaturation in low solubility systems is needed.

Many studies have attempted to develop new techniques for *in situ* control of crystallization by measurement of supersaturation. A method using the steady state fluorescence of extrinsic trace fluorescent probe molecules as sensors for monitoring the supersaturation of high solubility solutions was developed by Chakraborty and Berglund (3). This approach has been used to monitor the degree of supersaturation utilizing a peak intensity ratio (PIR) of pyranine in aqueous solutions of sucrose, glucose, fructose, and lactose (3). It has also been demonstrated that pyranine can be used as a fluorescent probe to measure supersaturation in citric acid solutions and that the probe responds to the solvent microenvironment as well as changes in the pH of the solution [4]. These studies were done with very highly concentrated solutions, often higher than 50 wt %. In such cases the PIR is a measure of the ratio of water associated with the solute to that not associated with the solute. Pyranine responds to the available water in its immediate environment. This behavior, in turn, is related to the amount of citric acid and sugar present in solution. Thus, the change in emission properties of pyranine can be related to the concentration of aqueous solution of citric acid. In other words the peak intensity ratio (PIR) can be used as an indicator of the degree of supersaturation. However, a technique that is suitable for *in situ* measurements for low concentration solutions, such as a few weight percent, has not been developed.

The current study utilizes pyranine as fluorescent probe by measuring the peak intensity ratio (PIR) versus solute concentration for solutions of tryptophan, nicotinic acid and benzoic acid with the aim of supersaturation measurement.

2.2. Materials and methods

Pyranine (8-hydroxy-1,3,6-pyrenetrisulfonate), also known as FDA D&C Green No. 8,was obtained from Lancaster, Windham, NH and used as received. Aqueous solutions of pyranine were prepared by dissolution of 0.026 g pyranine in 5ml HPLC grade water. Different concentrations of solutions were prepared by dissolving the appropriate amount of solute in 5ml HPLC water. Supersaturated solutions were prepared by heating the solution in the water bath until all the solute was dissolved and subsequent cooling to room temperature. The solutions were used as prepared without any degassing.

Probe molecules were introduced by addition of five microliters of the pyranine solution (10^{-2}M) to the aqueous tryptophan and benzoic acid solutions resulting in a probe concentration of 10^{-5}M, and 20 microliters of pyranine (10^{-2}M) for nicotinic acid resulting in a probe concentration of $4x10^{-5}$M. Fluorescence spectra of the pyranine in the aqueous solutions were collected within several hours of the preparation the solutions. All spectra were taken at room temperature with a Spex 1681 Fluorolog spectrometer equipped with a Xenon lamp source and a PMT detector. A quartz sample holder was used in all cases. Spectra was recorded at 1.00mm increment and an integration time of 1.0 sec. An excitation wavelength of 342nm for pyranine was used. The emission spectra were recorded over a range from 350-600nm for pyranine. Monochromator slits were 0.5 mm for spectra.

All experiments are conducted more than twice with a newly prepared solution series.

2.3. Results and discussions

2.3.1. Steady state fluorescence

Pyranine (8-hydroxy-1,3,6-pyrenetrisulfonate), whose chemical structure is shown in Figure 2.1, was used as a probe for all studies. Pyranine is water soluble and is known

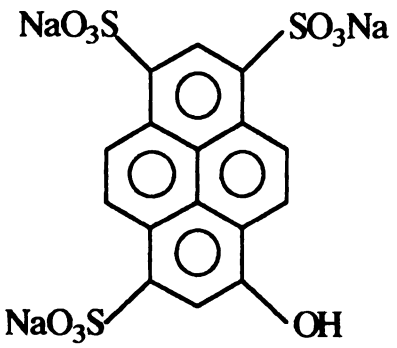

Figure 2.1 Molecular structure of 8-hydroxy-1,3,6-pyrenetrisulfonate (pyranine)

to have a highly sensitive, polarity dependent equilibrium between two excited states that fluoresce (5,6).

The photochemistry of pyranine has been well characterized (5) (Figure 2.2). In aqueous solution, pyranine exists with the sulfonate groups entirely dissociated. It has two excited fluorescent states: one in which the hydroxyl proton is associated with the molecule and one in which it is dissociated. Therefore, pyranine can be used to investigate the proton-accepting character of the solution microenvironment. In aqueous solution when pH is low, the absorption spectrum of pyranine is characteristic of the acidic form PyOH alone (max. 405nm) and the emission band at 440nm is the fluorescence of PyOH*. At high pH values, the absorption band at 445nm appears, revealing the presence of the basic form PyO^- in the ground state. The band at 510nm is the fluorescence of PyO^-*. When pH is between this high and low value, depending on the rate of proton transfer, emission can be observed from the protonated species, the ionized species, or both (Figure 2.2) (6).

Fluorescence spectra of pyranine in aqueous solution of tryptophan are shown in Figure 2.3. The emission spectrum of pyranine exhibits two bands: one is at 510nm which is assigned to deprotonated pyranine fluorescence and the other is a set of peaks 380nm to 440nm, which consists of three fine vibronic structure peaks. The spectra of pyranine in tryptophan solutions are different from the previous results in citric acid solutions in which the 445nm emission peak is missing in tryptophan solutions. In the previous work the concentration of citric acid was very high which is around 50wt%. The pH of the solution was low in such high concentrations so pyranine was in the form of PyOH* and the emission of 445nm is observed. In our systems the solubility of tryptophan is 1.136g/100ml H_2O and the solubility of nicotinic acid is 1.67g/100ml H_2O, and benzoic acid 0.34g/100ml H_2O at 25^{0}C. The pH of the solutions was pretty high (around 6). At this high pH pyranine exists in the form of PyOH mainly in the ground state and when it is excited it becomes PyOH*. We can not see the emission of PyOH in tryptophan solution, because of the fast excited-state proton transfer reaction (7). The high value of pK_a* (0.5)

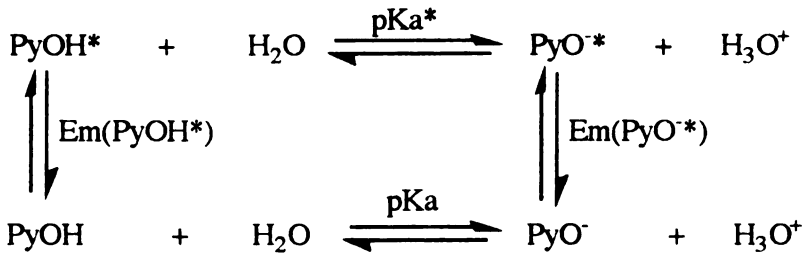

Figure 2.2 Scheme for acid-base equilibria in the ground state and excited state of pyranine. Deprotonated form of pyranine (PyO^-) will be excited at 440nm and emit at 510nm. Protonated form of pyranine (PyOH) will be excited at 405nm and emit at 450nm. pKa=7.5 and pKa*=0.5.

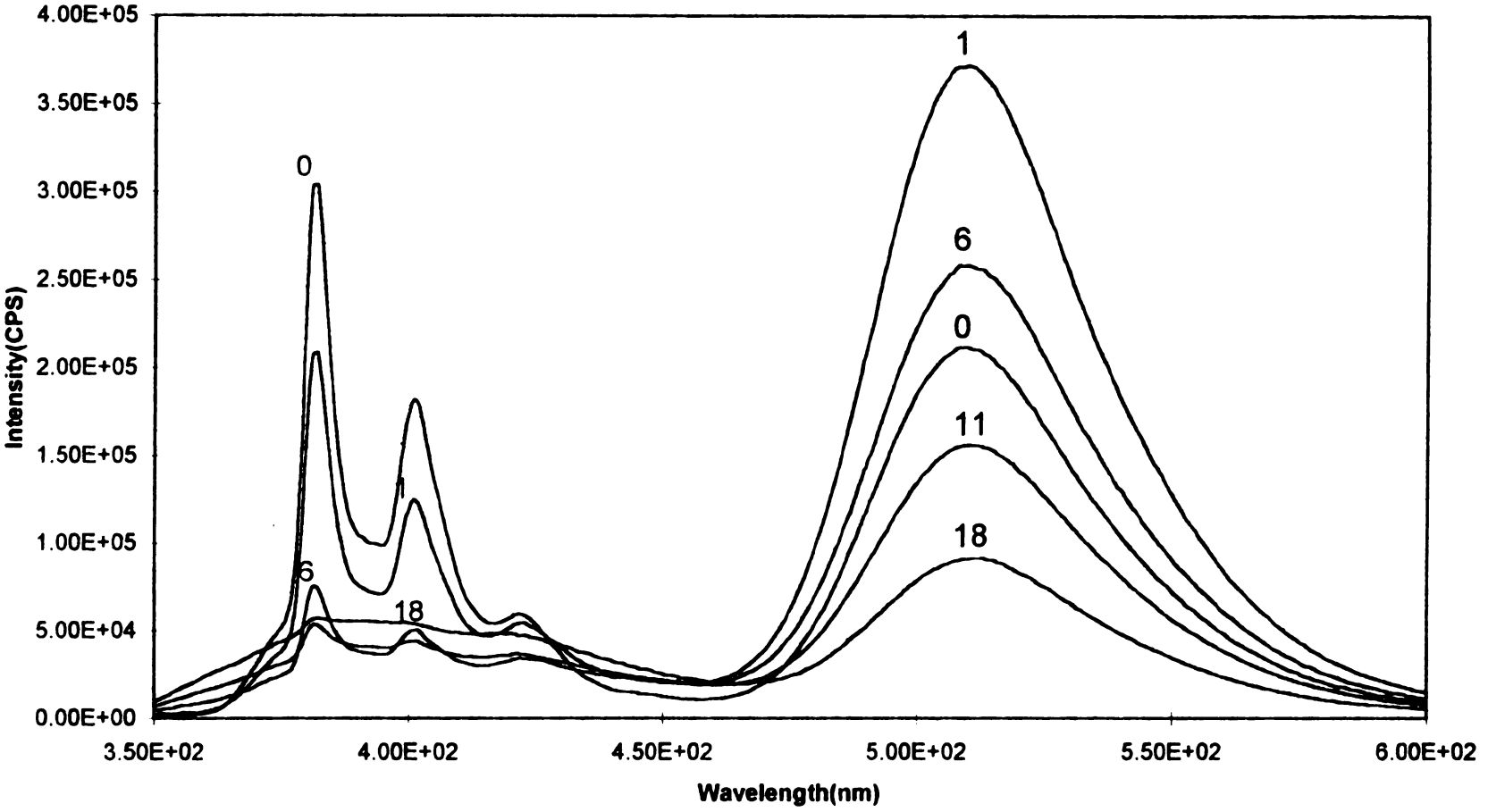

Figure 2.3 Fluorescence of pyranine in water (0) and in aqueous tryptophan solutions:
1 (0.0793g), 6 (0.51g), 11 (1.02g) and 18 (1.73g) tryptophan in 100ml H_2O at room temperature

in the excited state often differs greatly from the ground state value (pK_a=7.5), leading to deprontonation of the excited species. Although at ground state pyranine is in the form of PyOH, when it is excited the equilibrium between PyOH* and PyO^-* will favor PyO^-* due to the low concentration of H_3O^+ in the solution and the proton transfer from PyOH* to base is within the lifetime of fluorescence, so the fluorescence occurs from PyO^-* which results in that the 510nm peak. The absence of the 445nm peak in our spectra suggest that fast proton transfer occurred before the fluorescence of pyranine. Peak 445nm will show up in highly concentrated sugar solutions. From the equilibrium consideration, PyO^-* will be dominant form. But because of the high viscosity of sugar solutions, the proton transfer can not be done within the lifetime of fluorescence. So 445nm emission was observed. This supports the conclusion of fast proton transfer reaction in low solubility systems.

The 382nm, 401nm and 430nm emissions peaks can be attributed to typical emission spectra of the polycyclic aromatic heterocycle (PAH). The typical emission spectrum of the PAH monomer will consist of five major vibronic bands which are generally labeled as I-V in progressive order, such as the 0-0 band is labeled I, etc.(8,9). The possibility of a pyrene impurity was considered and discounted because pyrene is very hydrophobic and its solubility in water is very low (~5-8 x 10^{-7} M). Pure pyrene was purchased from Aldrich Chemical Co. (99+%). The emission spectrum of a saturated pyrene aqueous solution possessed two peaks at 371nm and at 390nm, but the intensity measured was much lower than corresponding intensities for pyranine emission. Therefore, we can conclude that the peaks around 400nm in pyranine are not the consequence of a pyrene impurity.

The fluorescence spectra show no differences in shape and maxima in the presence and absence of tryptophan at low tryptophan concentration. No new fluorescence peak is observed at longer wavelengths which indicates that no strong ground state complex formed. The intensity of the 510nm peak of pyranine increased upon addition of tryptophan in the solution as compared to the intensity of pyranine in pure water. If we compare the

intensity of pyranine emission at 510nm in different tryptophan concentrations, we see the peak intensity decreases with the increase of the tryptophan concentration.

The peak intensity of pyranine at 380-430nm decreases with the addition of tryptophan and keeps decreasing with the increased tryptophan concentration before a definite concentration. When the tryptophan concentration is very high, the peak intensity of pyranine at 380-430nm increases with the increase of tryptophan concentration, and high concentration of solute leads to the loss of fine vibronic structures of the emission spectra.

The shape and maximum of the fluorescence spectra of pyranine in nicotinic acid solution and in benzoic acid solution are the same as the fluorescence spectra of pyranine in tryptophan solutions. The effects of solute concentration on the peak intensity are different. The peak intensity of pyranine fluorescence at both 510nm and 380nm-430nm decreases with the addition of the benzoic acid in benzoic acid aqueous solution. The only difference between the fluorescence spectra of pyranine in benzoic acid solution and in nicotinic acid is that the intensity of fluorescence of pyranine decreases dramatically with the addition of nicotinic acid. The intensity keeps decreasing rapidly with the increase of the concentration of nicotinic acid. Here we should notice that the concentration of pyranine in nicotinic acid solution is four times higher than the concentration of pyranine in benzoic acid and in tryptophan solutions.

The decrease of the intensity with the increase of the solute concentration is due to the solute quenching of pyranine fluorescence. Tryptophan, benzoic acid and nicotinic acid have different quenching abilities to pyranine. Nicotinic acid can effectively quench pyranine fluorescence. Tryptophan and benzoic acid show more moderate quenching of pyranine fluorescence. The different pyranine fluorescence quenching behaviors of tryptophan, nicotinic acid and benzoic acid will be discussed in chapter 5.

2.3.2. Measurement of concentration

The peak intensity ratio (PIR), defined as the ratio of the peak intensity at 401nm, 382nm or 430nm to the intensity at 510nm is used to measure the concentration of solution. The use of a ratio as compared to simple intensity can provides an internal standard for the spectrophotometer. Graphs of the PIR versus concentration of tryptophan, nicotinic acid and benzoic acid are shown in Figures 2.4, 2.5 and 2.6, respectively. In order to determine the supersaturation of the solution it is necessary to develop a calibration curve to monitor signal versus concentration of solute. Changes in emission properties of pyranine can be related to the concentration of aqueous solutions. The smooth nature of the PIR curve indicates that it can be used to determine the concentration, hence the supersaturation, so it can serve as calibration curve to follow the concentration changes during the crystallization process. The measurement of supersaturation of solutions is realized by measuring PIR of the probe sensor fluorescence. The concentration of solutions can be read from the calibration curve. The supersaturation can then be calculated by the difference of concentration and the solubility. The presence of an upward curvature indicates that the response is nonlinear. It shows larger gain at high concentration region which is really desired in industrial practice because bigger signal response means higher sensitivity of the technique. It has been shown elsewhere (3,10) that the supersaturation measurement using the PIR is more sensitive than other techniques. We can tell the high sensitivity of fluorescence probe technique from our results since the concentration change in our research is from 0.5%-1.8% in tryptophan solutions, but the signal PIR changes from 0.29 to 0.72. So a remarkable signal can be realized by using fluorescence probe sensor technique.

A potential problem for using external probe is that the probe molecule may go into the crystal lattice. The cocrystallization of the probe in the crystal is not acceptable in industrial production because it will affect the purity of products. To test whether the probe

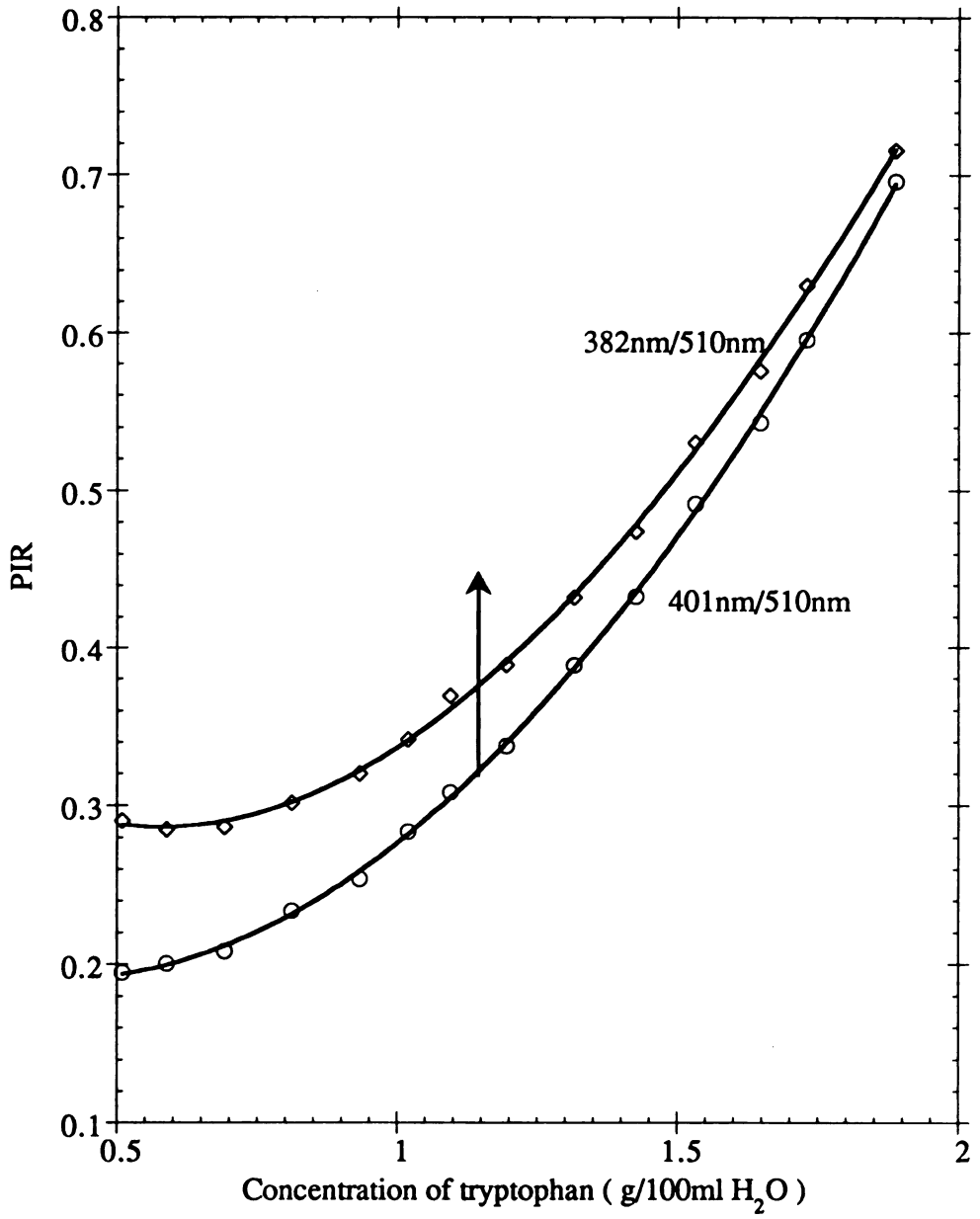

Figure 2.4 PIR (peak intensity ratio) of pyranine(10^{-5}M) versus concentration of aqueous tryptophan solutions at room temperature. Lines are polynomial fitting, and arrow indicates the solubility of tryptophan.

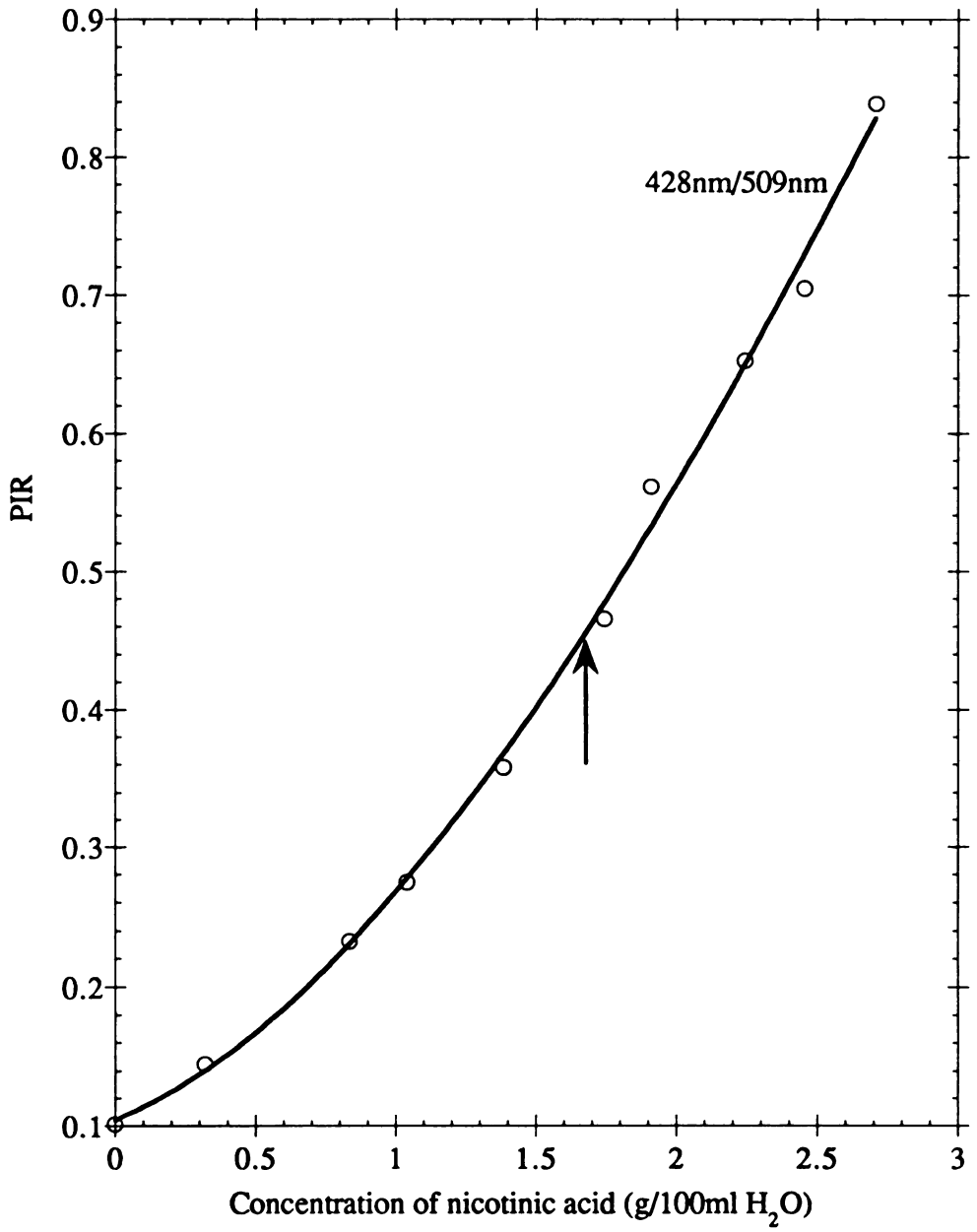

Figure 2.5 PIR (peak intensity ratio) of pyranine ($4x10^{-5}$M) versus concentration of aqueous nicotinic acid solutions at room temperature. The arrow indicates the solubility of nicotinic acid at 25^0C.

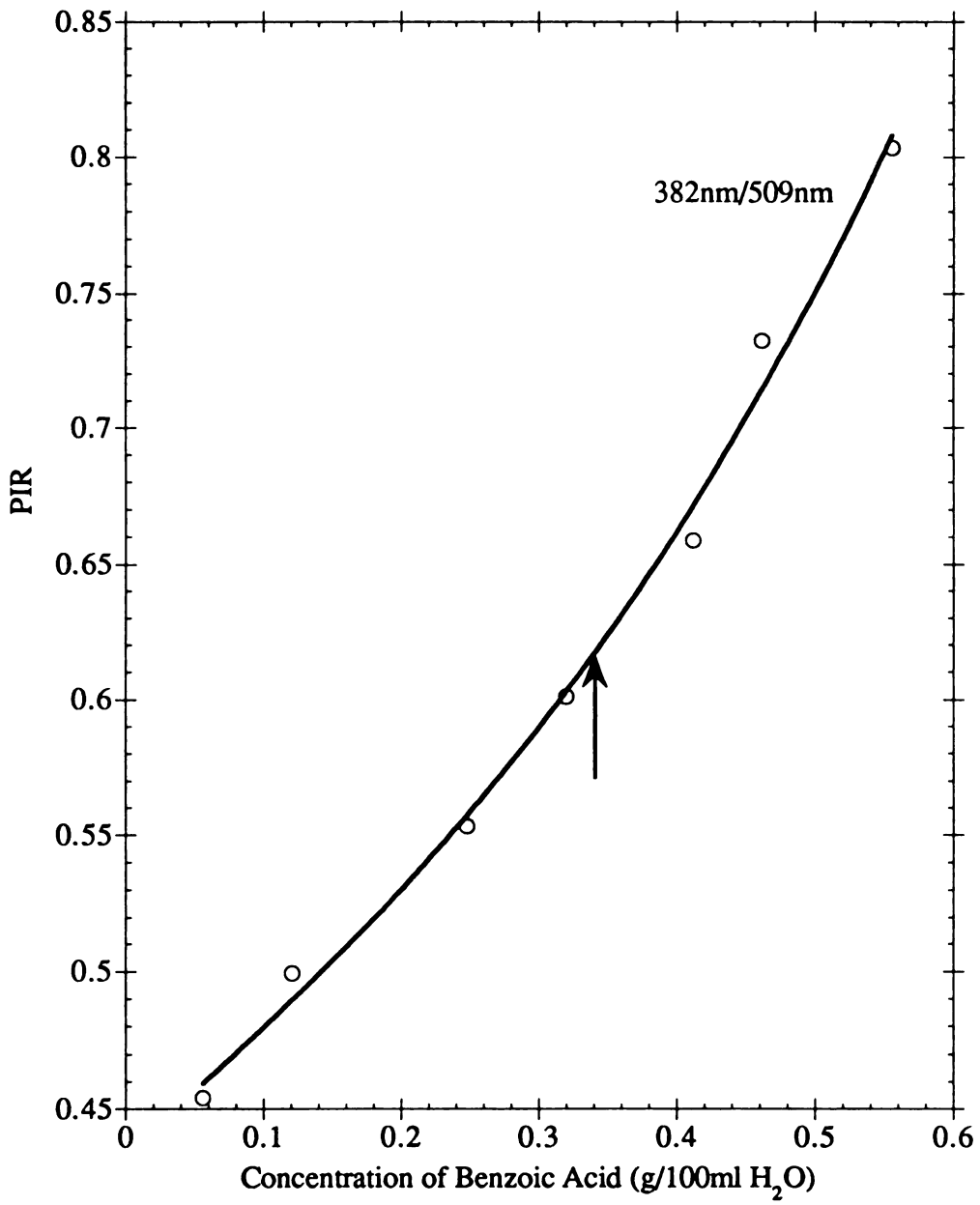

Figure 2.6 PIR (peak intensity ratio) of pyranine(10^{-5}M) versus concentration of aqueous benzoic acid solutions at room temperature. The arrow indicates the solubility of benzoic acid.

molecules will go into the crystal lattices. Recrystallized tryptophan with the presence of pyranine is dissolved into pure water and the fluorescence is measured by using 342nm excitation wavelength and scanning the emission spectrum from 350nm to 600nm. For comparison, a pure aqueous tryptophan emission spectrum is recorded by using 342nm excitation wavelength. The fluorescence spectra of both solutions are shown in Figure 2.7. Only one peak will show up for both case which is fluorescence of tryptophan. There are no peaks from the fluorescence of pyranine. Mass spectra also show no traces of pyranine in the recrystallized tryptophan. Therefore, we can conclude that pyranine does not go into the crystal lattice.

2.4. Conclusions

The emission properties of a fluorescence probe molecule like pyranine in trace amounts can be used to obtain an estimation of the supersaturation of low concentration solutions. The PIR is strongly correlated to the solute concentration and the relation between the PIR and concentration is highly non-linear and has an increasing signal in the supersaturated region of concentration. This technique is highly sensitive and experimentally simple which makes it promising for industrial use.

2.5. References

1. J. W. Mullin, *Crystallization* , Butterworth-Heinemann, Oxford, England (1993)
2. H. K. Zimmerman, *Chemical Review*, **51**, 25 (1952)
3. R. Chakraborty, and K. A. Berglund, *J. Crystal Growth*, **125**, 81-96 (1992)
4. S. K. Yedur, and K. A. Berglund, *Applied Spectroscopy*, **50**(7), 866-870 (1996)
5. H. Kondo, I. Miwa, and J. Dunamoto, *J. Phys. Chem.*, **86**, 4826-31 (1982)
6. V. Ramamurthy, *Photochemistry in Organized & Constrained Media,* VCH Verlagsgesellschaft mbH and VCH publishers (UK) Ltd. (1991)

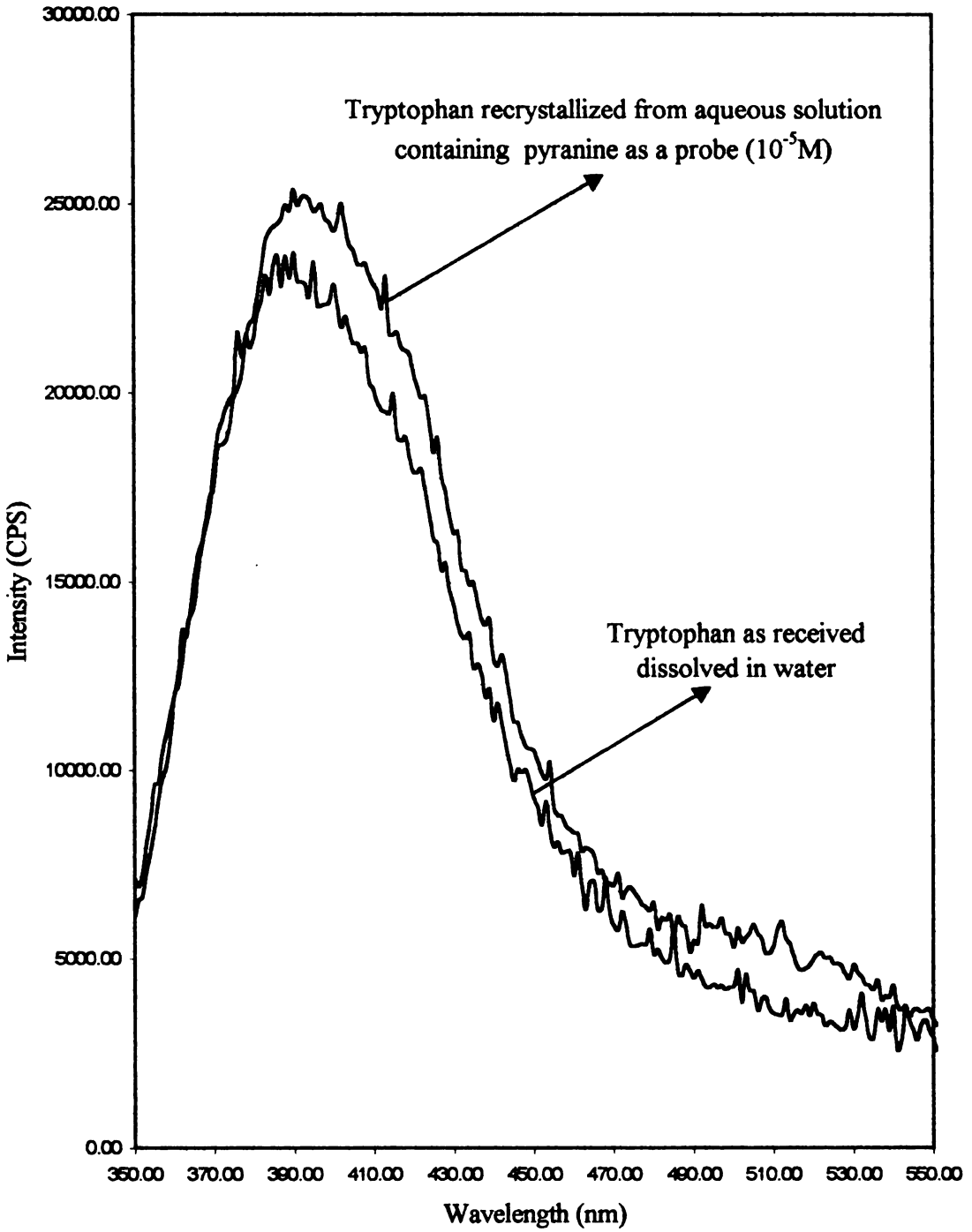

Figure 2.7 Fluorescence spectra of tryptophan excited at 342nm before and after recrystallization from aqueous solution containing pyranine at a concentration of 10^{-5}M

7. Q. Chen, W. J. Walczak, and M. D. Barkley, *J. Am. Chem. Soc.*, **117**, 556-7 (1995)

8 S. A. Tucker, W. E. Acree, JR., and M. J. Tanga, S. Tokita, K. Hiruta, and H. Langhals, *Applied Spectroscopy,* **46**(2), 229 (1992)

9 M. U. Kumke, H. G. Lohmannsroben and Th. Roch, *Analyst*, **119**, 997 (1994)

10 R. Chakraborty, and K. A. Berglund, *AICHE Symposium Series*, **284-7**, 114-123 (1991)

Chapter 3

SUPERSATURATION MEASUREMENTS BY USING THE STEADY STATE FLUORESCENCE OF IMMOBILIZED PYRANINE

3.1 Introduction

Steady state fluorescence of extrinsic trace fluorescent probe molecules as sensors as introduced by Chakraborty and Berglund (1) has been shown to be a very useful method to monitor the supersaturation of high solubility solutions. It has been used to monitor the degree of supersaturation with the peak intensity ratio (PIR) of pyranine in aqueous solutions of sucrose, glucose, fructose, lactose and citric acid (1, 2). In high solubility systems, the PIR is related to the available water in its immediate environment. Pyranine in solution can be used to monitor the crystallization of low solubility systems as well by explaining the pyranine quenching behavior the solutes as described in chapter 2. The PIR of pyranine was shown to change smoothly and nonlinearly with the concentration of tryptophan, nicotinic acid and benzoic acid, and had higher signal response in supersaturation region.

For previous studies pyranine ($1x10^{-5}M$) was introduced into the crystallization solution. A potential problem is that pyranine is not approved by the FDA as a food additive. Pharmaceutical applications of crystallization demand a high degree of purity which precludes the tolerance of even trace amounts of the probe incorporated in the crystal. The control of crystallization of food and pharmaceutical production processes is an important industrial need.

Previous studies have attempted to develop suitable methods to measure supersaturation of food and pharmaceutical crystallization. ATR-FTIR was shown to be a useful *in-situ* crystallization monitor for high solubility systems (3). ATR-FTIR can not be used to monitor low solubility systems, such as tryptophan and nicotinic acid solutions, due to low concentration changes which will produce not detectable signal. Pyranine is still the best probe to measure the supersaturation of low solubility systems due to its high signal response, sensitivity, stability and high quantum efficiency. Probe immobilization is an approach for avoiding contamination, however, the probe must response to the changes of the solution concentration. An immobilized pyranine probe is the target of current study.

In this research we have immobilized pyranine on an ion-exchange membrane and have determined the calibration curve of PIR (Peak Intensity Ratio) versus the concentration of solutions. The solutes studied are tryptophan, phenylalanine, and nicotinic acid all of which have low solubility around 2wt%.

3.2 Materials and Methods

Pyranine, also known by the FDA as D&C Green No. 8,was obtained from Lancaster, Windhamn, NH and used as received. Aqueous solutions of pyranine were prepared by dissolution of 0.026 g in 5ml HPLC grade water to get the pyranine at the concentration of 10^{-2}M.

Different concentrations of solutions were prepared by dissolving the appropriate amount of solutes in 5ml HPLC water. Supersaturated solutions were prepared by heating the solution in the water bath until all the solute was dissolved and subsequent cooling to room temperature. The solutions were used as prepared without any degassing.

Immobilized pyranine was prepared by immersing a membrane for 2.5mins in the pyranine solution ($4x10^{-5}$M) obtained by addition of 20ul pyranine at 10^{-2}M to 5ml HPLC water. The membrane was DEAE cellulose acetate NA45 anion exchange membrane with pore size 0.45 micro meter obtained from Schleicher & Schuell, Keene, NH. The

immobilized pyranine membrane was immersed in the solutions of tryptophan, nicotinic acid or phenylalanine for over 24 hours to saturate the membrane with the solutes before use in an experiment. Fluorescence spectra of the immobilized pyranine in the aqueous solutions were collected within a couple of hours of the preparation of the solutions. All spectra were collected at room temperature with a Spex 1681 Fluorolog spectrometer equipped with a Xenon lamp source and a PMT detector and a front angle set up. A quartz sample holder was used in all cases. Spectra were recorded at a 1.00mm increment and an integration time of 1.0 sec. An excitation wavelength of 342nm for pyranine was used. The emission spectra were recorded over a range from 350-600nm for pyranine. Monochromator slits were at 0.5 mm for all spectra.

3.3 Results and Discussion

3.3.1. Fluorescence spectra of immobilized pyranine

The spectra of immobilized pyranine and free pyranine in water are shown in Figure 3.1. There is a broad peak at 510nm for both immobilized and free pyranine. There is a set of peaks around 400nm which are different for immobilized pyranine and free pyranine. With free pyranine, three fine vibronic peaks will show up around 400nm. In immobilized pyranine, only two peaks will show up and the peak symmetry is not as good as free pyranine. Another remarkable difference is the relative intensity at 510nm and at 400nm. There is a big increase of peak intensity at 510nm and a big decrease of peak intensity at 400nm when pyranine is immobilized on membrane. The peak at 510nm is assigned as fluorescence of deprotonated pyranine and the other bands from 380nm to 420nm are characterized peaks of polycyclic aromatic hydrocarbon (PAH) (4,5).

As we know the amount of pyranine on the membrane is very low although we can not tell how much it is. We can tell that is low from the preparation of immobilized pyranine. Four piece membranes were immersed in pyranine solution ($4x10^{-5}M$) for 2.5mins at the same time. Even thought we can assume the ion exchange is very fast,

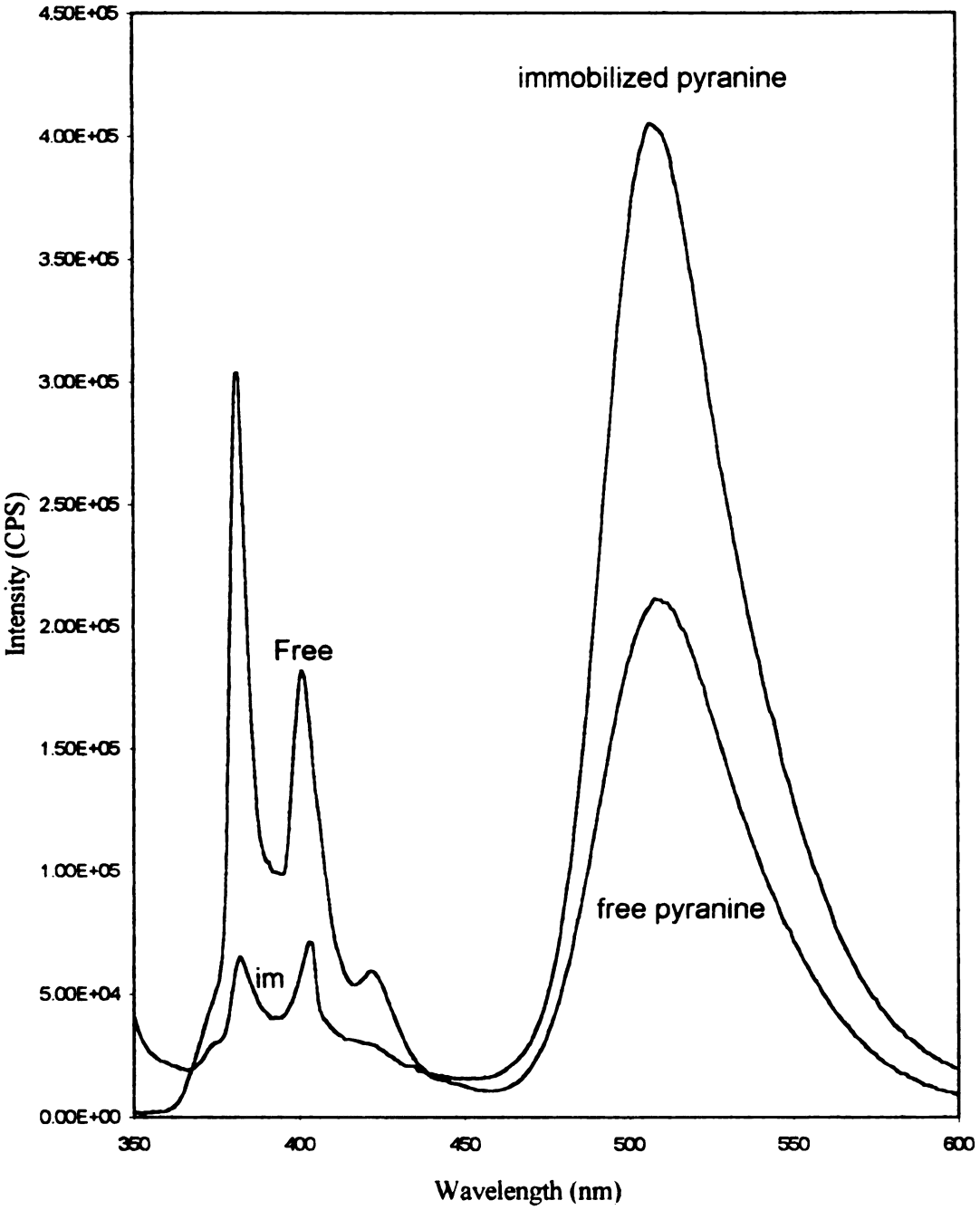

Figure 3.1 Fluorescence spectra of immobilized pyranine and free pyranine in water at room temperature

there is limitation of $1x10^{-5}$M. Actually we know it is impossible that all pyranine will be exchanged onto the membrane, but free pyranine concentration in water is 10^{-5}M. So the concentration difference is not hard to tell.

It is commonly known that the fluorescence intensity of an excited probe molecule can be drastically enhanced when bound to a micelle assembly (6,7,8). The enhancement of fluorescence in micelle system stem from altered micropolarity, restricted motion, effective shielding of the excited single state from quenchers present in solution (8). The shielding of the probe from vibrational quenching by the hydrogen-bond structure of water is also the reason for the enhanced fluorescence (6). Hoshino and Imamure also reported the increase of fluorescence of benzene derivatives by forming inclusion complexes with β-cyclodextrin in aqueous solution (10). The enhancement is due to the decrease of the rotational freedom of florescence molecules and the elimination surrounding fluorescent molecules in a aqueous solutions. It is obvious when pyranine is immobilized on membrane, the rotational freedom of pyranine molecule is restrained which will result in the increase of the fluorescence. Effective shielding of the excited single state from quenchers present in solution with immobilized pyranine and also the shielding of the probe from vibrational quenching by the hydrogen-bond structure of water are the results of the enhancement of immobilizes pyranine fluorescence too.

The fluorescence spectra of immobilized pyranine saturated with three different solutes, tryptophan, phenylalanine and nicotinic acid are shown in Figure 3.2. Immobilized pyranine saturated with phenylalanine has the same fluorescence spectrum as immobilized pyranine which is not saturated with solutes. There are no big change for the peak at 510nm either. But peaks around 400nm are different when immobilized pyranine saturated with tryptophan and nicotinic acid. Tryptophan blurred this set of peaks, and nicotinic acid enhanced the peak at 430nm. The differences of spectra saturated with different solutes can be interpreted as the different interaction of pyranine with tryptophan,

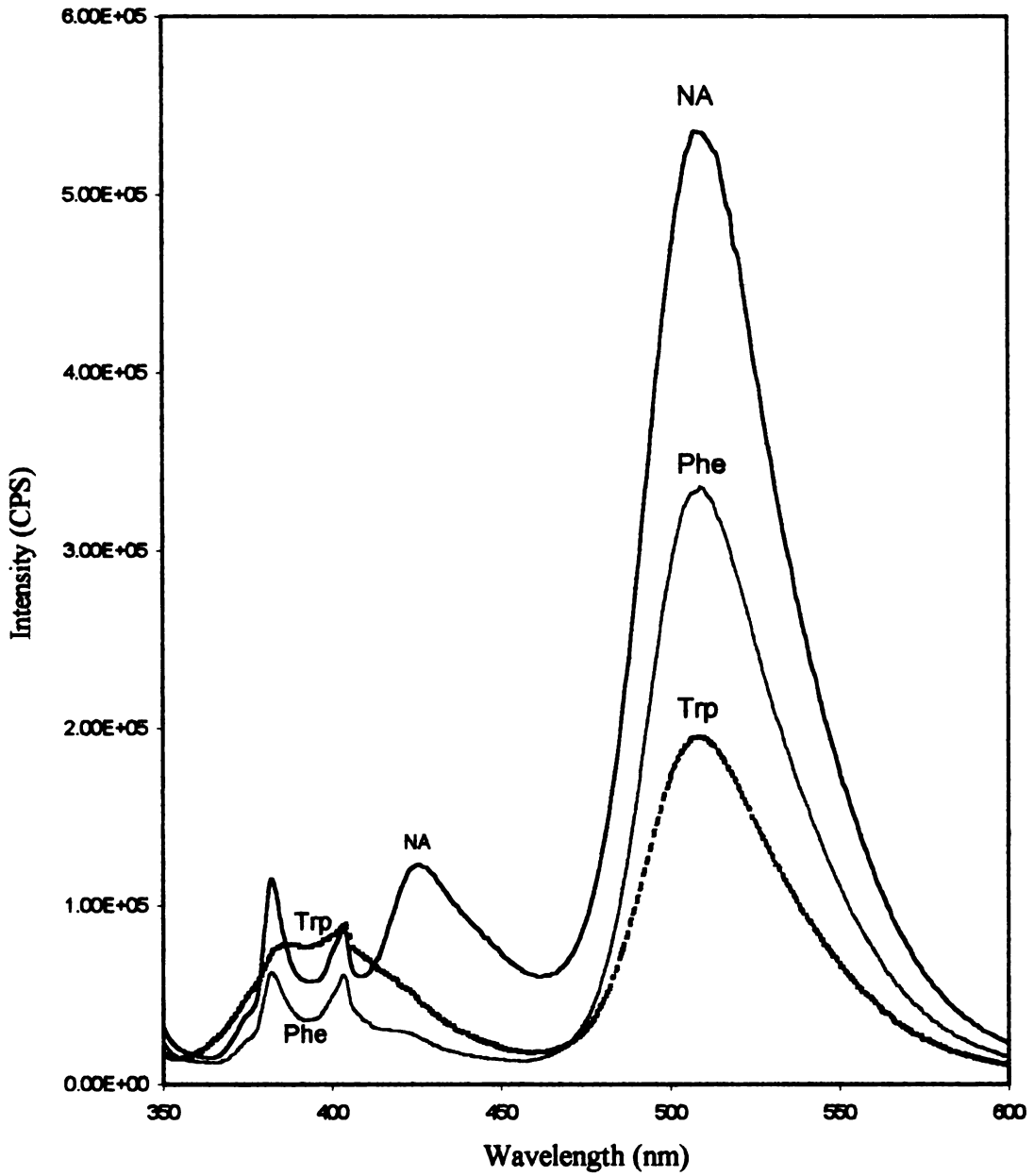

Figure 3.2 Fluorescence spectra of immobilized pyranine saturated with tryptophan, phenylalanine and nicotinic acid in pure water at room temperature

nicotinic acid and phenylalanine which are the results of different structures of solute molecules. As we know fluorescence occurs from the lowest vibronic level at fist excited state, but electrons will relax to different vibrational level of ground state. So fluorescence reflects the vibrational levels of ground states. The change of fluorescence at 400nm when immobilized pyranine saturated with tryptophan and nicotinic acid can be taken as the evidence of the stronger interaction with pyranine compared to phenylalanine which show no interference to immobilized pyranine. Nicotinic acid shows the strongest interaction with pyranine which changes the ground state energy profile of pyrnaine.

The fluorescence spectra of immobilized pyranine in tryptophan, phenylalanine and nicotinic acid solutions show no differences in shape and maxima in the presence and absence of tryptophan, phenylalanine and nicotinic acid. The immobilized pyranine fluorescence intensity changed with the concentration of solutes. But so many factors can result in the change of intensity so intensity change is unpredictable.

The fluorescence intensity of pyranine will increase with the addition of the solutes into the solution. When we immersed immobilized pyranine which did not contact with any solutes into tryptophan solution less than an hour, a very large fluorescence intensity enhancement at all bands can be realized. As we know nicotinic acid quenches pyranine strongly when pyranine is free in the water because the hydrogen bonding complex between pyranine and nicotinic acid (refer to chapter 5). Tryptophan will quench fluorescence of pyranine in solution too and phenylalanine will quench pyranine fluorescence in solution slightly. The different quenching ability of solutes results from the different interaction of pyranine with different solutes. When immobilized pyranine contacts with solutes, solute molecules will enter the membrane. Because the similar ring structure of pyranine as tryptophan, nicotinic acid and phenylalanine, the dipole moment interaction of pyranine with tryptophan, nicotinic acid and phenylalanine will be stronger than the interaction with water. This interaction is interpreted as the contact complex referred to chapter 5. The increase of the fluorescence intensity can be attributed to the

protection of quenching by water because of the formation of the contact complex between pyranine and solute molecules. Water quenching fluorescence by proton transfer has been proven by isotope effect (11,12). As we know the most important quenching mechanism is dynamic quenching which involves the collisional contact between quencher and fluorophore. When pyranine is immobilized in the membrane, the solute molecules can not diffuse into the membrane to quench the fluorescence of pyranine due to the bigger size of solute molecules. Water is much smaller molecules which are easier to diffuse to pyranine to quench the fluorescence. But the contact complex between pyranine and solute molecules provide the shielding of the probe from formation of hydrogen bonding with water molecules than from vibrational quenching by the hydrogen-bond structure of water. Thus the fluorescence intensity increases.

3.3.2. Measurement of supersaturation

The peak intensity ratio (PIR), defined as the ratio of the peak intensity at 401nm or 382nm to the intensity at 510nm for tryptophan and phenylalanine and 429nm to 510nm for nicotinic acid, is used to measure the concentration of solution. The use of this ratio can provide an internal correction in the spectrophotometer setup. The fluorescence intensity of immobilized pyranine is really unpredictable. So many different factors can affect the intensity, especially the membrane surface. Even different light shooting spot will alert the intensity. By using the PIR, these random change can really be corrected which is such a good news for us. Figure 3.3 is the calibration curves of immobilized pyranine in tryptophan, phenylalanine and nicotinic acid solutions. We can see the PIR changes with the concentration of solutes linearly. By measuring PIR, concentration of solutes can be read out from calibration curves and the supersaturation can be calculated by the difference of solubility and concentration. So we can control the supersaturation by adjusting the outer conditions, such as the temperature of environment. It has been shown that the supersaturation measurement using the PIR is more sensitive than other techniques,

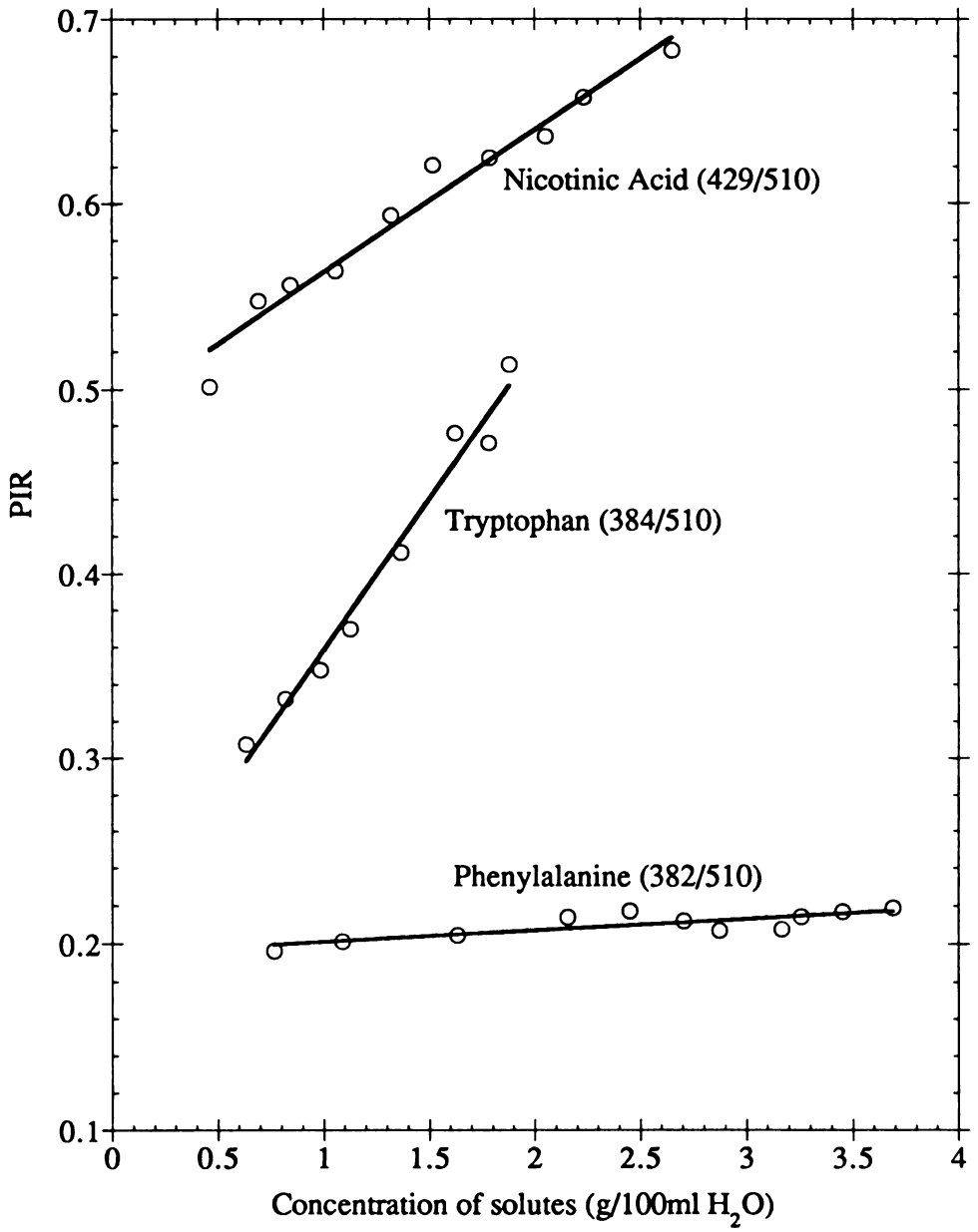

Figure 3.3 Peak intensity ratio (PIR) of pyranine versus concentration of tryptophan, nicotinic acid and phenylalanine aqueous solutions at room temperature. The values in parentheses represent the emission peaks for PIR.

we can see this in our research since the concentration change in our research is from 0.06%-1.8% of Tryptophan, PIR changes from 0.3 to 0.5. The concentration is 0.5% to 2.5% for nicotinic acid and the gain of PIR is from 0.5 to 0.7. This is a big signal response compared to traditional methods which changes occurs at fourth or even fifth decimal places.

Reproducibility of PIR versus the concentration was checked for both tryptophan and nicotinic acid solutions. It turned out different immobilized pyranine will give us different linear curves, but the same immobilized pyranine will have the same PIR versus concentration plots. Figure 3.4 shows two sets of the PIR vs. concentration of tryptophan and nicotinic acid with the same immobilized pyranine at different experiment dates. For tryptophan, two experiments were conducted by 6 days difference and nicotinic acid is 8 days difference. Two sets data for both tryptophan and nicotinic acid are overlap each other. Another experiment using the same immobilized pyranine and conducted in two different days in tryptophan solutions showed an overlap PIR versus concentration curves too which is not shown here. So we can conclude the relation between PIR and the concentration of solutes is reproducible.

Pyranine has very high solubility in water, so we have to consider whether immobilized pyranine will dissolve in water. If even trace dissolution happens, it will make this technique not good enough for monitoring food and pharmaceutical processing. So we immerse immobilized pyranine membrane into water, then detect the fluorescence of pyranine after the membrane was taken away. The spectra shows no fluorescence of pyranine. So we can conclude pyranine will not dissolve into water once it is immobilized in the membrane. It is safe for it to be used in food processing.

3.4. Conclusion

The fluorescence of immobilized pyranine was enhance due to the restriction of movements of pyranine molecule and also due to the protection of quenching by water

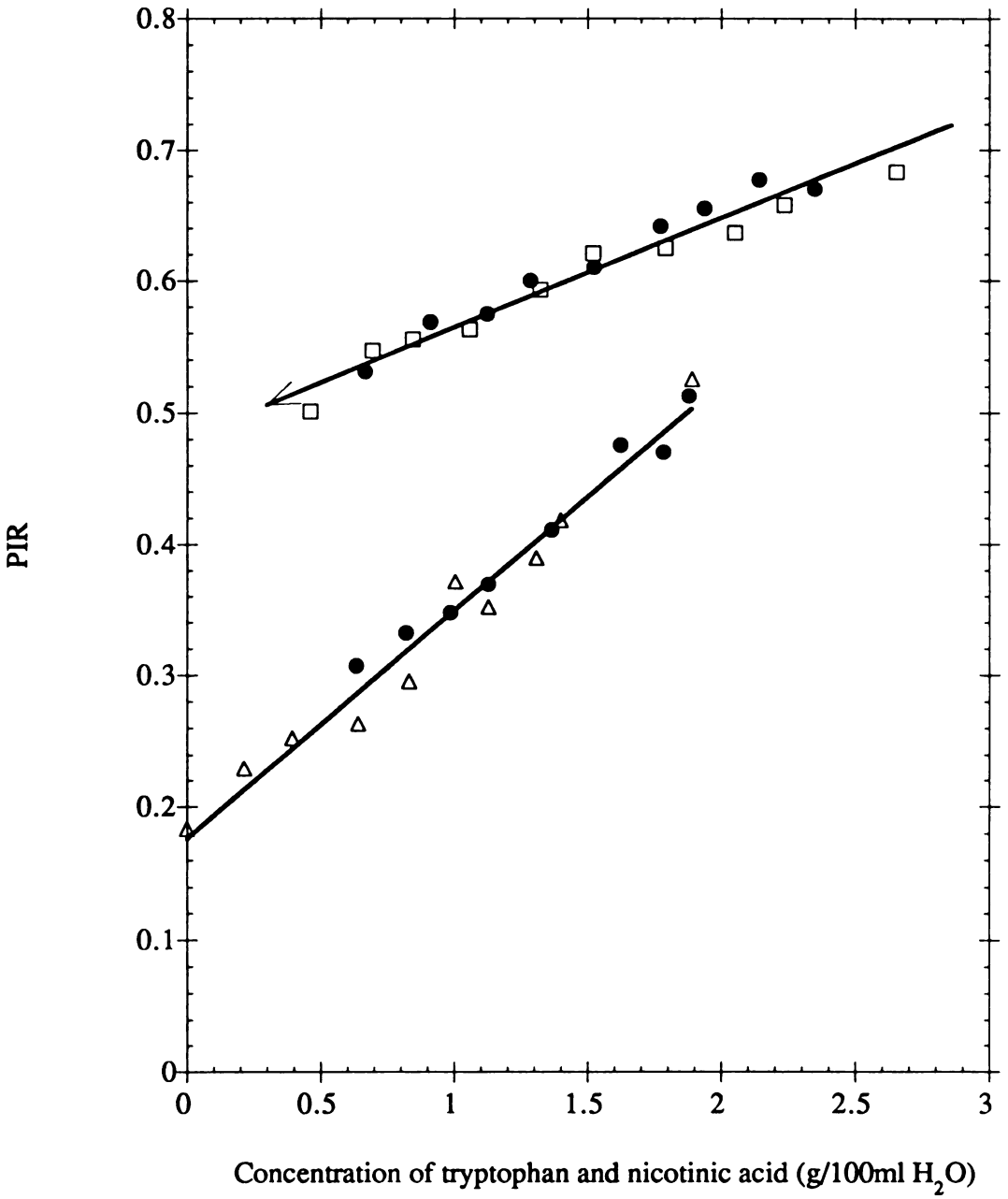

Figure 3.4 Reproducibility of peak intensity ratio (PIR) of pyranine versus concentrations for both tryptophan and nicotinic acid aqueous solutions at room temperature.

molecules. The introduction of solutes to immobilized pyranine on membranes will enhance the fluorescence intensity by formation of contact complex which will protect the quenching from water. The PIR of immobilized pyranine is strongly correlated to the solute concentration and the relation between the PIR of immobilized pyranine and concentration is linear. This technique is highly sensitivity which gives it more promise.

3.5. References

1. R. Chakraborty and K. A. Berglund, *J. Crystal Growth*, **125**, 81(1992)
2. Sanjay K. Yedur and Kris A. Berglund, *Applied Spectroscopy*, **50**(7), 866(1996)5.
3. Dunuwila, D. D., PhD Thesis, Michigan State University(1996)
4 S. A. Tucker, W. E. Acree, JR., and M. J. Tanga, S. Tokita, K. Hiruta, and H. Langhals, *Applied Spectroscopy*, **46**(2), 229, 1992
5 M. U. Kumke, H. G. Lohmannsroben and Th. Roch, *Analyst*, **119**, 997(1994)
6. W. L. Hinze, H. N. Singh, Yoshimi Baba and Noel G. Harvey, *Trends in Anal. Chem.*, **3**(8), 193(1984)
7. H. N. Singh and W. L. Hinze, *Analyst*, **107**, 1073(1982)
8. H. N. Singh and W. L. Hinze, *Anal. Lett.* **15**, 221(1982)
9. M. Hoshino, M. Imamura, K. Ikehara and Y. Hama, *J. phys. Chem.* **85**, 1820(1981)
10. J. D. Ingle, Jr.., and S. R. Crouch, *Spectrochemical Analysis*, Prentice-Hall, Inc., 1988
11. L. P. McMahon, W. J. Colucci, M. L. McLaughlin and M. D. Barkley *J. Am. Chem. Soc.*, **114**, 8442-8448(1992)
12. Yu Chen, Bo Liu, Hong-Tao Yu and Mary D. Barkley, *J. Am. Chem. Soc.*, **118**, 9271-9278(1996)

Chapter 4.

THE EXPLORATION OF OTHER POSSIBLE PROBES--PBA AND CA

4.1. Introduction

It was shown in chapter 2 that pyranine is a good probe for measurement of supersaturation in low solubility systems. The PIR (peak intensity ratio) curves of pyranine with the concentration of tryptophan, nicotinic acid are smooth, nonlinear curves which have a larger gain at higher concentrations.

Our goal is to evaluate other probes and compare them to pyranine. PBA (1-Pyrenebutyric acid) is another useful probe which is used widely to study micellar properties and fluorophores' location in membranes (1, 2). The molecular structure of PBA (1-Pyrenebutyric acid) is shown in Figure 4.1. PBA has strong fluorescence in aqueous solution. There are three emission peaks for PBA in MeOH originating from the first excited singlet state and shows fine structure as is common for many PAH compounds (3). Pharmaceutical and food production applications of crystallization demand a high degree of purity which precludes the tolerance of even trace amounts of the probe incorporated in the crystal. Pyranine and PBA, which are not approved by the FDA as food additives, can't be added directly in food and pharmaceutical processing to monitor the process if there is a possibility of the probe contamination in the product. Although we already have shown pyranine will not go into crystal lattice, the addition of pyranine is not allowed by FDA in food processing. We need to explore other possible probes approved by FDA. Carminic acid (CA) is a choice.

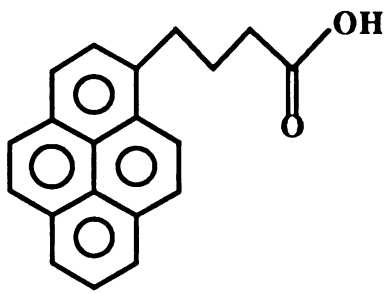

1-pyrene butyric acid (PBA)

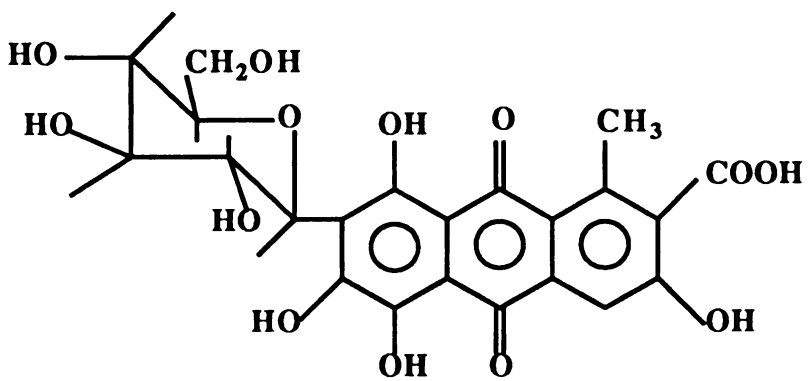

Carminic acid (CA)

Figure 4.1. Molecular structures of 1-pyrene butyric acid (PBA) and carminic acid (CA)

Carminic acid (CA), shown in Figure 4.1, is a natural food pigment making it a potentially good probe for food processing and pharmaceutical processing. Carminic acid is the major coloring substance of cochineal used in food and beverages, and can be added directly into pharmaceutical and food processing.

CA is weakly fluorescent in aqueous solution. The photochemistry of CA has been studied and results show that the fluorescence of carminic acid is moderately dependent on pH in acidic and neutral aqueous solution. There are four species of CA in solution--- LH_3(CA), LH_2^-, LH^{2-},and L^{3-} (4,5). Each species has a different emission spectrum.

The state of supersaturation is an essential requirement for all crystallization operations. The formation of nuclei is the beginning point of the crystallization. The nucleation of solute must somehow depend upon the solute molecules in a supersaturated solution and also depend upon the various molecular interactions, such as solute-solute and solute-solvent interactions (6). Understanding the structure of supersaturated solutions can help us better design and control the crystallization.

Fluorescence quenching requires the contact of the quenchers and fluorophores so fluorescence quenching technique is a very useful tool to study the interaction of fluorophore and quencher then information about the organization of solution can be deducted from quenching data. Different quenching behaviors are the results of different interaction of fluorophors and quenchers.

In this chapter we measure the fluorescence spectra of PBA and CA in aqueous solutions to evaluate the feasibility of PBA sand CA for measurement of supersaturation in low solubility systems. The quenching behavior of tryptophan and phenylalanine to PBA and CA are also studied to probe the organization of solute molecules in solutions.

4.2. Material and Methods

PBA (1-Pyrenebutyric acid) was obtained from Eastman Kodak, Rochester NY and used as received. PBA solutions were prepared by dissolution of 0.0134g PBA in 20ml

ethanol because the solubility of PBA in water is pretty low. Different concentrations of solutions were prepared by dissolving the appropriate amount of solute in 5ml HPLC water. Supersaturated solutions were prepared by heating the solution in the water bath until all the solute was dissolved and subsequent cooling to room temperature. The solutions were used as prepared without any degassing.

Probe molecules were introduced by addition of five microliters of the PBA solution ($4x10^{-3}M$) to the aqueous tryptophan and phenylalanine solutions resulting in a probe concentration of $4x10^{-6}M$. Fluorescence spectra of PBA in the aqueous solutions were collected within two hours of the preparation of the solutions. All spectra were taken at room temperature with a Spex 1681 Fluorolog spectrometer equipped with a Xenon lamp source and a PMT detector. A quartz sample holder was used in all cases. Spectra were recorded at a 1.00mm increment and an integration time of 1.0 sec. An excitation wavelength of 326nm for PBA was used. The emission spectra were recorded over a range from 340-4500nm for PBA. Monochromator slits were at 0.5 mm for spectra.

Carminic acid was obtained from Aldrich Chemical Company, Inc. Milwaukee, WI and used as received. Carminic acid solutions were prepared by suspending 0.01g CA in 20ml H_2O. The suspension was centrifuged in a Eppendorf Centrifuge 5415C at the speed of $14x1000min^{-1}$ for 5 mins to obtain a saturated aqueous solution of CA. The appropriate concentration of CA was introduced by addition of 5 microliters of the saturated CA solution to the aqueous tryptophan and phenylalanine solutions which were prepared by dissolving the appropriate amount of solute in 5ml HPLC water. Fluorescence spectra of CA in the aqueous solutions were collected within two hours of the preparation the solutions. All spectra were taken at room temperature with a Spex 1681 Fluorolog spectrometer equipped with a Xenon lamp source and a PMT detector. A quartz sample holder was used in all cases. Spectra were recorded at a 1.00mm increment and an integration time of 1.0 sec. An excitation wavelength of 500nm was used. The emission

spectra were recorded over a range from 530nm to 700nm. Monochromator slits were set at 4 mm.

4.3. Results and Discussions

4.3.1. Steady state fluorescence of PBA as probe

There are two peaks in the PBA emission spectra in tryptophan solution shown in Figure 4.2, one peak is at 375nm and the other is at 395nm. This is a typical emission spectrum of a polycyclic aromatic hydrocarbon (PAH). The typical emission spectrum of the PAH monomer will consist of five major vibronic bands which are generally labeled as I-V in progressive order, such as the 0-0 band is labeled I, etc.(3,7,8). The fluorescence intensity versus the concentration of PBA (Figure 4.3) shows that the intensity of fluorescence decreases with the concentration of tryptophan at both wavelengths. The intensity shows a larger decrease at 375nm. The intensity differences at 375nm and 395nm are smaller with the increase of the concentration of tryptophan. When the concentration of tryptophan is high, the fluorescence intensity increases very little with the concentration of tryptophan, especially the intensity at 395nm. The intensity of fluorescence at 375nm and 395nm approach the same value at high tryptophan concentrations. The intensity decrease with the concentration of tryptophan showed the quenching of tryptophan to PBA.

The emission spectra of PBA in aqueous phenylalanine solution has the same shape and peak position as in tryptophan solutions. There are two peaks, one is at 375nm and the other is at 395nm. The intensity of both peaks changes little with the concentration of phenylalanine which means phenylalanine does not quench the fluorescence of PBA.

4.3.2. Calibration curve of PBA as probe

The peak intensity ratio (PIR) is defined as the ratio of intensity at 395nm and 375nm in tryptophan solutions. The PIR increases with the increase of concentration of

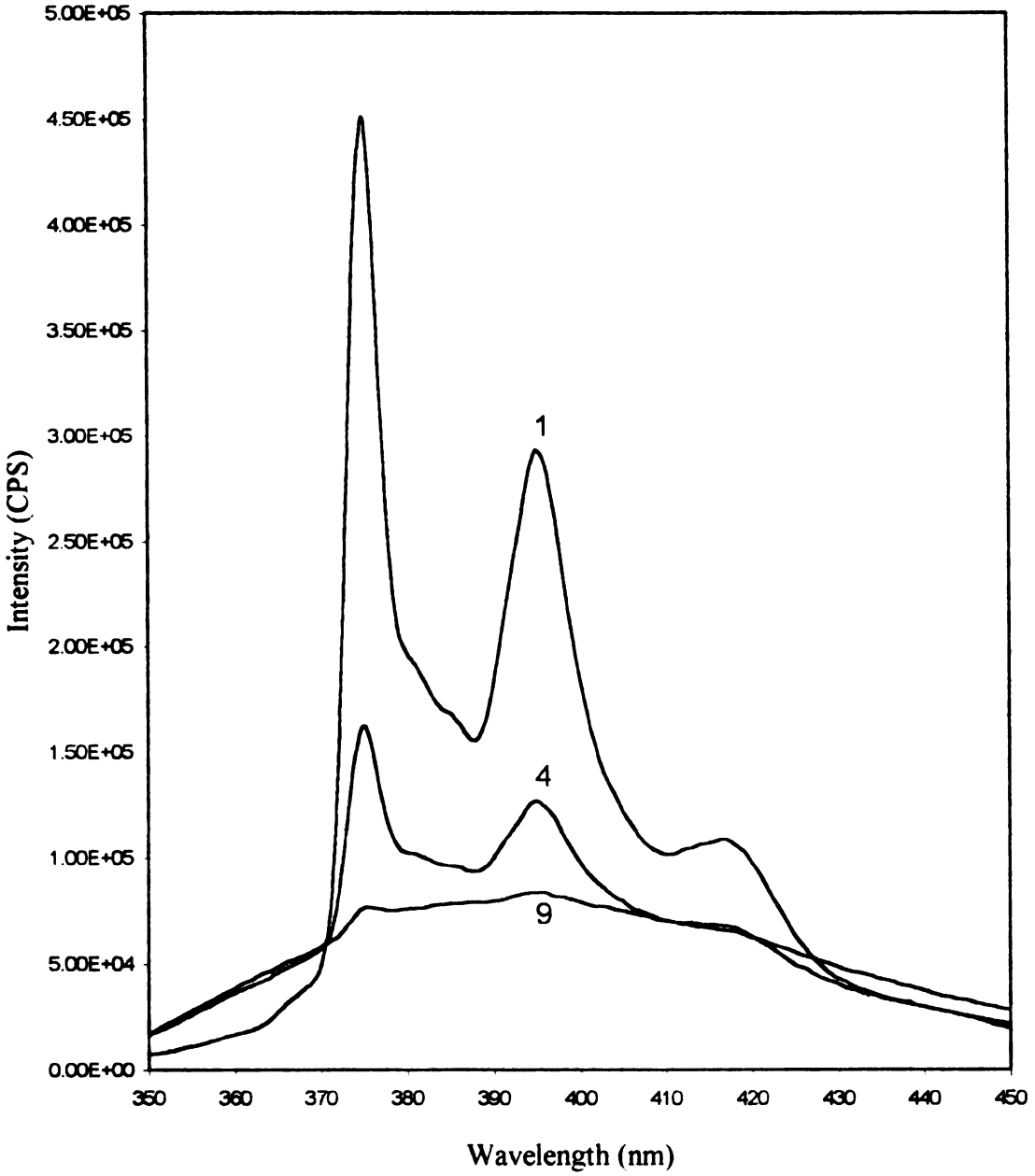

Figure 4.2 Fluorescence spectra of PBA in aqueous tryptophan solutions:
1(0.0118M), 4(0.0410M) and 9(0.100M)

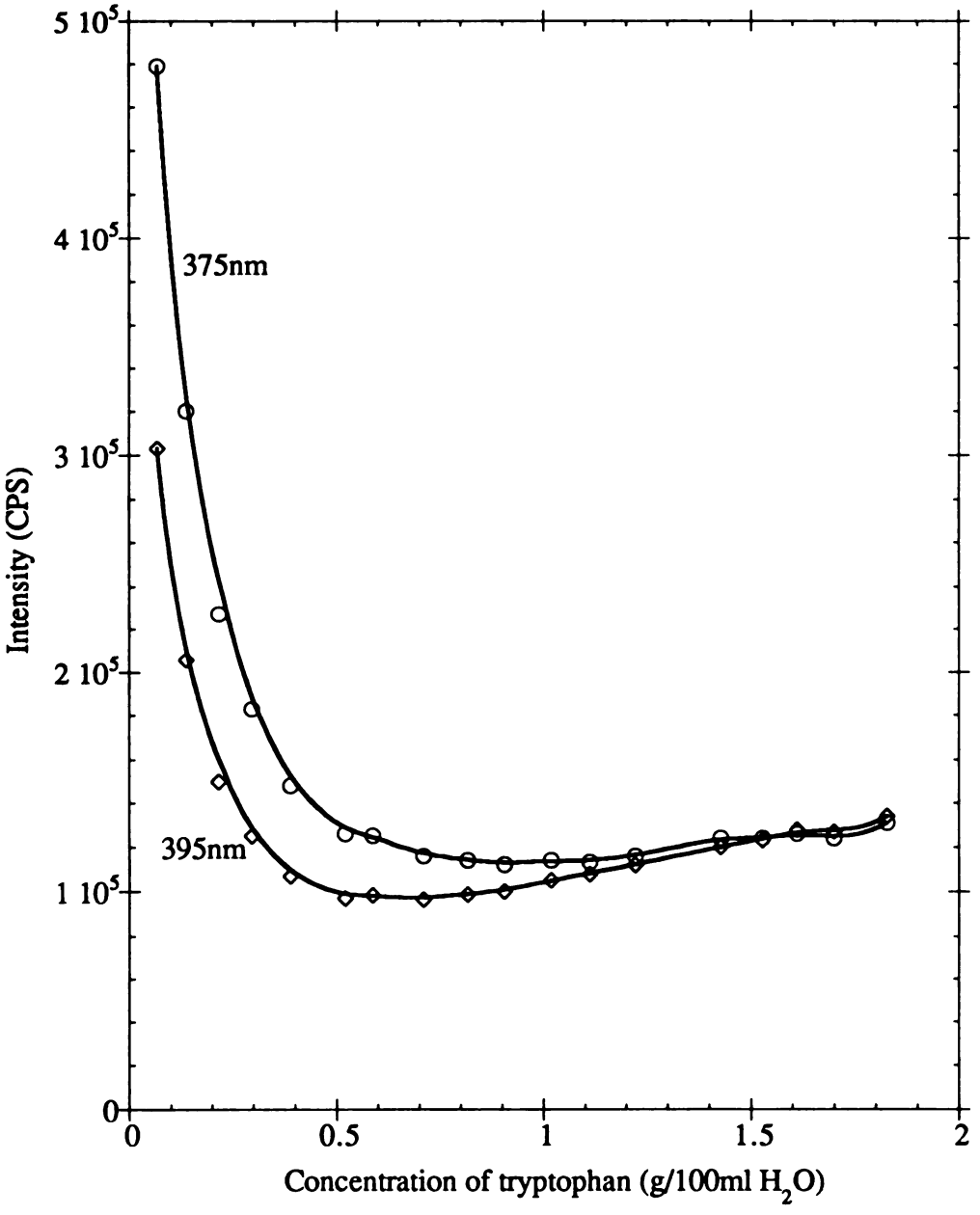

Figure 4.3 Fluorescence intensity of PBA versuses the concentration of tryptophan in aqueous solution at room temperature. The lines are smooth fit of data.

tryptophan shown in Figure 4.4. The increase is smooth, but there is not a larger gain at higher concentration as shown with pyranine as the probe in chapter 3. In contrast the PIR plot curves downward at higher tryptophan concentration; However, the PIR curve is changing with the concentration of tryptophan smoothly and the signal is big enough to be used to measure the supersaturation of tryptophan solutions.

The intensity of PBA did not change with the concentration of phenylalanine, so the PIR of 395nm/375nm is constant at all concentrations of phenylalanine. Therefore, PBA can not be used as probe to measure the supersaturation of phenylalanine.

4.3.3. Steady state fluorescence of carminic acid as a probe

There are four emission peaks in the emission spectra of carminic acid because there are four species in the solution (5). They are difficult to deconvolute because they overlap each other. In general, we obtain one broad peak, or one wide peak with a shoulder when one species is dominant. From the emission spectra (Figure 4.5) we can see that in tryptophan and phenylalanine solutions there are two different dominant species, which position at 580nm in phenylalanine and 595nm in tryptophan. The emission intensity of carminic acid increases with the concentration of phenylalanine (Figure 4.6), but decreases with the concentration of tryptophan (Figure 4.7). The PIR is defined as the peak intensity ration of 580nm/595nm. No changes of the PIR occurs with the concentration changes of phenylalanine. Therefore peak intensity will be used as the signal to measure the supersaturation for CA as probe. From Figure 4.6 the fluorescence intensity of CA will increase with the concentration of phenylalanine smoothly and can be used as the calibration curve to measure the supersaturation of the phenylalanine solutions. From previous results we know phenylalanine does not quench the fluorescence of PBA and quenches the fluorescence of pyranine weakly shown in chapter 2, therefore it is hard to get strong signal to measure the concentration of phenylalanine using PBA and pyranine as

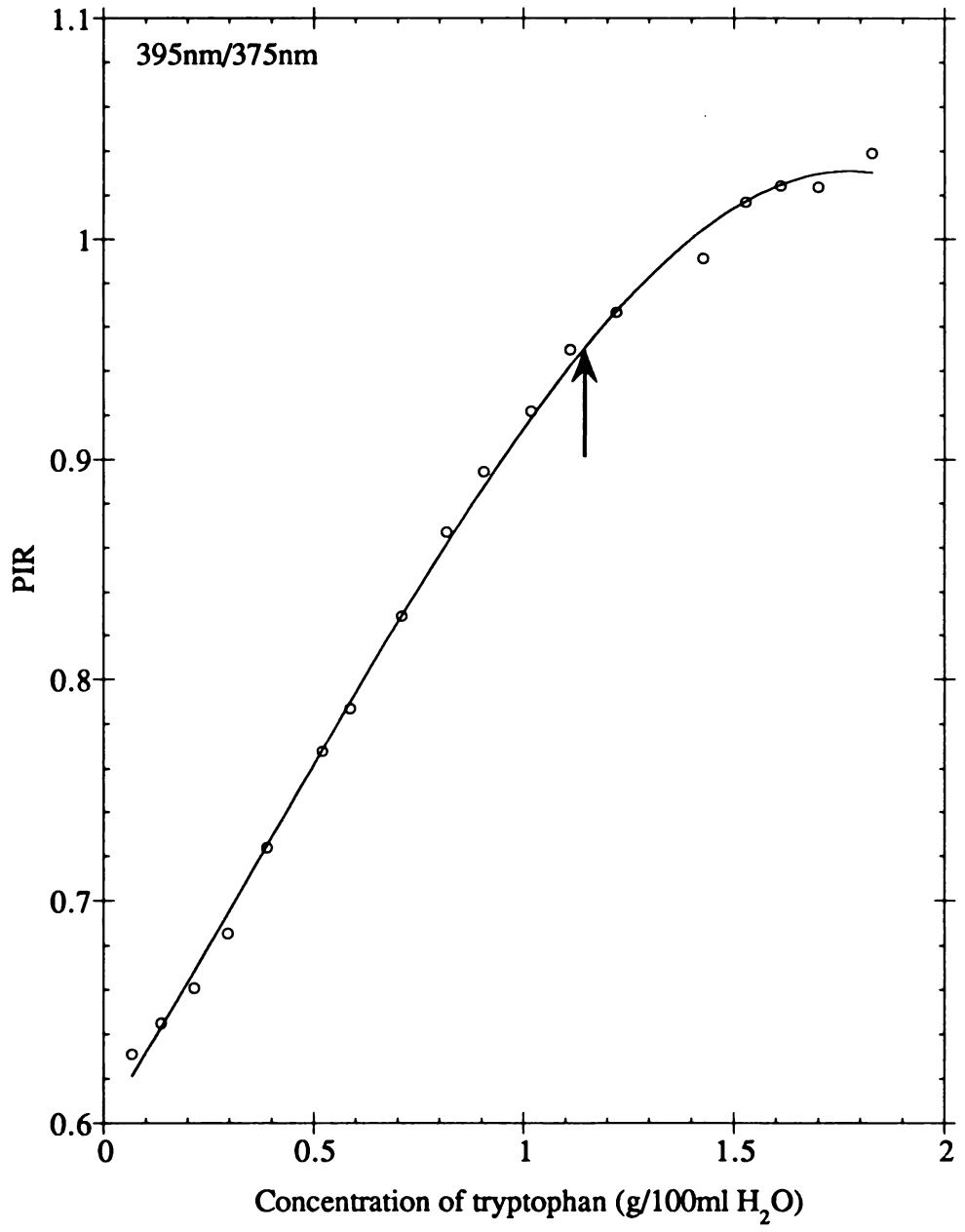

Figure 4.4 Peak intensity ratio (PIR) of PBA versus the concentrations of tryptophan in aqueous solutions at room temperature.

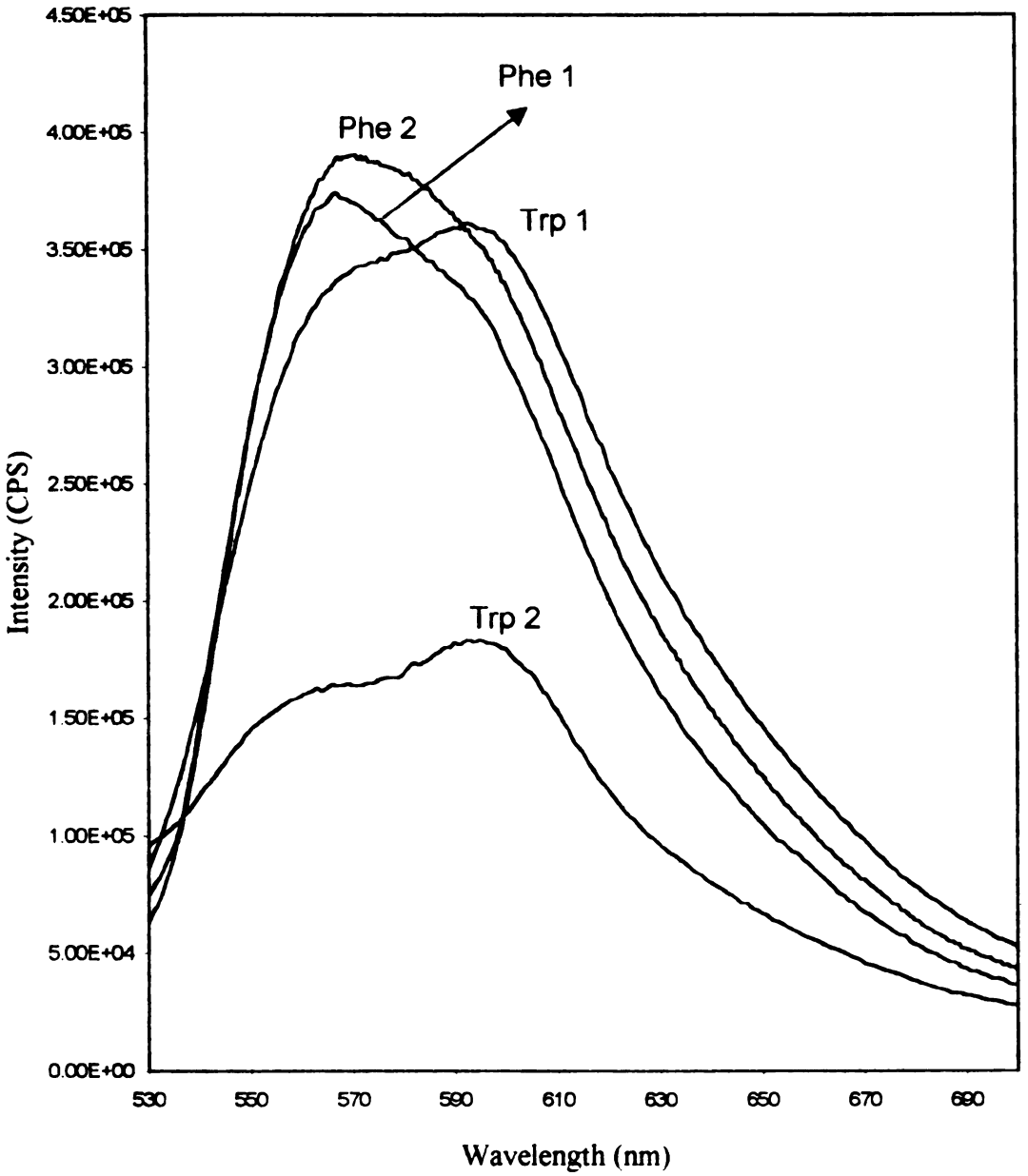

Figure 4.5 Fluorescence spectra of carminic acid in aqueous tryptophan solutions and phenylalanine solutions at room temperature. Phe 1: 0.0128M, Phe 2: 0.0138M, Trp 1: 0.0119M and Trp 2: 0.0702M

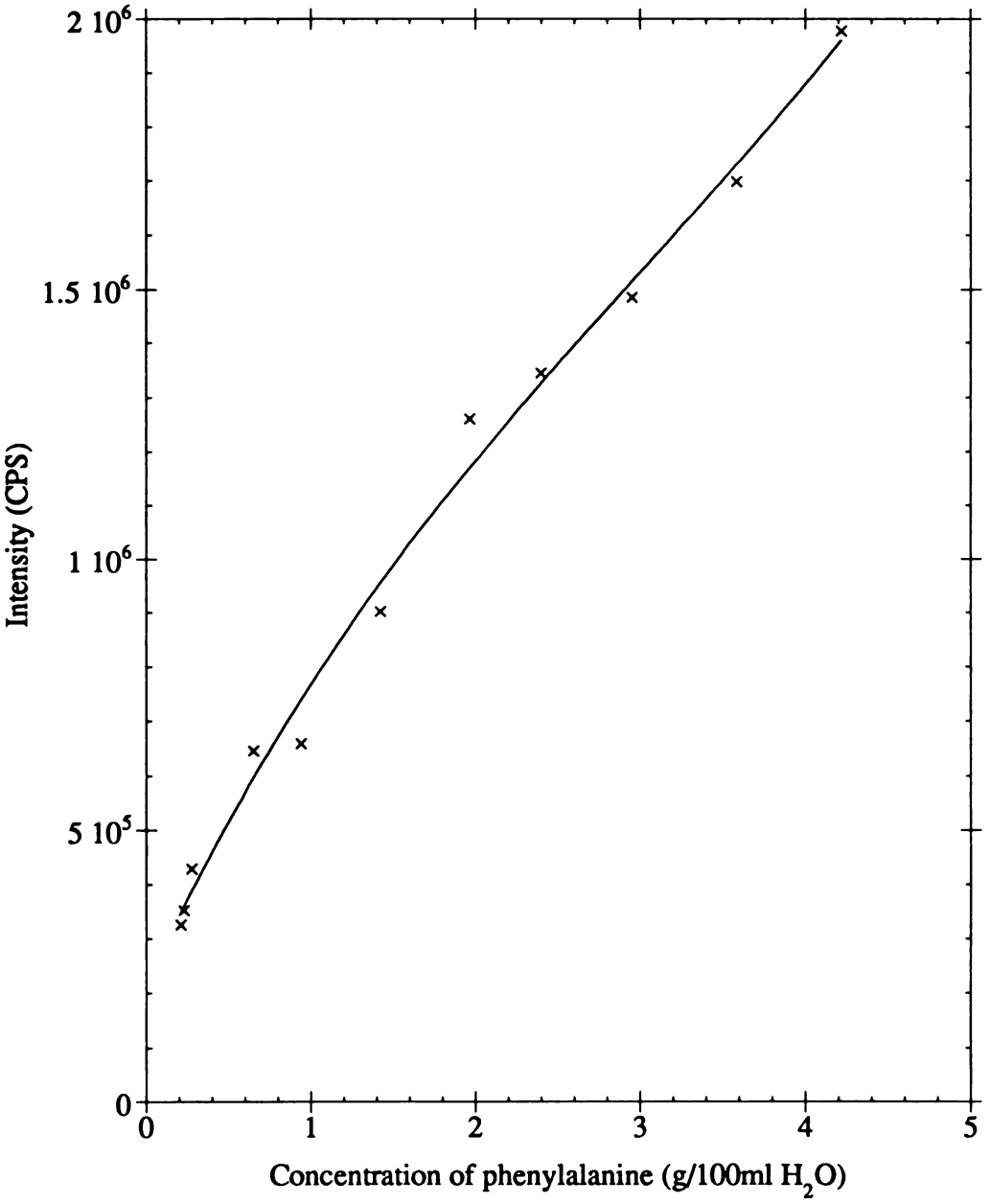

Figure 4.6 Fluorescence intensity of CA at 595nm versus concentration of phenylalanine in aqueous solutions at room temperature. The plot is polynomial fitting.

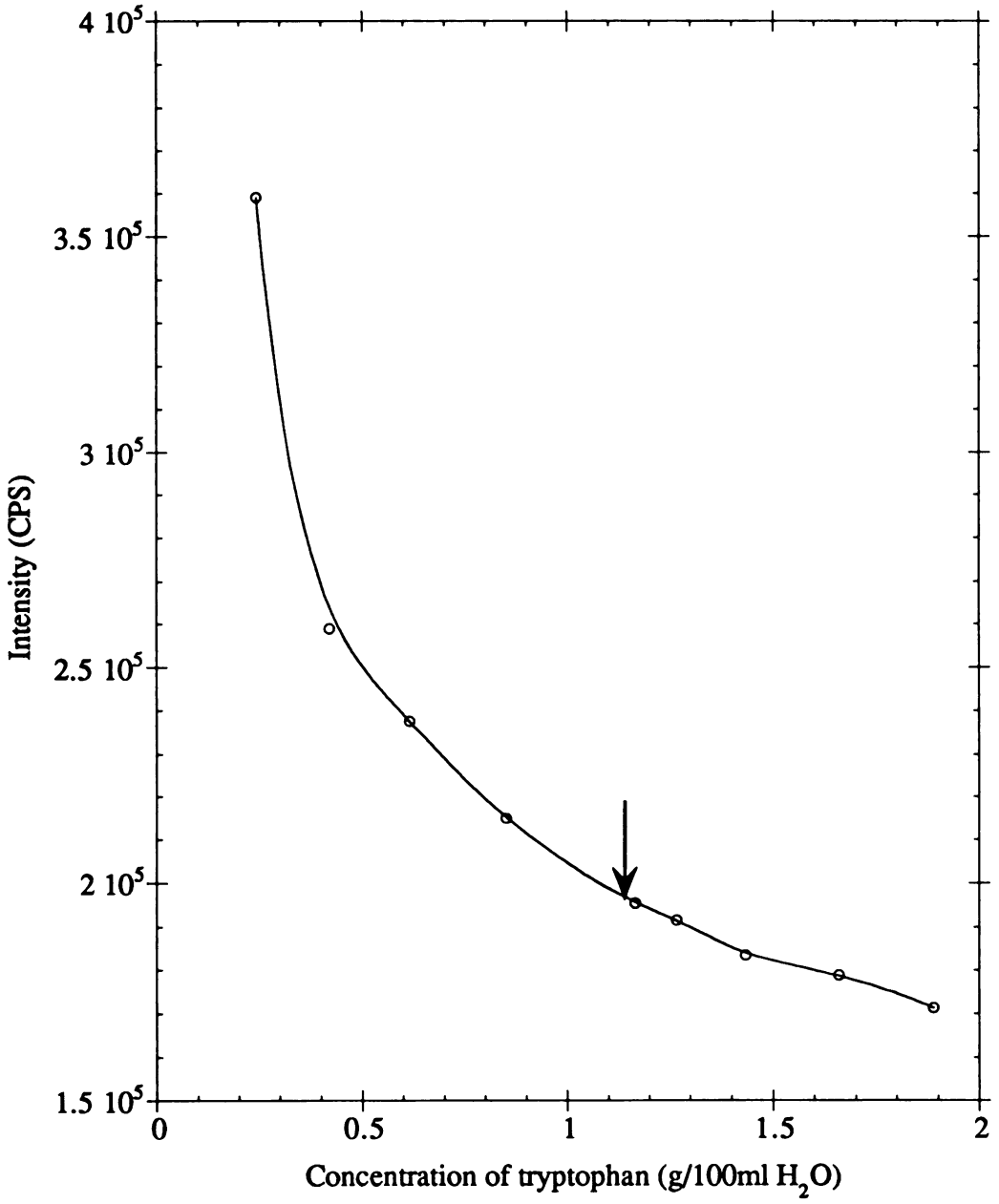

Figure 4.7 Fluorescence intensity of carminic acid at 595nm versus concentration of aqueous tryptophan at room temperature.

The arrow indicates the solubility of tryptophan at 25^{0}C.
The line is smooth fitting of data.

probes. Here we show CA will work as a probe for phenylalanine. However, CA can not be used to measure the supersaturation of tryptophan solutions because the PIR curve doesn't change with the concentration of tryptophan and fluorescence intensity of CA decreased with the concentration of tryptophan.

4.3.4 Quenching behavior of tryptophan and phenylalanine

The decrease of the fluorescence intensity of PBA in tryptophan solutions is the result of quenching by tryptophan. The Stern-Volmer quenching curve of PBA by tryptophan is shown in Figure 4.8. Quenching of PBA by tryptophan follows a straight line at low concentration of tryptophan at both wavelengths. When the concentration of tryptophan increases, the plot curves downward. When the concentration of tryptophan increases, aggregates of tryptophan probably form in the solution reducing the quenching efficiency, so the plot curves down. The fluorescence intensity of PBA does not change with the concentration of phenylalanine which indicates that phenylalanine does not quench the fluorescence of PBA.

The fluorescence intensity of CA in tryptophan solutions decreases with the concentration of tryptophan, but increases with the concentration of phenylalanine solutions. So we can conclude tryptophan quenches the fluorescence of CA but phenylalanine does not quench the fluorescence of CA. The quenching curve of CA by tryptophan in solutions is shown in Figure 4.9. The graph shows a downward quenching curve. The downward curvatures can be the result of the heterogeneity of the system or selective quenching. Different binding sites in large molecules make some fluorophores easier to be quenched than others (9). The negative deviation from the Stern-Volmer law can be described by modified Stern-Volmer Law III (10).

$$\frac{I_0}{I_0 - I} = \frac{1}{fK_{sv}}\frac{1}{[Q]} + \frac{1}{f} \qquad (4.1)$$

f is the fraction of the fluorescence accessible to quenching.

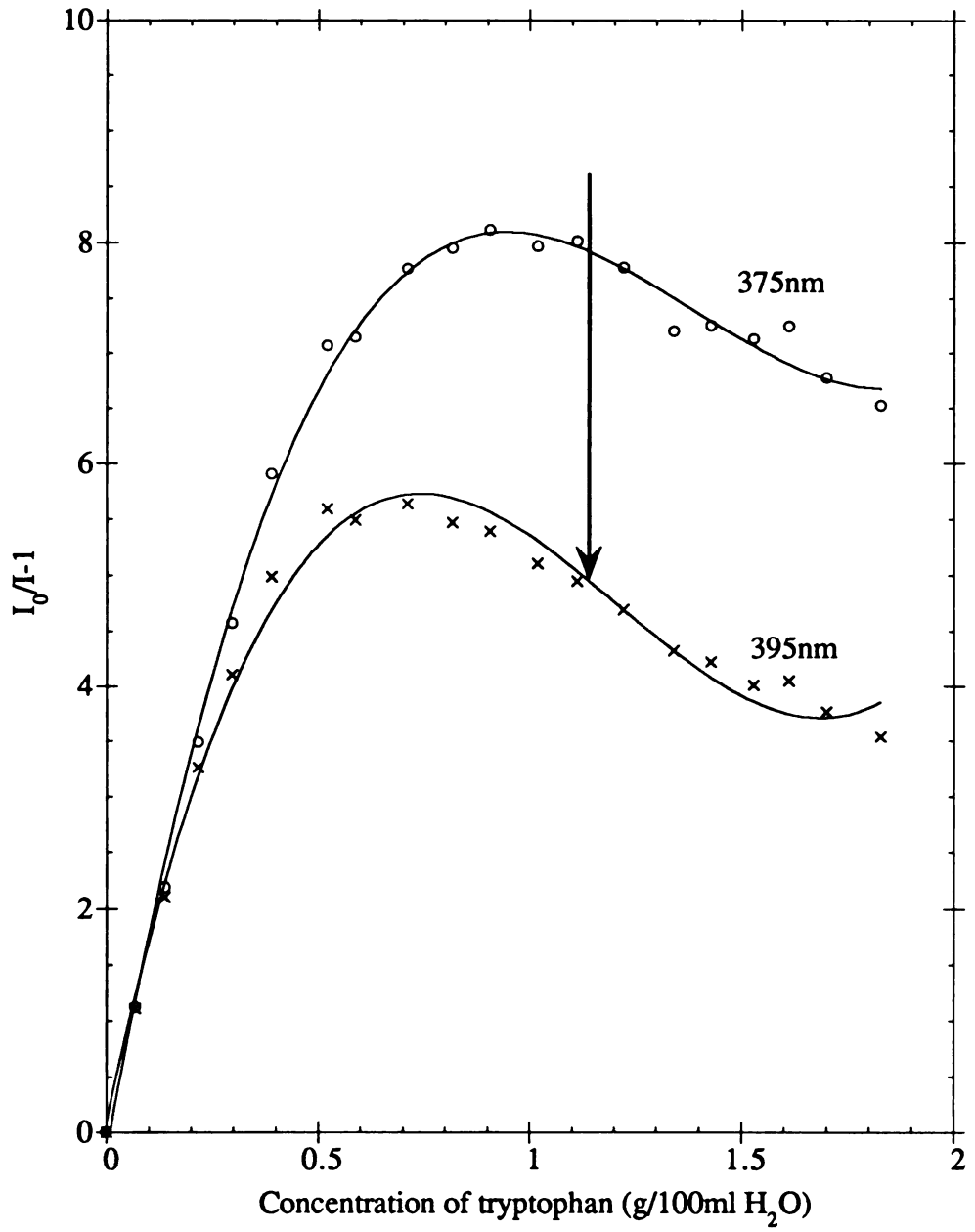

Figure 4.8 Quenching of PBA by tryptophan in aqueous solutions at 375nm and 395nm fit to Stern-Volmer law at room temperature. The arrow indicates the solubility of tryptophan at 25^0C.

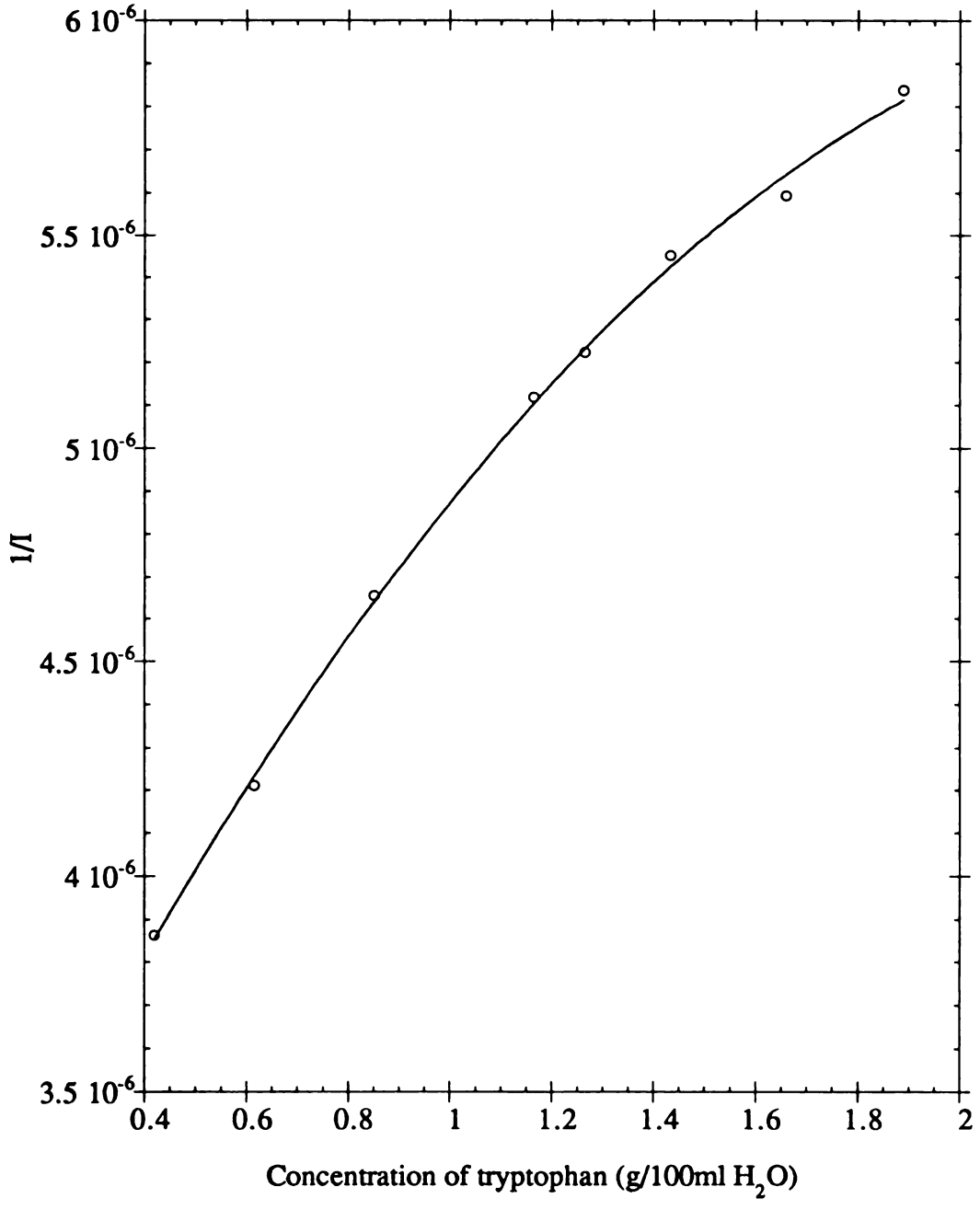

Figure 4.9 Quenching of carminic acid at 595nm by tryptophan in aqueous solutions fit to $1/I=1/I_0+(K/I_0)[Q]$ at room temperature.

By using this modified Stern-Volmer curve to fit the quenching data, Figure 4.10 is obtained which is a straight line. The intercept 1.372 results in the fraction of the fluorescence accessible to the quenching as 73% and the quenching constant is 1.2 (g tryptophan/100ml H_2O/)$^{-1}$. Some of tryptophan molecules can not access CA to quench the fluorescence because of the formation of multiple molecular associates among tryptophan molecules. Detailed discussion regarding the structure of tryptophan in solution will be presented in chapter 5 and chapter 7.

The different quenching behaviors of tryptophan and phenylalanine stem from the different host-probe interaction of probe molecules with solute molecules resulting from the different structures of solute molecules. We know the structural difference of tryptophan and phenylalanine is only in the ring, tryptophan has an indole ring and phenylalanine has a benzene ring. If the dynamic quenching were the quenching mechanism, phenylalanine should have a larger quenching ability due to its relative smaller size compared to tryptophan. However, phenylalanine does not show any quenching ability at all; therefore we interpret the quenching from tryptophan is static domain quenching due to the amine in the ring.

4.3.5. Detection of PBA and CA in crystalline products

In order to test if PBA and CA will enter the crystals lattice of tryptophan, an experiment is conducted as follows: dissolving tryptophan in solution, adding PBA and CA into the solution, then recrystalizing tryptophan from solutions with PBA and CA in the solutions. Recrystalized tryptophan is dissolved in water and the fluorescence of PBA and CA is recorded. For tryptophan recrystallized from PBA solution, the solution was excited at 326nm, spectra were collected from 340nm-450nm. For tryptophan recrystallized from CA solution, the solution was excited at 500nm. The spectra for material recrystallized from PBA exhibits the peaks from PBA indicating that PBA is incorporated into the crystal

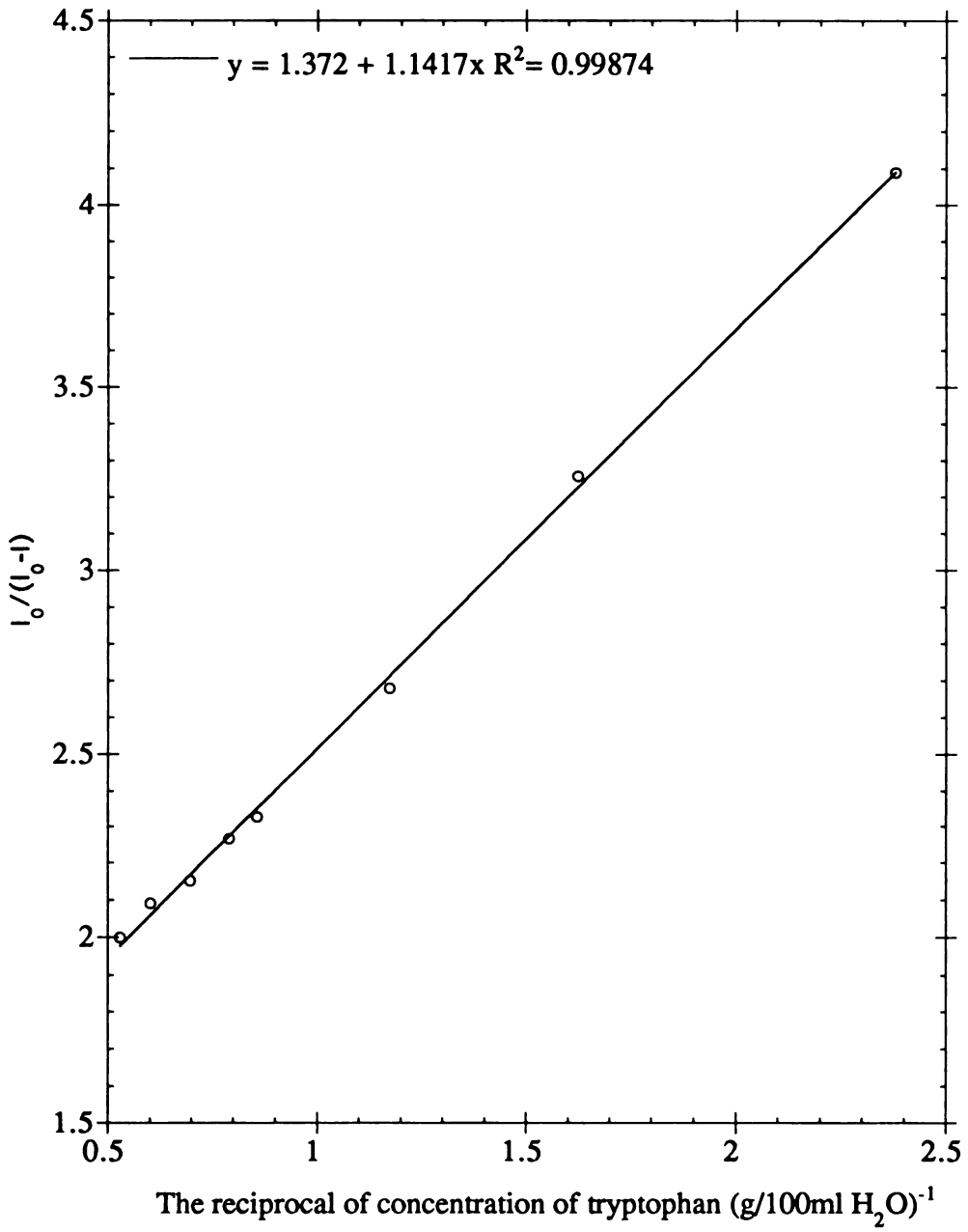

Figure 4.10 The quenching curve of tryptophan in aqueous solutions to CA at 595nm fit to $I_0/(I_0-I)=(1/[Q])(1/fKsv)+1/f$ at room temperature.

of tryptophan. Therefore, PBA can not be used to measure the supersaturation because it will contaminate the crystal product. Conversely, no fluorescence of CA is detected which tells us that CA does not go into the crystal of tryptophan.

4.4. Conclusion

Tryptophan will quench the fluorescence of PBA, but phenylalanine will not. This can be interpreted as the static quenching domain in the tryptophan quenching behavior. The formation of aggregates in high concentration solution reduce the quenching efficiency resulting in the downward curvature of the quenching plot.

However, PBA can incorporate into the lattice of the crystal of tryptophan which will contaminate the product; therefore, PBA can not be used as the probe to monitor the crystallization.

Carminic acid is an excellent potential probe for the food processing because it is a food additive. The fluorescence intensity of carminic acid at 595nm changes smoothly with the concentration of solutes. Monitoring the change of the intensity we can determine the concentration of the solution. It is shown that carminic acid will not go into the lattice of the tryptophan crystal. In conclusion, carminic acid can be used as *in situ* monitors to follow the crystallization of phenylalanine.

Tryptophan shows a quenching ability for CA and phenylalanine will enhance the fluorescence of CA by protecting CA from quenching by water. Only 73% of tryptophan can access CA which confirms that multiple molecule associates form among tryptophan molecules in tryptophan solution.

4.5. References

1 F. H. Quina and V. G. Toscano, *J. Phys. Chem.* **81**(18), 1750(1977)

2. M. Deumie, M. El Baraka and E. Quinones, *J. Photochem. Photobio, A: Chemistry*, **87**, 105-113(1995)

3. T. L. Netzel, Min Zhao, K. Nafisi, J. Headrick, M. S. Sigman and B. E. Eaton, *J. Am. Chem. Soc.,* **117**, 9119-9128(1995)

4. H. Stapelfeldt, J. Huang, and L. H. Skibsted, *Food Chemistry*, **48**, 1-11(1993)

5. M. J. Schwing-Weill, *Analusis*, **14**(6), 290-295(1986)

6. J. W. Mullin, *Crystallization*, Butterworth-Heinemann, Oxford, England(1993)

7. S. A. Tucker, W. E. Acree, JR., and M. J. Tanga, S. Tokita, K. Hiruta, and H. Langhals, *Applied Spectroscopy*, **46**(2), 229(1992)

8. M. U. Kumke, H. G. Lohmannsroben and Th. Roch, *Analyst*, **119**, 997(1994)

9. M. R. Eftink and C. A. Ghiron, *Biochemistry*, **15**(3), 672(1976)

10. J. R. Lakowicz, *Principles of Fluorescence Spectroscopy*, Plenum Press, New York and London(1983)

Chapter 5

MECHANISM OF PYRANINE FLUORESCENCE QUENCHING AND THE APPLICATION IN THE STUDY OF SUPERSATURATED SOLUTION

5.1. Introduction

Fluorescence quenching is a very useful method used to study both physical and biochemical phenomena (1-5). Fluorescence quenching experiments can yield valuable information about fluorophore and quencher interactions. The diffusion-controlled process of fluorescence quenching has been used to study various dynamic properties of aggregated systems of micelles and lipid vesicles (1). Quenching processes require the contact of quencher and fluorophore, so quenching measurements can reveal the accessibility of fluorophores to quenchers. By studying the interaction between the probe molecules and solute molecules, we can get insight about the organization of solute molecules. Therefore, fluorescence quenching is a potential technique to allow us to study the structure of supersaturation solution.

Crystallization takes place by the formation of a stable crystal nucleus from a homogeneous supersaturated solution first, then those nuclei will grow to form crystals. The formation of nuclei is the beginning point of the crystallization. The nucleation of solute must somehow depend upon the solute molecules in a supersaturated solution and also depend upon the various molecular interactions, such as solute-solute and solute-solvent interactions. Supersaturated solutions definitely have different structures from unsaturated solutions. Understanding of the structure of supersaturated solutions can help us in the control of industrial crystallization. Several studies have focused on the structure

of supersaturated solutions and many techniques have been applied, such as NMR, X-ray diffraction and Raman spectroscopy, and many theories about the structure of supersaturated solution have been proposed (6-10). Mullin and Leci suggested that solute clusters form in a supersaturated solution of citric acid by observing an isothermal column of a supersaturated solution of citric acid which generated a concentration gradient over period of several days. The concentration gradient developed as a result of the density difference between the clusters and the solution (6). Cussler observed different rates between cluster diffusion and molecular diffusion in many binary systems, which supported the cluster assumption (7). Myerson and co-workers observed the decrease in the diffusivities of urea and glycine solutions, which provided evidence for molecular aggregation (8). Hussman et al. and McMahon et al. also confirmed cluster formation on alkali nitrate solutions by using Raman spectroscopy (9,10). Although significant work has been done on structure study, there are still no generally accepted theories.

Previous research focused on studying high solubility systems with solubility exceeding 50wt%. No information about the organization of supersaturated solutions of lower solubility systems has been reported. A suitable method is needed to study lower solubility systems to get information about the organization of supersaturated solutions. The interaction between s solute and a probe can be studied by fluorescence quenching combined with the sensitivity of fluorescence spectroscopy which makes fluorescence quenching a possible technique for low solubility systems. Fluorescence quenching will be used to study the organization of supersaturated solutions in this research.

In this chapter fluorescence quenching of pyranine by tryptophan, phenylalanine, and nicotinic acid in aqueous solutions are studied to probe the organization of solutions. Tryptophan, phenylalanine and nicotinic acid showed different quenching behaviors which are the results of the different interactions between the pyranine and solutes. By interpreting the different quenching behaviors, insight into the organization of solution can be gained.

5.2. Theory

Fluorescence quenching involves a variety of processes, such as excited state reactions, excited state proton transfer, excited state electron transfer, energy transfer, complex formation and collision quenching (11). The quenching from diffusion-controlled encounters, the most common quenching process, is called dynamic quenching.

Dynamic quenching of fluorescence can be described by the Stern-Volmer Law (11)

$$\frac{I_0}{I} - 1 = K_{sv}[Q] \qquad (5.1)$$

I_0 is initial intensity without the quencher, I is emission intensity of single-emission wavelength with the quencher. K_{sv} is the Stern-Volmer quenching constant. Q is the concentration of quencher. If the mechanism of quenching is by dynamic quenching, a straight plot of I_0/I versus concentration of quencher will be obtained and the slope of the line is the Stern-Volmer quenching constant.

Static quenching is a frequent complicating factor in the analysis of dynamic quenching. Static quenching can be described by a ground state complex model or a sphere of action static quenching model. Ground state complex static quenching occurs as a result of the formation of a nonfluorescent ground state complex between the fluorophore and quencher. When this complex absorbs light it immediately returns to the ground state without emission of a photon (11). The sphere of action static quenching model for static quenching is described as "active sphere" which is the volume around a quencher molecule. The fluorophore is quenched without the need for a diffusion-controlled collision interaction if it is in the active interaction volume (12). In many instances the fluorophore can be quenched both by collisions and also by static quenching. The characteristic feature of the Stern-Volmer plots in such circumstances is an upward curvature, concave towards the y axis. In the ground state complex model the modified form of Stern-Volmer law I (11) can be expressed as

$$\frac{I_0}{I} = (1 + K_s[Q])(1 + K_d[Q]) \qquad (5.2a)$$

$$\frac{I_0/I - 1}{Q} = K_s + K_d + K_sK_d[Q] \qquad (5.2b)$$

K_s and K_d are the quenching constants of static and dynamic quenching respectively. When $K_s >> K_d$ static quenching is dominant or when $K_d >> K_s$ dynamic quenching is dominant, the Stern-Volmer quenching plot will follow a straight line. When there is no dominant form of quenching, which means K_s is very close to K_d, the Stern-Volmer plot will be upward, but the plot of $(I_0/I-1)/[Q]$ versus [Q] (equation 5.2b) should be a straight line. From the slope and intercept we can get static and dynamic quenching constants.

Birks (12) described the active sphere model using the modified Stern-Volmer Law II

$$\frac{I_0}{I}\exp(-V[Q]) = 1 + K_{sv}[Q] \qquad (5.3)$$

K_{sv} is the collision quenching constant, and V is the interaction volume or is called the static quenching constant which is related to the probability of finding a quencher molecule close enough to a newly formed excited state. A plot of $(I_0/I)\exp.(V[Q])$ versus Q by adjusting V should result in a straight line.

Downward curvature of the S-V plot was reported by Lakowicz (11), Eftink and Ghiron (13), Kikuchi and Sato (14) and by Pan and Cherry (15). Negative deviations from the Stern-Volmer Law are the results of multiple emitters with different quenching constants or inefficient quenching (11,13). Pan and Cherry pointed out that the downward curvature is the characteristic of the particular quenching effect. Also, downward curvatures can be the results of the heterogeneity of the system or selective quenching, such as different binding sites in large molecules which make some fluorophores easier to be quenched than others (16). The negative deviation from the Stern-Volmer law can be described by modified Stern-Volmer Law III (27).

$$\frac{I_0}{I_0 - I} = \frac{1}{fK_{sv}}\frac{1}{[Q]} + \frac{1}{f} \qquad (5.4)$$

f is the fraction of the fluorescence accessible to the quenching.

Different fits of the Stern-Volmer plot indicates the different quenching mechanism. By interpretation of the different quenching mechanisms we can infer the interaction of the probe and the solute and the organization of solution.

5.3. Materials and methods

Pyranine, also known as FDA D&C Green No. 8, was obtained from Lancaster, Windhamn, NH and used as received. Aqueous solutions of pyranine were prepared by dissolution of 0.026 g in 5ml HPLC grade water. Different concentrations of solutions were prepared by dissolving the appropriate amount of solutes in 5ml HPLC water. Supersaturated solutions were prepared by heating the solution in the water bath until all the solute was dissolved and subsequent cooling to room temperature. The solutions were used as prepared without any degassing.

Probe molecules were introduced by addition of five microliters of the pyranine solution to 5ml aqueous tryptophan and phenylalanine solutions resulting in a probe concentration of 10^{-5}M and 20 microliters of the pyranine to 5ml nicotinic acid aqueous solutions resulting in a probe concentration of $4x10^{-5}$M. Fluorescence spectra of the pyranine in the aqueous solutions were collected within two hours of the preparation the solutions. All spectra were collected at room temperature with a Spex 1681 Fluorolog spectrometer equipped with a Xenon lamp source and a PMT detector. A quartz sample holder was used in all cases. Spectra were recorded at a 1.00mm increment and an integration time of 1.0 sec. An excitation wavelength of 342nm for pyranine was used. The emission spectra were recorded over a range from 350-600nm for pyranine. Monochromator slits were at 0.5 mm.

Absorption spectra were collected by using a Perkin-Elmer Lambda Array 3840 UV/Vis Spectrophotometer. The absorption spectra of pyranine in water were recorded with HPLC water as the reference and the absorption spectra of pyranine in solution of tryptophan, phenylalanine and nicotinic acid were taken by using the same concentration of tryptophan, phenylalanine and nicotinic acid solutions as references.

5.4. Results

5.4.1. Tryptophan quenching of pyranine

The fluorescence spectra of pyranine in aqueous tryptophan solutions (Figure 2.3) exhibit no differences in shape and maxima in the presence and absence of tryptophan when the concentration of tryptophan is not very high although there is appreciable quenching, i.e. reduction in the intensity in the presence of tryptophan. When the concentration of tryptophan is very high, peaks around 400nm started losing their vibronic fine structure. No new fluorescence peak is observed at longer wavelengths indicating that no excimers or exciplex are formed.

The Stern-Volmer quenching curve of pyranine by tryptophan at 382nm is shown in Figure 5.1 and shown that when the concentration of tryptophan is low, the quenching response of tryptophan to pyranine is linear. With the increase of the concentration a maximum is reached and then the quenching plot curves downward.

With the addition of tryptophan in water, the fluorescence intensity at 510nm will increase compared with the intensity of pyranine in pure water. But with the increase of the concentration of tryptophan the fluorescence intensity of pyranine will decrease. Tryptophan quenches the fluorescence of pyranine but we can not fit the data by using a normal Stern-Volmer law because of the lower of I_0 than I. We just rearrange it as follows:

$$\frac{1}{I} = \frac{1}{I_0} + \frac{K_{sv}}{I_0}[Q] \qquad (5.5)$$

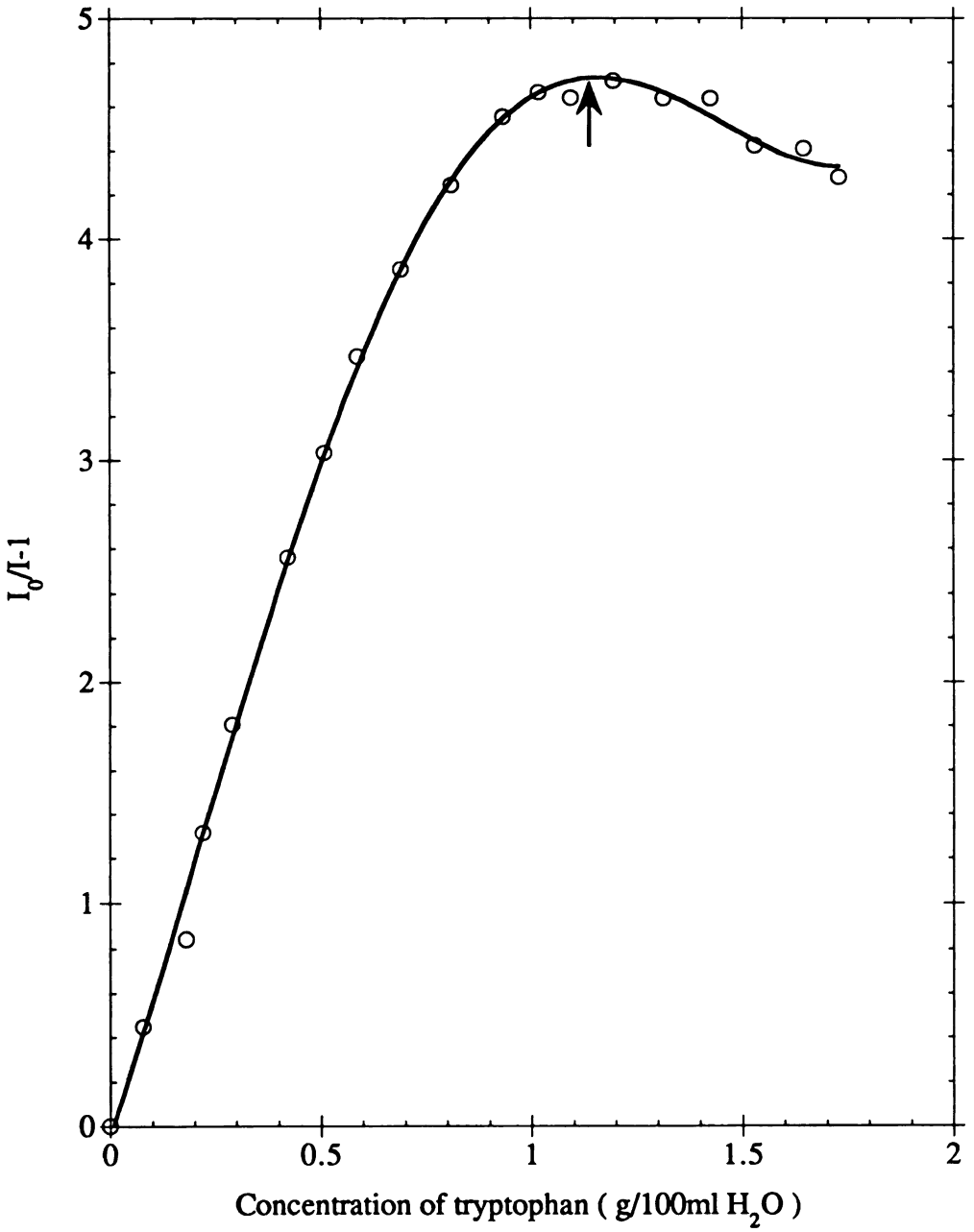

Figure 5.1. Quenching of pyranine(10^{-5}M) fluorescence at 382nm by tryptophan in aqueous solutions at room temperature fit to $I_0/I-1=K_{sv}[Q]$. The arrow shows the solubility of tryptophan at 25^0C.

In this case the intercept will be the reciprocal of initial intensity. The different initial intensity I_0 will not change the shape of the quenching curve. The only thing can be changed by initial intensity is the intercept which will not affect the interpretation of our results. The quenching of pyranine fluorescence at 510nm by tryptophan in aqueous solution can be fitted by using equation 5.5 and is shown in Figure 5.2. The upward curve shows up which tells us the quenching of pyranine by tryptophan at 510nm is coexisting of static and dynamic quenching.

5.4.2. Phenylalanine quenching of pyranine fluorescence

The fluorescence spectra of pyranine in phenylalanine aqueous solutions have the same shape and maximum as in tryptophan aqueous solutions and show no differences in shape and maxima in the presence and absence of phenylalanine at low phenylalanine concentration. No new fluorescence peak is observed at longer wavelengths indicating that no excimers or exciplex are formed.

The Stern-Volmer quenching curve of pyranine fluorescence at 382nm by phenylalanine is shown in Figure 5.3. The quenching curve deviated downward smoothly with the concentration of phenylalanine. The difference means that the quenching mechanism of pyranine by phenylalanine and by tryptophan was different. The quenching data were fitted to the modified Stern-Volmer Law III (Equation 5.4), and a straight line was obtained with intercept 1.37 and slope 1.30 (Figure 5.4). The intercept is the reciprocal of the fraction of the fluorescence accessible to the quenching. The fraction of phenylalanine accessible to pyranine is calculated as 72.8%. This value suggests there are only 73% of phenylalanine molecules accessible to pyranine and 27% of phenylalanine can not access pyranine. The quenching constant from the slope is 1.05. If we fit the quenching curve at 382nm by normal Stern-Volmer Law, the quenching constants of pyranine by phenylalanine can be obtained from the initial slope of the quenching curve which is 0.9.

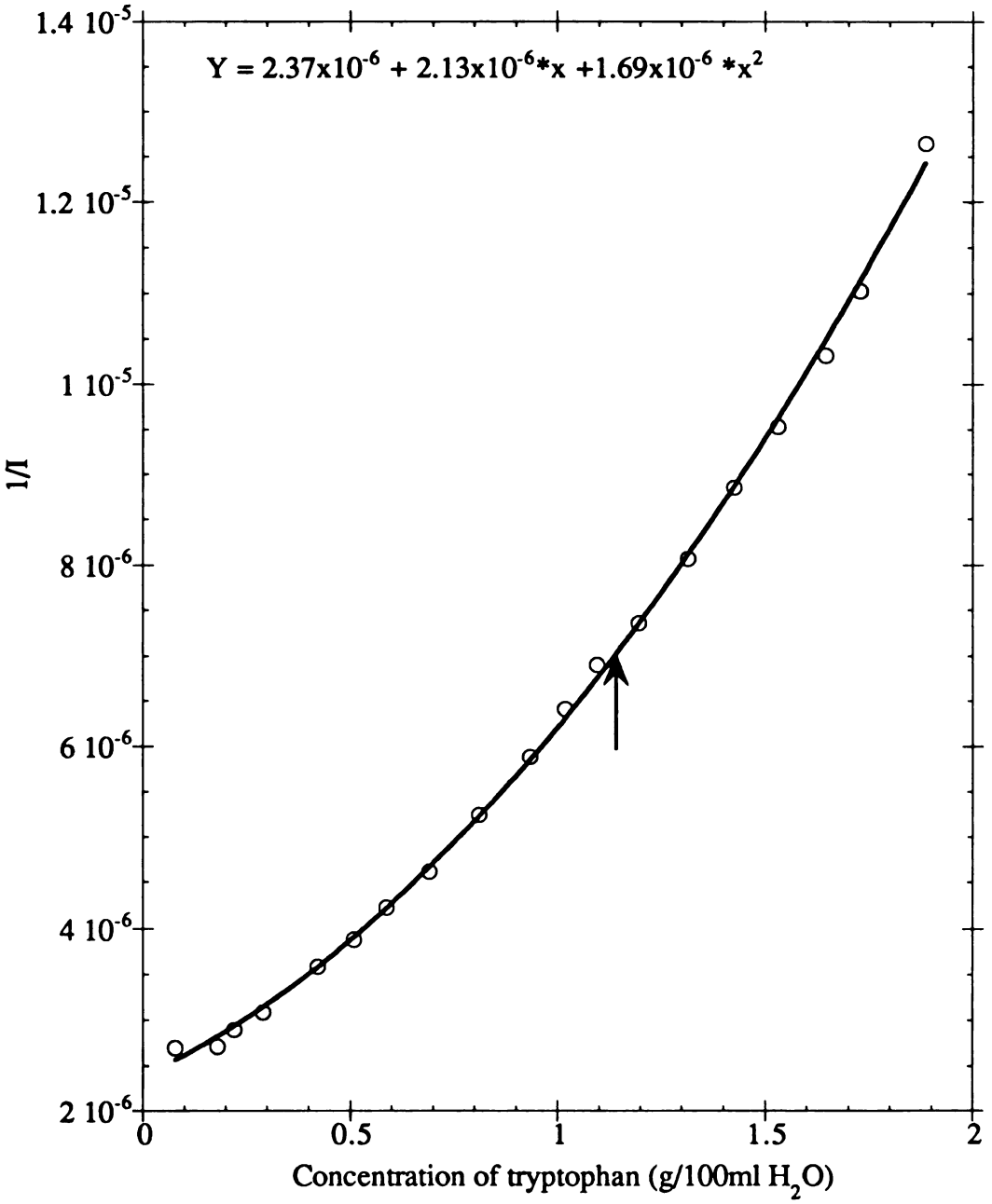

Figure 5.2 Quenching of pyranine fluorescence at 510nm by tryptophan in aqueous solutions at room temperature fit to $1/I=1/I_0+(K_{sv}/I_0)[Q]$.

The arrow indicates the solubility of tryptophan at 25^0C.

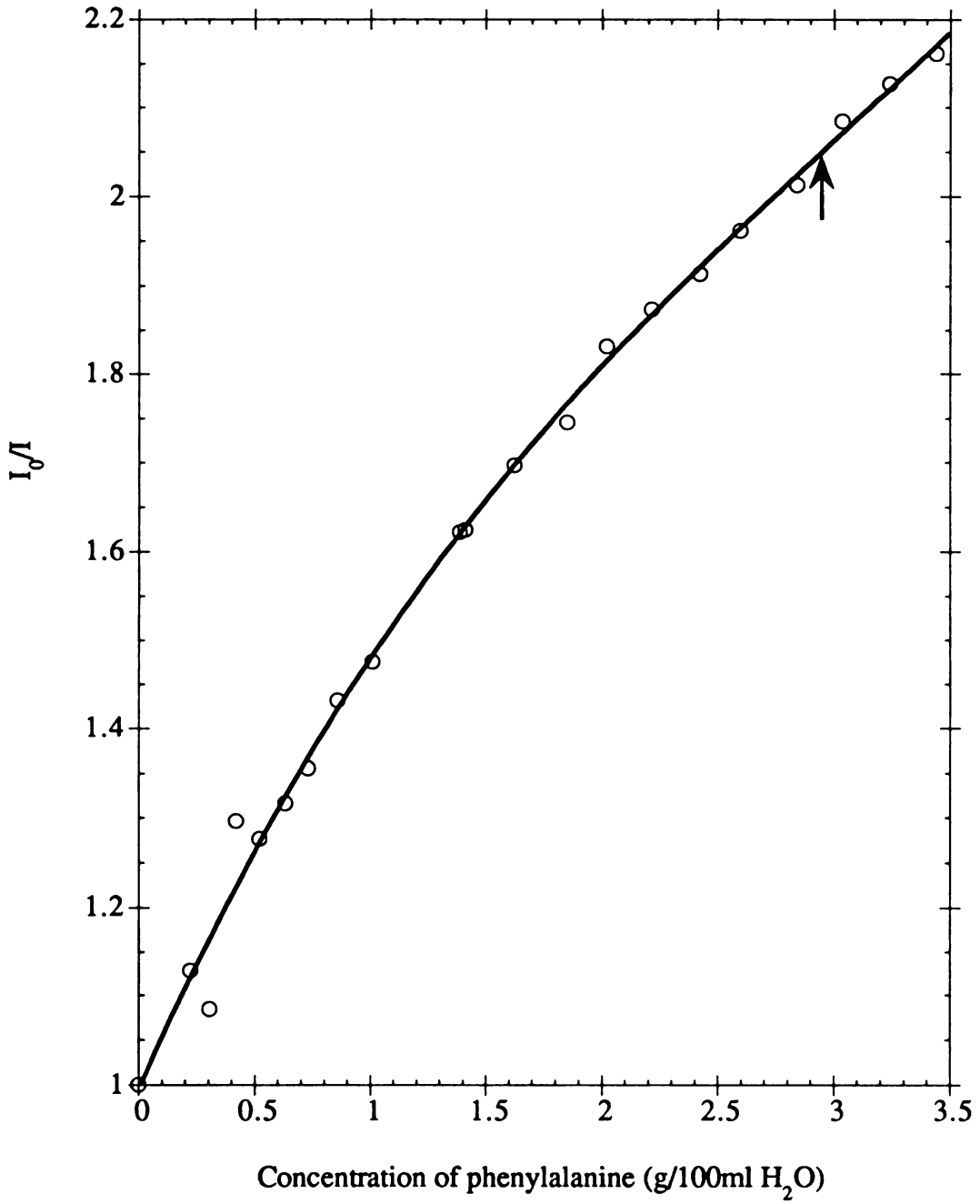

Figure 5.3 Quenching of pyranine fluorescence (10^{-5}M) at 382nm by phenylalanine in aqueouse solutions at room temperature. The arrow shows the solubility of phenylalanine. The curve is fit to $I_0/I-1=K_{sv}[Q]$.

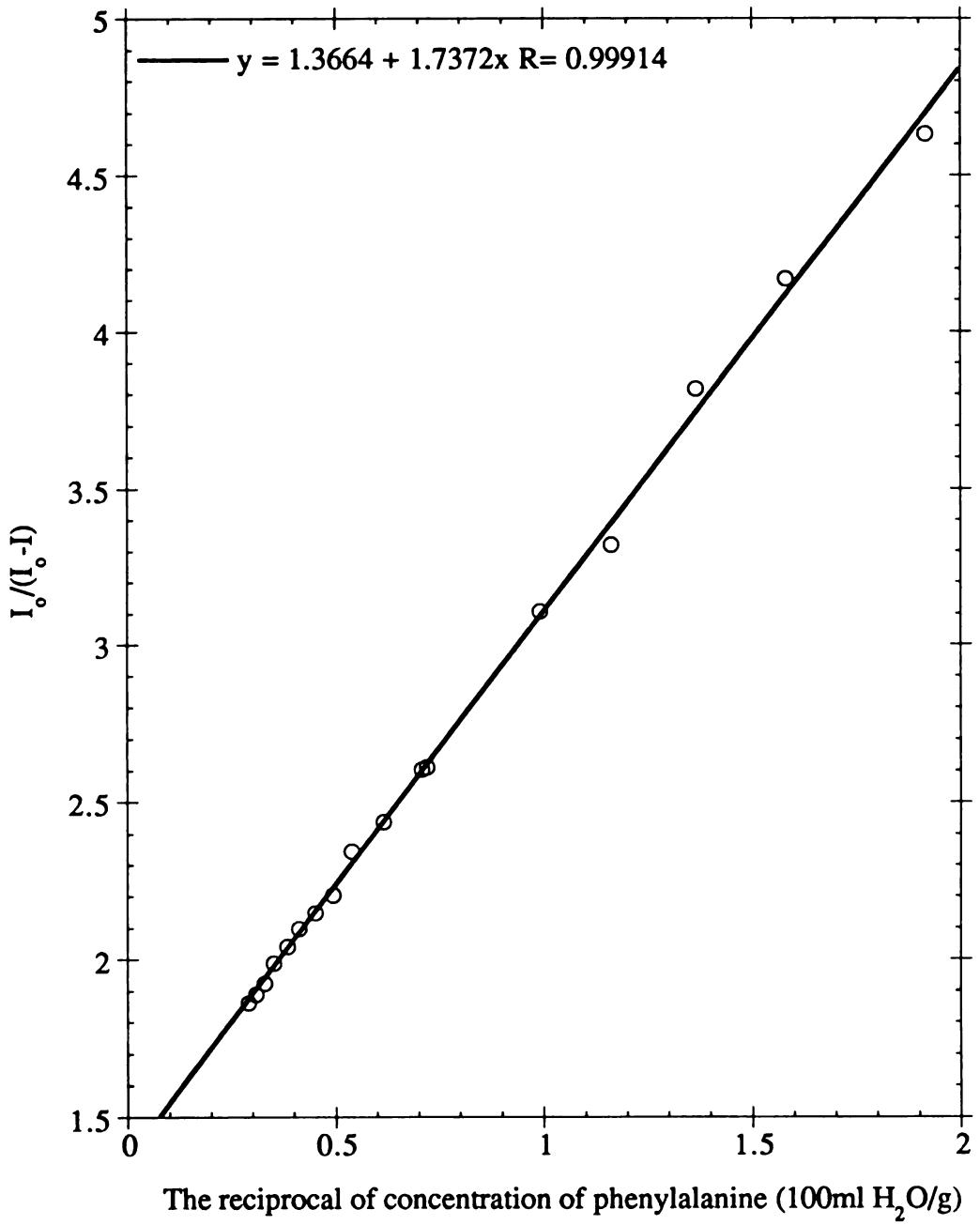

Figure 5.4. Quenching of pyranine fluorescence at 382nm by phenylalanine in aqueous solutions at room temperature fit to $I_0/(I_0-I)=(1/[Q])(1/fKsv)+1/f$.

5.4.3. Nicotinic acid quenching of pyranine fluorescence

The spectra of pyranine in nicotinic acid aqueous solutions have the same shape and maximum as in aqueous tryptophan solutions and show no differences in shape and maxima in the presence and absence of nicotinic acid although there is strong quenching in the presence of nicotinic acid. With the addition of nicotinic acid into pure water, the fluorescence intensity of pyranine decreased dramatically. The spectra were not excitation wavelength dependence. No new fluorescence peak is observed at longer wavelengths indicating that no excimers or exciplex are formed.

The Stern-Volmer quenching plot of pyranine fluorescence at 328nm by nicotinic acid curved upward (Figure 5.5) which was the evidence of coexistence of dynamic quenching and static quenching. The initial slope of Stern-Volmer plot was 11.6 ± 0.8.

Fitting the quenching data to the modified Stern-Volmer law I (equation 5.2) yields the plot of $(I_0/I-1)/[Q]$ versus [Q] shown in Figure 5.6. The quenching curve is a straight line at lower concentrations. Quenching constants obtained by using the straight part of the plot are 8.6 ± 0.9 and 1.6 ± 0.3. At high concentrations, the plot curves downward.

The quenching data were fitted to a modified Stern-Volmer law II $(I_0/I)\exp(-V[Q])$ versus [Q] (Figure 5.7). When the concentration of nicotinic acid was low we obtain a straight line with the slope 14.5 ± 0.8, the dynamic quenching constant and V=0.45, the static quenching constant.

The quenching plot of pyranine fluorescence at 510nm shows upward curvature (Figure 5.8). From the curve we can see two sets of data at different excitation wavelengths 342nm and 360nm overlapped each other which tells us the excitation wavelength does not affect the quenching behavior at 510nm.

Fitting data to the modified Stern-Volmer law I (Equation 5.2b) we can obtain plots which would still curve a little bit upward for both excitation wavelengths. Fitting data to the modified Stern-Volmer law II (Equation 5 3), we can see when the concentration of

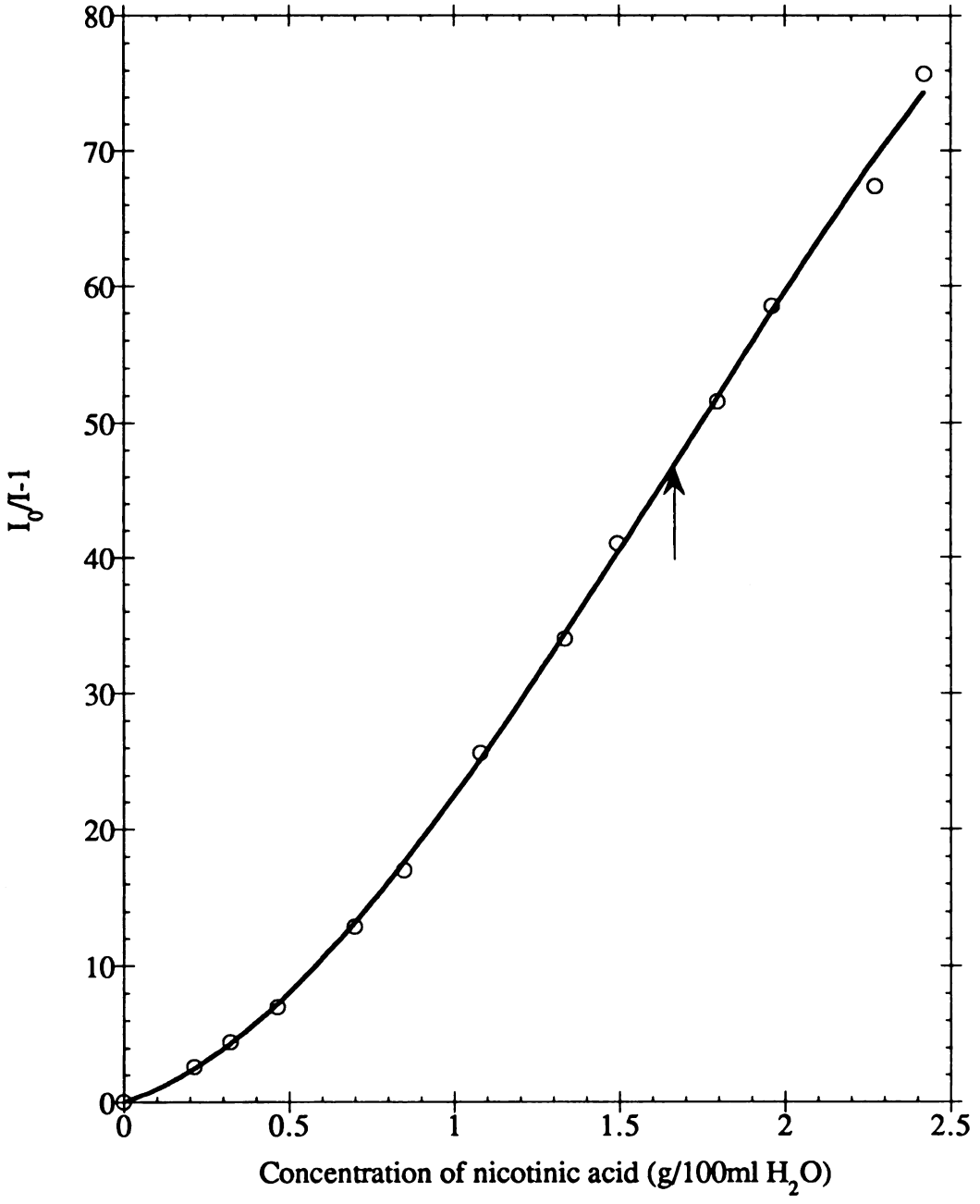

Figure 5.5 Quenching of pyranine fluorescence at 382nm by nicotinic acid in aqueous solutions at room temperature fit to $I_0/I-1=K_{sv}[Q]$.

The arrow indicates the solubility of nicotinic acid at 25^0C.

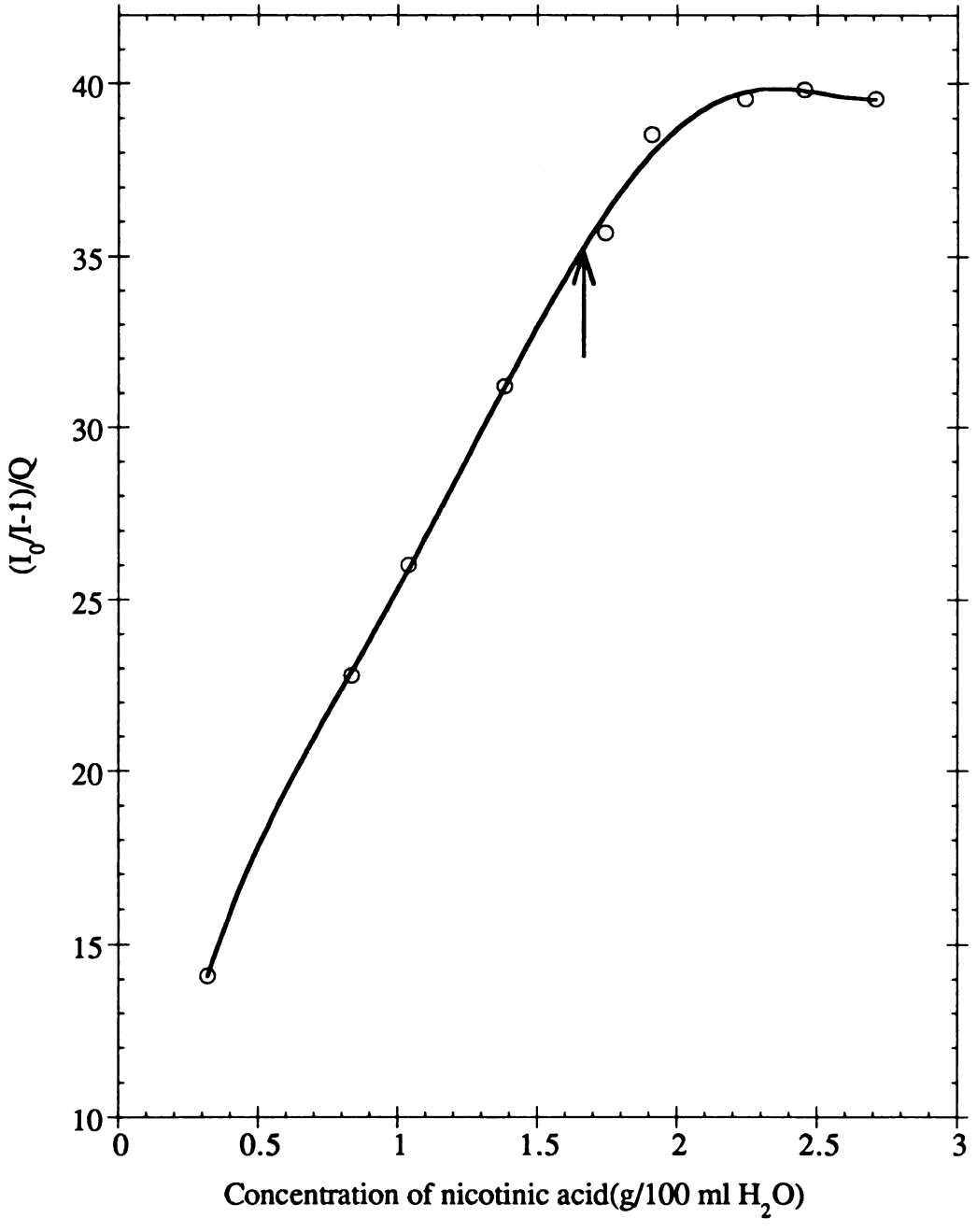

Figure 5.6. Quenching of pyranine fluorescence at 382nm by nicotinic acid in aqueous solutions at room temperature fit to $(I_0/I-1)/[Q]=K_1+K_2[Q]$.

Arrow indicates the solubility of nicotinic acid at 25^0C.

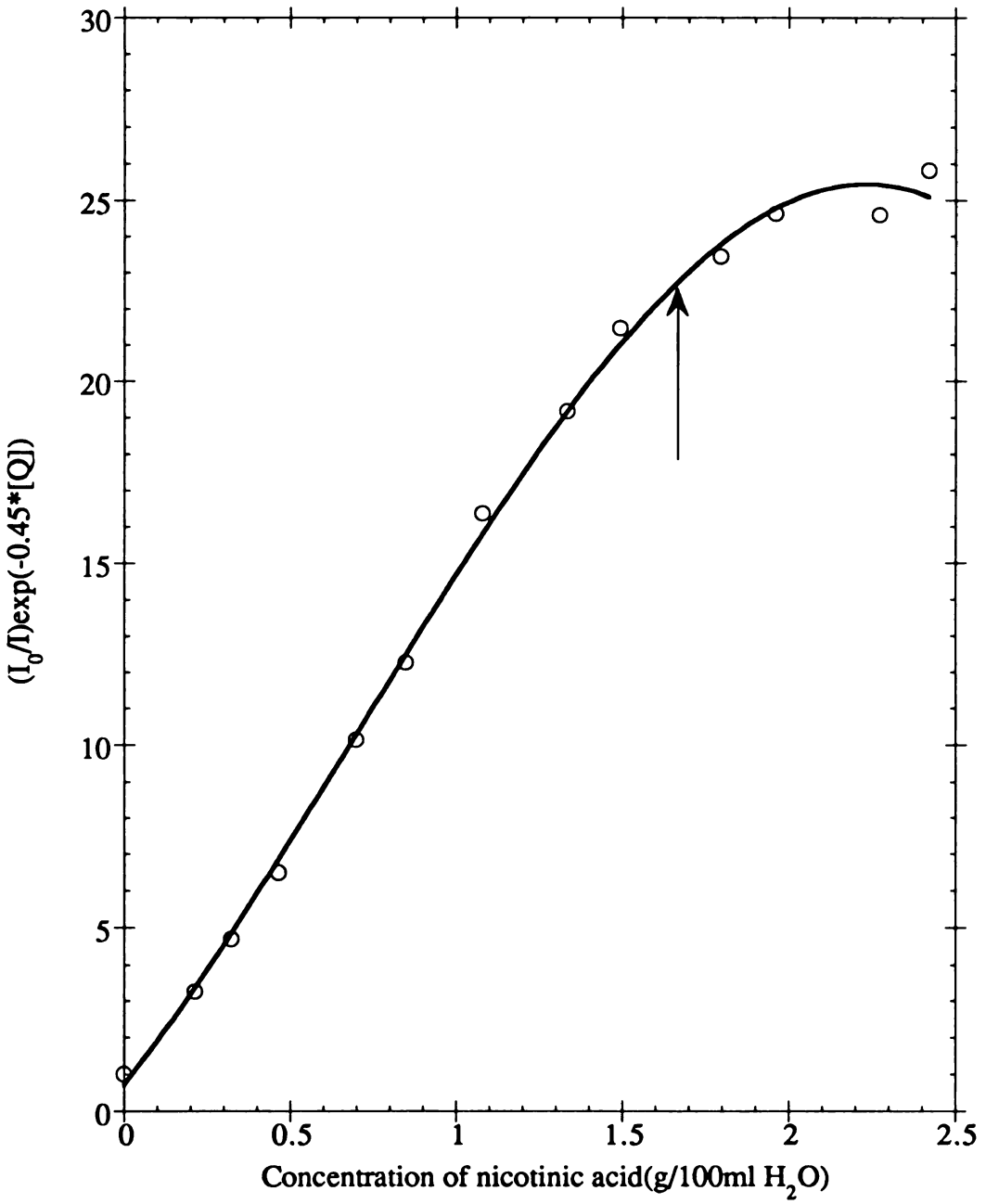

Figure 5.7 Quenching of pyranine fluorescence at 382nm by nicotinic acid in aqueous solutions at room temperature fit to $(I_0/I)\exp(-V[Q])=1+K_{sv}[Q]$

Arrow indicates the solubility of nicotinic acid at 25^0C.

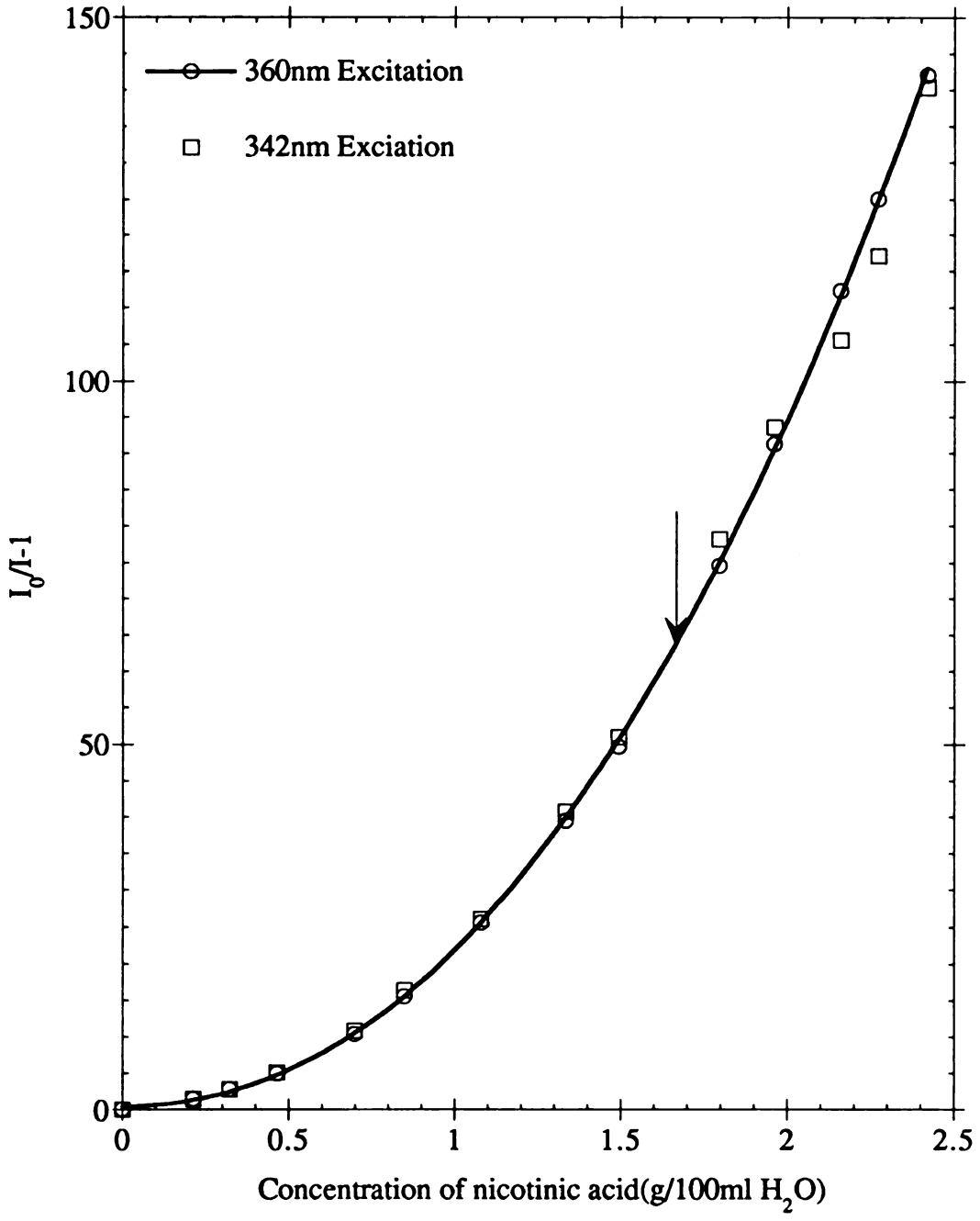

Figure 5.8 Quenching of pyranine fluorescence at 510nm by nicotinic acid at room temperature at different excitation wavelengths of 342nm and 360nm fit to $I_0/I-1=K_{sv}[Q]$. Arrow shows solubility of nicotinic acid.

nicotinic acid is low the quenching curves are straight lines with the slope 7.9 ± 0.2, the dynamic quenching constant, and V=0.9, the static quenching constant. When the concentration is high the plots curve downward. Quenching curves showed different behavior of unsaturated and supersaturated solutions.

5.4.4. The absorption spectra of pyranine in water and in solutions

The absorption spectra shown in Figure 5.9 showed that low wavelength bands 236nm and 246nm were missing by introducing tryptophan, nicotinic acid and phenylalanine and the broad band around 454nm was missing in the presence of tryptophan, phenylalanine and nicotinic acid too. Absorption bands at 282nm and 291nm were missing with the addition of tryptophan and nicotinic acid into solution.

5.5. Discussion

The structures of tryptophan, nicotinic acid and phenylalanine are shown in Figure 5.10. Tryptophan and phenylalanine are different only in the ring, one is benzene and the other is the indole ring which has a nitrogen heteroatom in a five member ring. Nicotinic acid is a six member ring with one nitrogen heteroatom in the ring. Both nicotinic acid and tryptophan have strong quenching ability for pyranine, which implies that the ring nitrogen contributed to the quenching of pyranine or a ground and/or excited state complex form through nitrogen in the ring.

The formation of a transient excited state complex or exciplex as an intermediate in the fluorescence quenching process was proposed by many workers (17-26). Such as exciplex can be emissive which will present broad and structureless emission spectra at longer wavelength (18). In many cases there were non-emissive exciplexes as involved in the excited state quenching. An exciplex is defined as a complex of simple integer stoichiometry formed between an excited molecule and one or more non-excited molecules(19). The formation of an exciplex is the result of intermolecular forces or

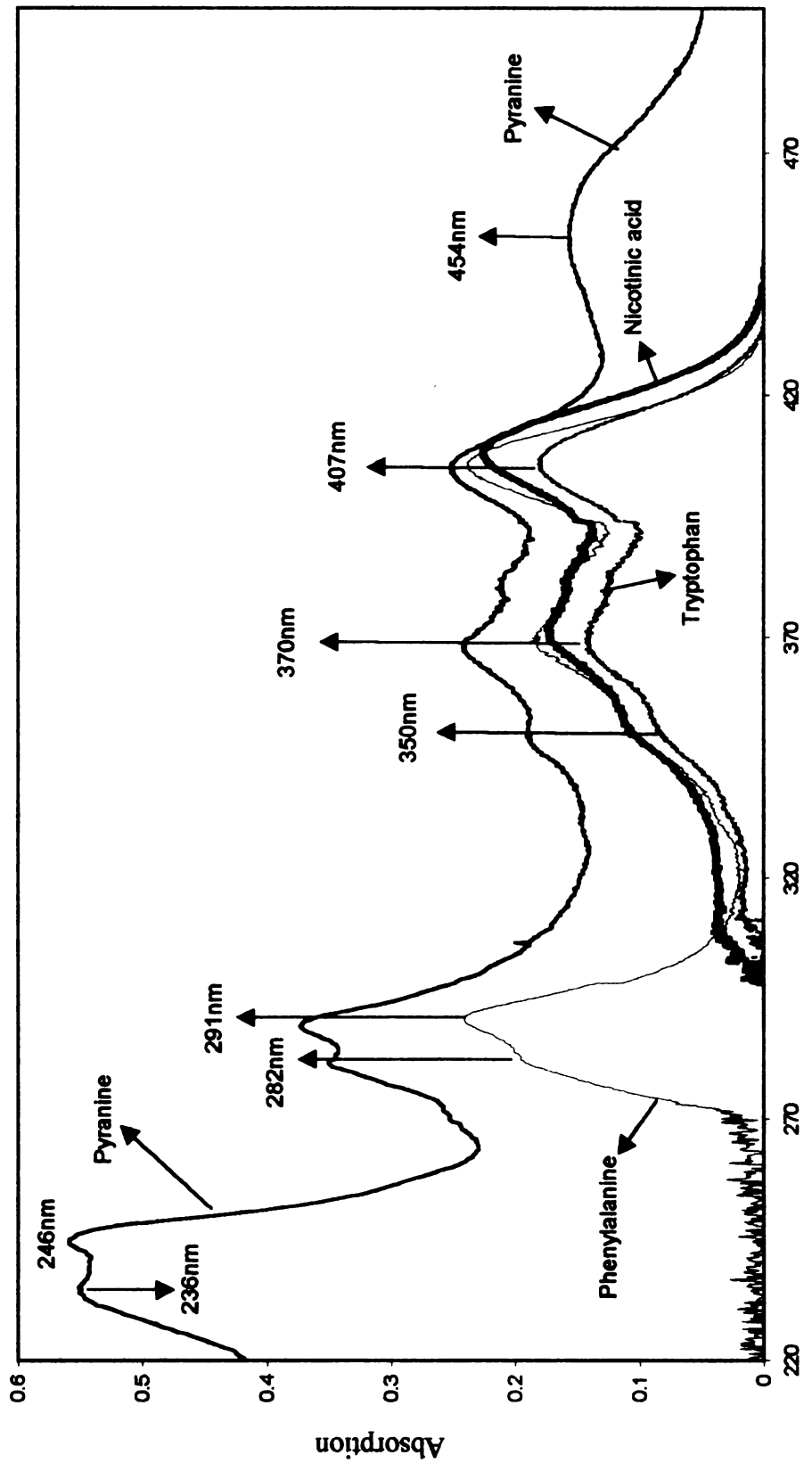

Figure 5.9. Absorption spectra of pyranine in water with water as reference and in tryptophan, phenylalanine and nicotinic acid aqueous solutions with the same concentration of solution as reference. The concentrations of all solutions are at solubility.

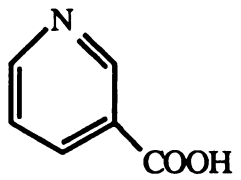

Nicotinic acid (NA) (1.67g/100ml H_2O)

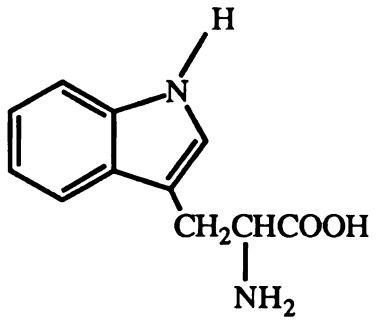

Tryptophan (Trp) (1.14g/100ml H_2O)

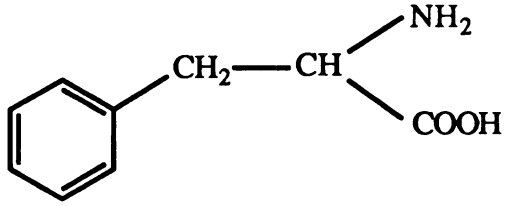

Phenylalanine (Phe) (2.96g/100ml H_2O)

Figure 5.10 The molecular structures of nicotinic acid, tryptophan and phenylalanine. Solubility in water at 25^{0}C is given in parentheses

Van der Waals interactions which have an electromagnetic origin and arise in a variety of ways such as dipole-dipole, polarizability-dipole, polarizability-polarizability and dispersion interactions. Hydrogen bonding interaction is often cited as an efficient quenching mechanism by charge transfer or electron transfer via the hydrogen bond or by proton transfer (20). The orbital overlap interactions play an important role in the correct exciplex geometry and also help to stabilize the exciplex but they can not become a dominant factor for the formation of exciplex (19).

Pyridine which has the same structure as nicotinic acid except the carboxyl group in nicotinic acid was reported to be a strong fluorescence quencher to many fluorophores such as 1-pyrenol, 2-naphthol, 1-aminopyrene and 13H- and 7H-dibenzocarbazole which was suggested as hydrogen bonding interaction between pyranine and fluorophore in the hydrogen bonded complex (20).

The strong quenching ability of nicotinic acid and tryptophan for pyranine comes from the hydrogen bonding with pyranine. Amines are shown to be very efficient quenchers of aromatic molecules because they are organic electron donors (21). Amines can form a hydrogen bonding complex with pyranine in the ground state. But the fluorophore-quencher interaction did not change the absorption and fluorescence spectral properties, because the ground-state complex formed between pyranine and tryptophan or nicotinic acid were not sufficiently stable owing to weak interaction and the exciplexes are non emissive species. We are able to tell there are ground state complexes because the absorption spectra bands shown in Figure 5.7 show a small red shift for tryptophan, and a larger red shift for nicotinic acid, which tell us the stabilization of the excited state will be improved due to the hydrogen bonding interaction. With the addition of nicotinic acid and tryptophan all peaks at lower wavelengths disappear. Those lower peaks can be assigned to some structure of pyranine with water molecules. The absence of those peaks is due to the formation of a complex of pyranine with nicotinic acid and tryptophan which will destroy the structure of pyranine with water. At our experimental conditions (pH~7 and

low concentration of acid) pyranine (pK_a=7.5) will exist as a protonated species. This protonated species will form a hydrogen bonding complex with tryptophan and nicotinic acid. When pyranine is excited, the proton transfer will take place between pyranine and amine due to the low pK_a (0.5) in the excited state. The excited energy will be lost by proton transfer then will quench the fluorescence of pyranine. The mechanism of quenching, including both the ground state complex and exciplex, is summarized in the scheme shown in Figure 5.11.

The Stern-Volmer plot of tryptophan-pyranine is a straight line when the concentration of tryptophan is low. With the increase of the concentration of tryptophan the Stern-Volmer plot curves downward. Negative deviations from the Stern-Volmer Law are the results of multiple emitters with different quenching constants or inefficient quenching (11,13) or many possible quenching mechanisms existing at the same time. Kikuchi and Sato (14) showed in their paper that the quenching curve of oxygen sometimes would deviate downward from a straight line when the concentration of oxygen was high which was reported as the evidence for exciplex formation. Negative curvatures of the plots in the pyranine-tryptophan system is the result of the two or three dimensional structure among tryptophan molecules which can be proved by the excitation dependence of tryptophan fluorescence (see chapter 7 for details). In pH range 4-8 the predominate species of tryptophan is the zwitterion $^{+}H_3NRCOO^{-}$, so the Coulombic interaction and/or hydrogen bonding between two or more zwitterions can form chain structures or a three dimensional structure such as

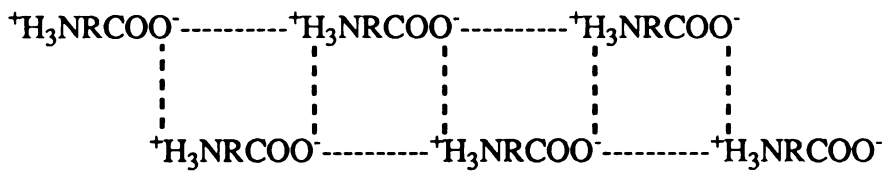

We refer these two or three dimensional structure as associates.

The effective concentration of quenchers will not be directly proportional to true concentrations because the molecules in the center of the associates could hardly contact

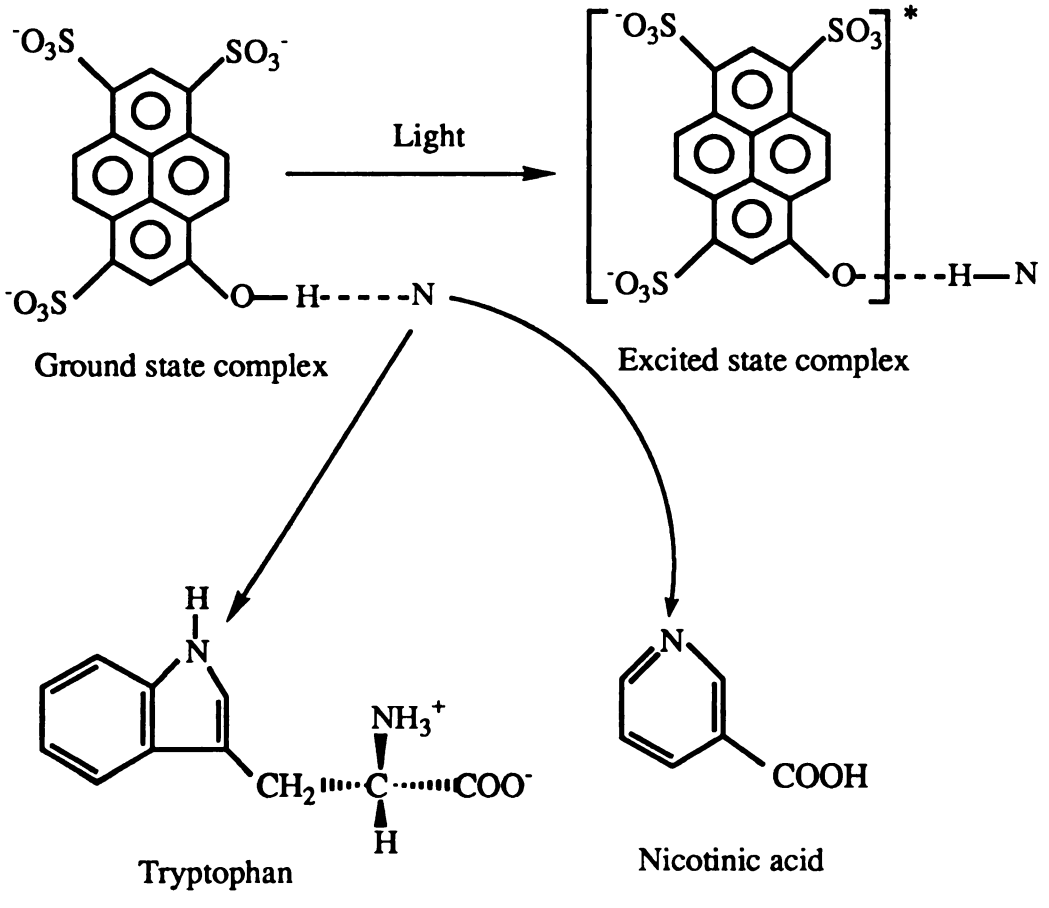

Figure 5.11 Scheme of quenching mechenism of pyranine by amine in tryptophan and nicotinic acid ring through hydrogen bonding complex at ground and excited state

with pyranine, making the quenching by dynamic encounter inefficient. Quenching by diffusion was also inhibited due to the larger size of associates. The Stern-Volmer plot should curve upward with the coexistence of static quenching and dynamic quenching. The coexistence of dynamic quenching and static quenching appear in the pyranine-tryptophan system which can be seen from the quenching plot of fluorescence at 510nm shown in Figure 5.2. The associates causes the downward curvature and coexistence of dynamic and static quenching causes an upward curve. These two effects cancel each other to result in a straight quenching plot of pyranine fluorescence at 382nm at low concentration of tryptophan. We notice the difference of quenching curves between 510nm and 382nm. The emission at 510nm is from the deprotonated form PyO^-. The hydrogen bonding occurs at the hydroxyl group, so the hydrogen bonding complex will affect the emission of PyO^- much more. The emission at 382nm is the result of general $\pi \leftrightarrow \pi^*$ polycyclic aromatic hydrocarbon (PAH) transmission. The hydrogen bonding complex will not affect the 382nm emission as much as the 510nm emission resulting in more static quenching effects in the quenching of pyranine at 510nm. Also the hydrogen bonding between tryptophan and pyranine is not as strong as the bonding between pyranine and nicotinic acid, which explains why the quenching plots show the similar upward curves at 382nm and 510nm in nicotinic acid solutions.

When the concentration of tryptophan is high, a different situation exists. Aggregates will form in the solution at high concentration of tryptophan. As we know at high concentration in high solubility systems, the observation of a concentration gradient was taken as the evidence of the formation of aggregates in solution (6). In low solubility systems, the concentration gradient will not be noticeable. The much lower quenching ability occurs at very high concentration which implies the formation of aggregates in a low solubility system such as tryptophan solutions. The aggregates will have much less ability to quench fluorescence of pyranine due to their relatively large size which reduces diffusion. Some of the molecules in the middle of aggregates can not contact with pyranine

which is the requirement for the quenching, therefore, quenching plots will curve downward.

The similar associates should appear in the phenylalanine solutions. But phenylalanine does not have a cyclic amine in its structure, so there is no hydrogen bonding complex between pyranine and phenylalanine. It is reasonable for us to infer the formation of a contact complex between pyranine and phenylalanine because they both have benzene rings. Phenylalanine will like pyranine better than phenylalanine likes water. The missing of two lower peaks in adsorption spectra of pyranine with the addition of phenylalanine shows that phenylalanine destroys the structure of pyranine with water. The interaction is not as strong as tryptophan so only two peaks disappear. The contact complex between pyranine and phenylalanine is not strong enough to quench fluorescence of pyranine effectively. Quenching requires the contact of fluorophores and quenchers. Some molecules in the middle of associates can not contact with pyranine even they can diffuse to pyranine during lifetime. The data fit to the modified Stern-Volmer law III (Equation 5.4) shown in Figure 5.4 shows only 73% of phenylalanine were accessible to pyranine. These 27% of phenylalanine that could not reach pyranine may be in the middle of associates or may be too big to effectively diffuse to pyranine.

The higher concentration of tryptophan and phenylalanine, the more the associates present, and the more downward the quenching plot would curve. When the concentration was very high almost all molecules are involvec in the formation of associates or aggregates which makes the quenching much more inefficient and the curve would go down instead of curving down.

The higher quenching ability of nicotinic acid to pyranine is because nicotinic acid can not form associates among molecules. When the concentration of nicotinic acid was low all the single molecules were good quenchers. Some of them which were far from fluorophores would diffuse to pyranine, meet pyranine and quench fluorescence. Other molecules would form a hydrogen bonding complex with pyranine and they would quench

pyranine by proton transfer from excited pyranine to nicotinic acid. Both dynamic quenching and static quenching exist at the same time which result in the upward Stern-Volmer plot. At the 510nm emission fitting to the modified Stern-Volmer I (equation 5.2) still results in an upward curve. So we can tell how strong the static quenching is. The red shift of adsorption spectra of pyranine in nicotinic acid solutions provides the evidence of the formation of ground state complex between pyranine and nicotinic acid. The ground state complex model can better explain the quenching behavior of pyranine fluorescence by nicotinic acid also.

When the concentration of nicotinic acid was high the quenching was not as effective as for lower concentrations. Thus, the quenching curve would not follow the same trend. We can interpret this result as aggregate formation which makes the diffusion of molecules more difficult, then the dynamic quenching was restrained. Also the formation of aggregates inhibited the formation of the complex between pyranine and nicotinic acid, so the static quenching was restrained too.

The higher quenching ability of nicotinic acid can be because it does not have a benzene ring beside the amine, so less spatial hindrance occurs for the formation of the complex between pyranine and nicotinic acid as compared to tryptophan. The complex between pyranine and nicotinic acid is more stable than the complex between pyranine and tryptophan. The proof comes from the absorption spectra which show a larger red shift in nicotinic acid solutions as compared to the red shift in tryptophan solutions.

In all three systems the discontinuity occurs in the quenching plots at high concentration. All quenching curves will curve downward at high concentration of solutes. We can interpret this result as the different structure of supersaturated solutions and unsaturated solutions. The structure of supersaturation solutions is always an interesting topic since the supersaturation is the starting point for crystallization. But in very few cases the discontinuity of physical properties on concentration have been observed. In our quenching study, the quenching plot changes at high concentration in all cases. The change

of quenching shows the different quenching behavior of low and high concentration. High concentration solutions show weaker quenching ability. This phenomenon is taken as a evidence of the formation of aggregates at high concentration. So we can conclude aggregates will form in the low solubility system as in the high solubility system at high concentration. Especially in tryptophan solutions, the zwitterion form will help the formation of aggregates, so the change of the quenching plots is really dramatic. At high concentration the plot will go down with the increase of concentration (Figure 1). In nicotinic acid the quenching plot will just curve downward at high concentration to indicate the formation of aggregates.

The fluorescence quenching technique is a very easy and simple method. However, the quenching studies can be performed with a great degree of precision and get very important information about the organization of solutes.

5.6. Conclusion

Fluorescence quenching is a useful tool for studying solute behavior. Different quenching behaviors of tryptophan, phenylalanine and nicotinic acid to pyranine indicate the differences of the host-probe interaction. The differences come from different structures of tryptophan, phenylalanine and nicotinic acid. Nicotinic acid and tryptophan will form a hydrogen bonding complex with pyranine for both ground and excited state due to the electron deficiency of amine. Aggregates are proposed in the supersaturated solution which are the reason for the discontinuity of the quenching curves.

5.7. References

1. H. G. Marcelo, and F. C. De Schryver, *Chem. Rev.*, **93**, 199(1993)

2. F. S. Abrams, and E. London, *Biochemistry*, **31**, 5312(1992)

3. K. Kachel, E. Asuncion-Punzalan, and E. London, *Biochemistry*, **34**, 15475(1995)

4. C. Peviani, W. Hillen, N. Ettner, H. Lami, S. M. Doglia, E. Piemont, C. Ellouze, and M. Chabbert, *Biochemistry*, **34**, 13007(1995)

5. M. R. Eftink, and C. A. Ghiron, *Biochemistry*, **15**(3), 672-680(1976)

6. J. W. Mullin, and C. L. Leci, *Phil. Mag.*, **19**(1969)

7. E. L. Cussler, *AIChE J.* **26**(1), 43 (1980)

8. L. S. Sorrel, and A. S. Myerson, *AIChE J.*, **28**(5), 772(1982)

9. G. A. Hussman, M. A. Larson, and K. A. Berglund, *Industrial Crystallization '84* S. J. Jancic, and E. J. DeJong, Eds. Elsevier, Amstrdam (1984)

10. P. M. McMahon, K. A. Berglund, and M. A. Larson, *Industrial Crystallization '84*, Jancic, S. J. and DeJong, E. J. Eds. Elsevier, Amstrdam (1984)

11. J. R. Lakowicz, *Principles of Fluorescence Spectroscopy*, Plenum Press, New York and London(1983)

12. J. B. Birks, *Photophysics of Aromatic Molecules*, New York, Wiley-Interscience(1970)

13. M. R. Eftink and C. A. Ghiron, *Anal. Biochem.* **114**, 199(1981)

14. K. Kikuchi, C. Sato, M. Watabe, H. Ikeda, Y. Takahashi and T. Miyashi, *J. Am. Chem. Soc..*, **115**, 5180(1993)

15. Rui-jun Pan and Richard J. Cherry, *Biochemistry*, **34**, 4880(1995)

16. M. R. Eftink and C. A. Ghiron, *Biochemistry*, **15**(3), 672(1976)

17. D. Goswami, R. S. Sarpal and S. K. Dogra, *Bull. Chem. Jpn.*, **64**, 3137(1991)

18. H. Pal, D. K. Palit, T. Mukherjee and J. P. Mittal, *Chem. Phys. Letts.* **173**, 354(1990)

19. *Photochem. Photobio*, **27**, 819(1978)

20. H. Miyasaka, A. Tabata, S. Ojima, N. Ikeda and N. Mataga, *J. Phys. Chem.* **97**, 8222(1993)

21. M. Mac, J. Najbar and J. Wirz, *Chem. Phys. Letts.*, **235**, 187(1995)

22. A. Sharma, O. S. Wolfbels and M. K. Machwe, *Anal. Chim. Acta*,

230, 213(1990)

23. St. L. Logunov and M. A. Rodgers, *J. Phys. Chem.*, **96**, 2915(1992)

24. U. Graf, H. Niikura, and S. Hirayama, *J. Phys. Chem.* A, **101**, 1292(1997)

25. E. M. Talavera, B. Quintero and J. M. Alvarez,
J. photochem. Photobiol. A: Chem., **66**, 171(1992)

26. H. Pal, D. K. Palit, T. Mukherjee and J. P. Mittal,
J. Chem. Soc. Faraday Trans., **89**(4), 683(1993)

27 M. Tabak, G. Sartor, P. Neyroz, A. Spisni and P. Canatorta,
J. *of Luminescence*, **46**, 291-299(1990)

Chapter 6

QUENCHING STUDY BY MEASUREMENT OF LIFETIME OF PYRANINE IN DIFFERENT SOLUTIONS

6.1 Introduction

Time-resolved fluorescence is a powerful optical spectroscopic technique for monitoring the dynamics of macromolecular interactions in solution and a useful tool to study the interactions of solute and solvent (1-4). A wealth of information about the organization and dynamics of solvent-solute interactions in the microenviornment of a probe molecule can be obtained by studying the relaxation processes on a variety of time scales. Time-resolved techniques are able to directly separate and quantify the relevant fluorescence parameters that contribute to the steady-state emission parameters. The emission lifetime of a probe molecule is highly sensitive to the solvation. The measurement of lifetime can determine static and dynamic conformational information about macromolecules, make state assignments, and provide information on the solvent polarity as well as diffusive processes such as collision quenching and proton transport. The use of time resolved fluorescence methods to investigate the microscopic interactions between the solvent and solute and the crystallization behavior should result in a more directed and rational approach to understand and control the crystallization.

Frequently, materials having very similar spectra can have greatly different lifetimes which can be used to identify different materials. The lifetime is defined as the time required for the population of the excited state to decrease to 1/e of its original value after

the excitation source is turned off. Lifetime measurements have become an indispensable tool in the physical and biological sciences (4).

Fluorescence quenching is another very useful method used to study both physical and biochemical phenomena (5-9). Fluorescence quenching experiments can yield valuable information about fluorophore and quencher interactions. The quenching from diffusion-controlled encounters is called dynamic quenching. Dynamic quenching is very common in the bimolecular systems. Fluorescence of fluorophore can be quenched by collisional processes between fluorophore and quencher. The dynamic quenching can be expressed as Stern-Volmer Law

$$I_0/I-1=K_{sv}[Q] \qquad (6.1)$$

Static quenching is a frequent complicating factor in the analysis of dynamic quenching. When the fluorophore and quencher are close enough, the fluorescence can be quenched immediately on excitation. Static quenching decreases the emission intensity but has no effect on the lifetime of the unassociated excited fluorophores. In order to distinguish dynamic quenching and static quenching we use the lifetime form of the Stern-Volmer Law to describe dynamic quenching

$$\tau_0/\tau-1=K_{sv}[Q] \qquad (6.2)$$

τ_0 is the lifetime of fluorophore without quencher, and τ is the lifetime with quencher.

The two plots should be indistinguishable if the simple diffusional quenching model holds. The discrepancies between the I and τ Stern-Volmer plots can supply useful chemical information. There are, however, times when only τ data can be used conveniently. These include situations in which the quencher absorbs intensely in the region of excitation and/or emission. Under these conditions, trivial absorption can produce unacceptable distortions of intensity quenching data unless complicated, and frequently unreliable, corrections are applied.

The coexistence of static quenching and dynamic quenching will result in upward, nonlinear Stern-Volmer plots. It can be described as

$$\frac{I_0/I - 1}{Q} = K_s + K_d + K_s K_d[Q] \qquad (6.3)$$

Where K_s and K_d are the static and dynamic quenching constants respectively.

Static quenching does not affect the lifetime Stern-Volmer plot. Therefore from lifetime quenching data we can get the dynamic quenching constant, then the static quenching constant can be obtained readily.

Chapter 5 focused on steady state quenching of pyranine fluorescence by solutes in aqueous solutions. In this chapter more attention will be given to the dynamic quenching study by lifetime measurements with pyranine as probe in solutions of tryptophan, phenylalanine and nicotinic acid to investigate the interaction between the host system and probe. Some steady state fluorescence quenching will be shown as a comparison to the time resolved results.

6.2 Materials and methods

Pyranine, also known as FDA D&C Green No. 8, was obtained from Lancaster, Windharn, NH and used as received. Aqueous solutions of pyranine were prepared by dissolution of 0.026 g in 5ml HPLC grade water. Different concentration of solutions were prepared by dissolving the appropriate amount of solutes in 5ml HPLC water. Supersaturated solutions were prepared by heating the solution in the water bath until all the solute was dissolved and subsequent cooling to room temperature. The solutions were used as prepared without any degassing.

Probe molecules were introduced by addition of five microliters of the pyranine solution to 5ml aqueous tryptophan and phenylalanine solutions resulting in a probe concentration of 10^{-5}M and 20 microliters of the pyranine to 5ml nicotinic acid aqueous solutions resulting in a probe concentration of $4x10^{-5}$M for the lifetime measurement at

510nm. For the lifetime measurement at 382nm, 25 microliters of pyranine solutions were added into tryptophan solutions and phenylalanine solutions and 150 microliters of pyranine were added into nicotinic acid solutions to compensate for the weaker fluorescence at 382nm. Lifetime measurements of pyranine in the aqueous solutions were collected within several hours of the preparation the solutions. All lifetimes were measured by using the single photon counting time correlated method with PMT as the detector and a YAG laser with LDS 698 dye as excitation light source. The excitation wavelength was 342nm and emission wavelengths were 382nm and 510nm. The other conditions were high voltage 3200v, TAC range 100ns, power 120mw/cavity dump.

6.3 Results and Discussion

6.3.1. Fluorescence lifetime quenching of pyranine in different solutions at 510nm

The decay curve of pyranine is fit to a first order kinetic processes. The lifetimes of pyranine in different concentrations of tryptophan, phenylalanine and nicotinic acid were measured by using the single photon counting technique. The results show that the fluorescence lifetime of pyranine in tryptophan solutions will decrease with the increase in the concentration of tryptophan. The same decrease of lifetime was observed in nicotinic acid solutions. Conversely, the lifetime of pyranine in phenylalanine solutions increased with increased concentrations of phenylalanine. The decrease of the lifetime with the increase of concentrations is due to the fluorescence quenching of pyranine by tryptophan and nicotinic acid. The increase of lifetime of pyranine with the increase of concentration of phenylalanine is due to the protection of pyranine from quenching by water. Water quenching fluorescence by proton transfer has been proven by the isotope effect (10,11).

Lifetime Stern-Volmer quenching curves are shown in Figures 6.1 and 6.2 for tryptophan and nicotinic acid, respectively. The quenching of pyranine by phenylalanine at 510nm for steady state and lifetime Stern-Volmer Law are shown in Figure 6.3. In tryptophan solutions the plot is linear at lower concentration and then curved downward at

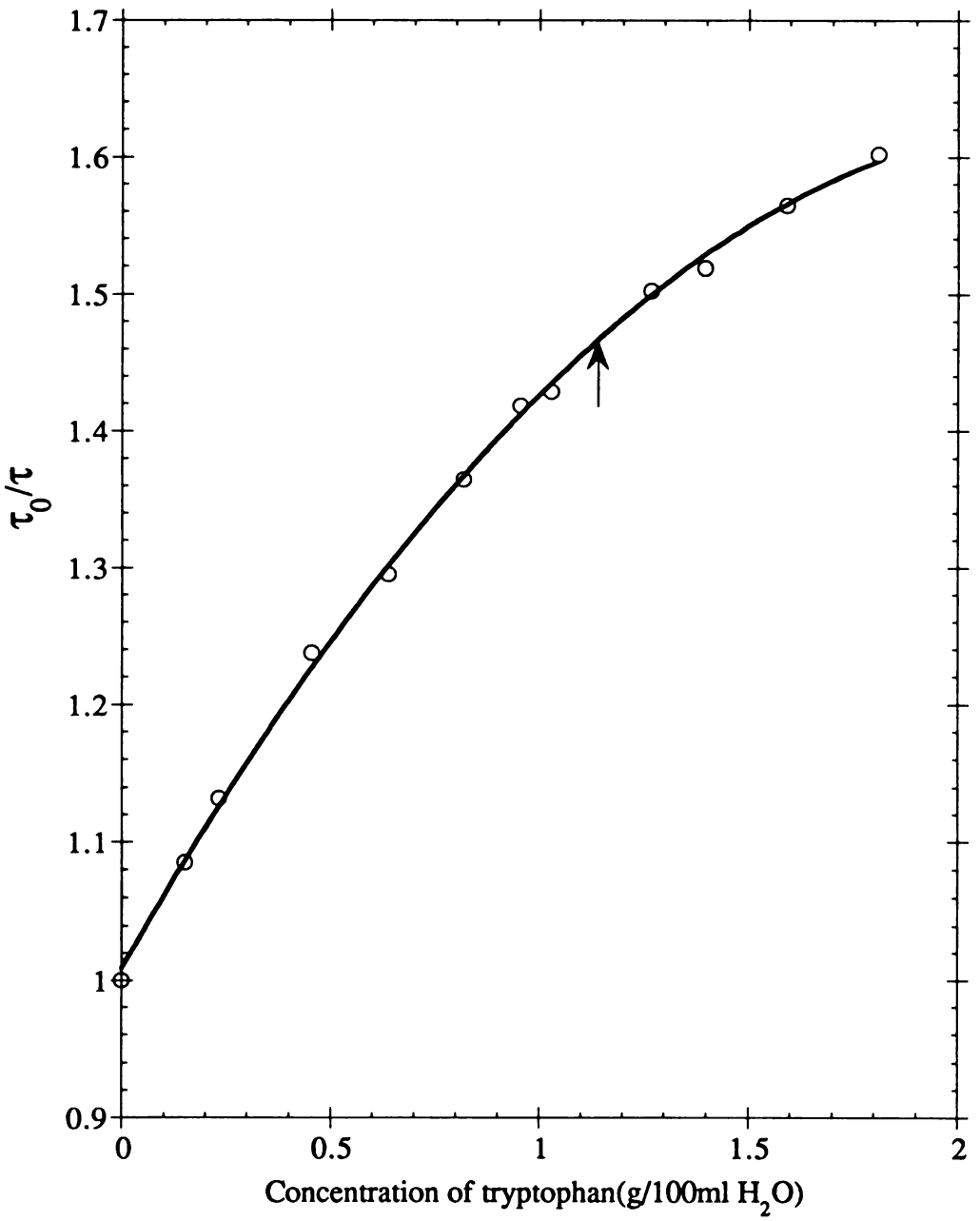

Figure 6.1 Lifetime Stern-Volmer quenching of pyranine fluorescence at 510nm by tryptophan in aqueous solutions at room temperature. The arrow indicates the solubility of tryptophan at 25^0C.

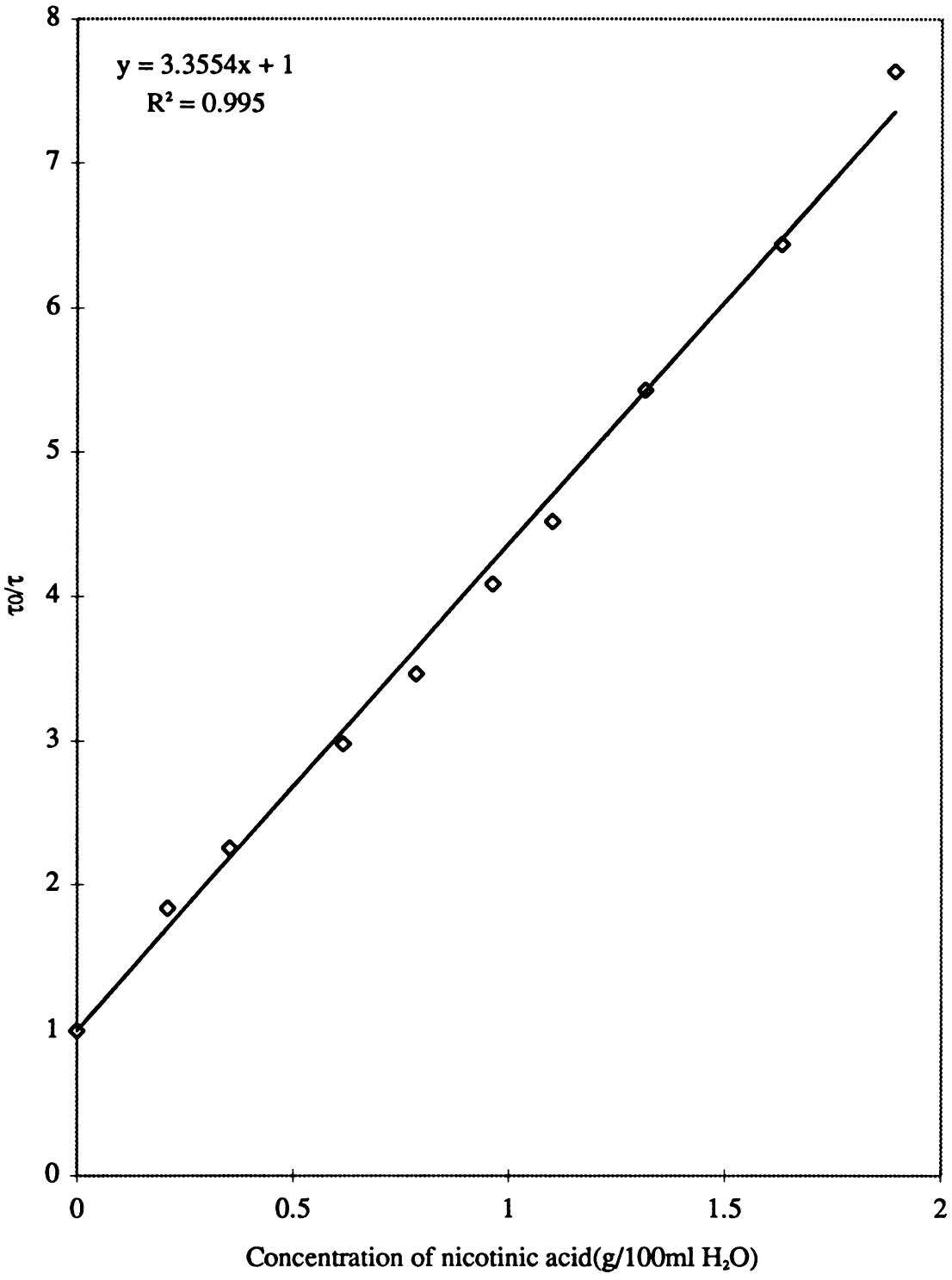

Figure 6.2 Lifetime Stern-Volmer quenching of pyranine fluorescence at 510nm by nicotinic acid in aqueouse solutions at room temperature. The equation shown is linear fitting.

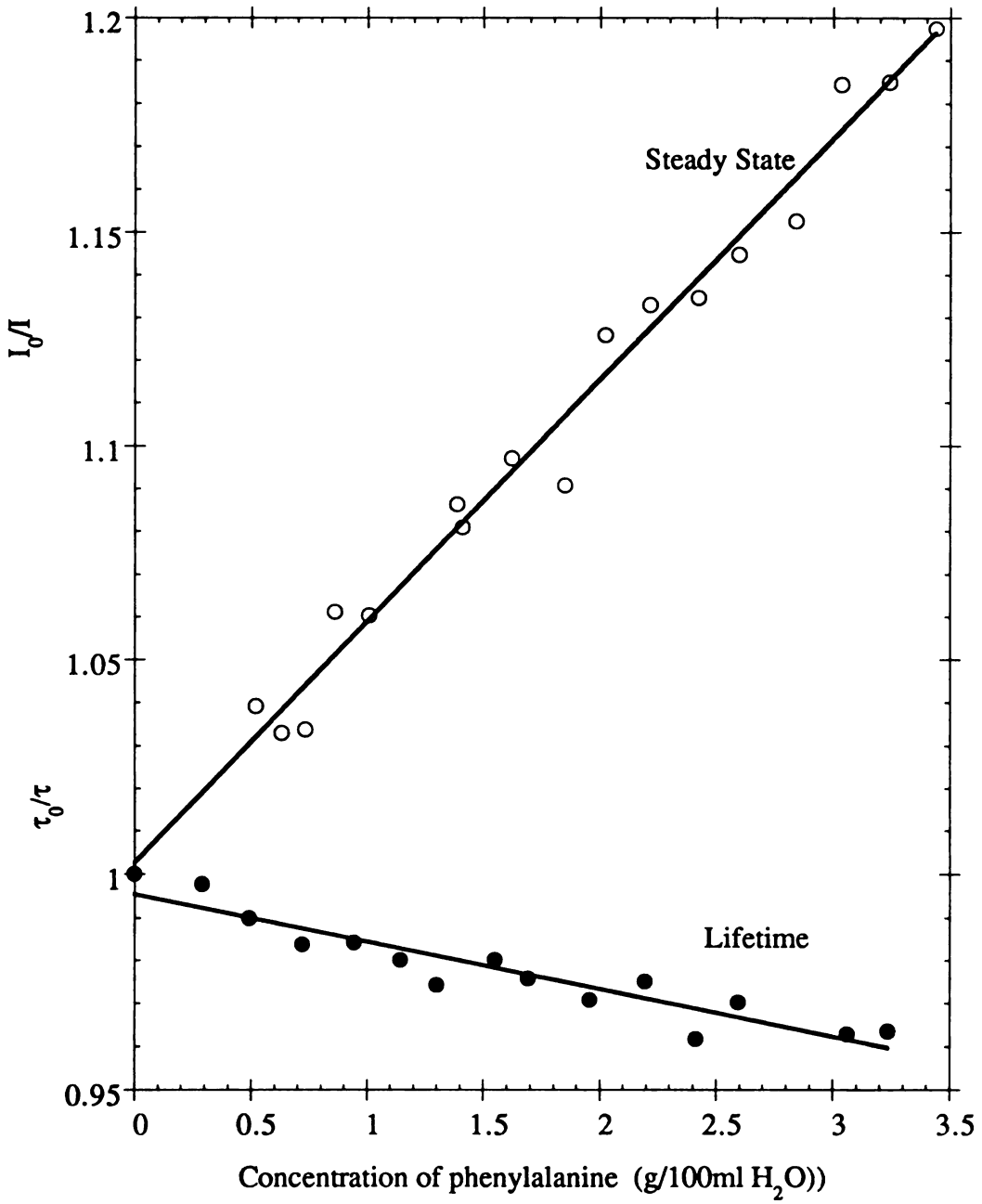

Figure 6.3 Lifetime and steady state quenching of pyranine fluorescence at 510nm by phenylalanine in aqueous solutions at room temperature fit to Stern-Volmer Law.

higher concentrations. In nicotinic acid the plot is linear. In phenylalanine solutions, the lifetime plot goes downward with the increase in concentration of phenylalanine which is seldom observed and the steady state plot is going up with the increase of the concentration.

The linear Stern-Volmer plot for nicotinic acid shows that the lifetime Stern-Volmer law holds for nicotinic acid. The slope is the dynamic quenching constant which is 3.4 (100g H_2O/g nicotinic acid). At low concentration of tryptophan, the dynamic quenching Stern-Volmer law holds. As previously discussed, tryptophan tends to form associates among themselves. With the increase of concentration, the population of associates will increase. At very high concentration, aggregates will form in the solution. Those associates and aggregates can not quench fluorescence of pyranine efficiently due to the larger size and also the lack of contact of molecules in the middle of associates, thus the lifetime decrease will not follow the same trend. The plot curves downward. In phenylalanine solutions, the lifetime quenching plot goes down with the concentration of phenylalanine which can be interpreted that phenylalanine will not quench the fluorescence of pyranine at 510nm dynamically. Steady state phenylalanine shows quenching behavior to pyranine with an increasing quenching curve. We can conclude phenylalanine will quench pyranine fluorescence statically but not dynamically. Alternatively we can say phenylalanine is poorer quencher as compared to H_2O because water can form a hydrogen bonding complex with pyranine which was shown a very effective quenching mechanism. When phenylalanine is added to water, a contact complex will form between pyranine and phenylalanine. This contact complex will protect pyranine from quenching by water. This contact complex will quench fluorescence of pyranine statically by formation of an exciplex.

6.3.2. Fluorescence lifetime quenching of pyranine at 382nm in different solutions

The fluorescence decay of pyranine at 382nm is a first order kinetic process with life time around 4ns. The fluorescence lifetime of pyranine at 382nm was measured in tryptophan, phenylalanine and nicotinic acid at different concentrations. The results show that lifetime decreases with the increase of the concentration of solutions. In tryptophan and nicotinic acid solutions the increase is greater. The decrease in the lifetime of pyranine with the increase of concentration of solutes results from the fluorescence quenching of pyranine by the solutes.

The quenching plots of pyranine in tryptophan solutions for steady state and time resolved measurements are shown in Figure 6.4. The lifetime quenching plot is linear at low concentration of tryptophan and curves downward at higher concentration which is taken as the evidence of the formation of aggregates at the higher concentrations. From the linear part, the dynamic quenching constant is shown to be 4.3 (100g H_2O/g tryptophan). The steady state quenching curve is distinguishable from the lifetime quenching curve, which tells us the steady state quenching at low concentration is not just dynamic quenching although it is straight line. As discussed in chapter 5, a straight line at low concentration of tryptophan is result of the double functions of static quenching and associates of tryptophan in solutions. The steady state quenching curve has a larger slope which means higher quenching constants. The higher quenching constant is dynamic quenching plus static quenching.

The quenching plots of pyranine in nicotinic acid for steady state and time resolved measurements are shown in Figure 6.5. Because nicotinic acid has a strong quenching capability for pyranine, the peak intensity is low which makes the measurement of the lifetime difficult. We can measure some lifetimes by increasing the concentration of pyranine. The concentration of pyranine can not be too high in the solution because of the selfquenching of pyranine. Therefore, the fluorescence lifetime of pyranine can be measured only at low concentrations of nicotinic acid. The lifetime quenching plot shows

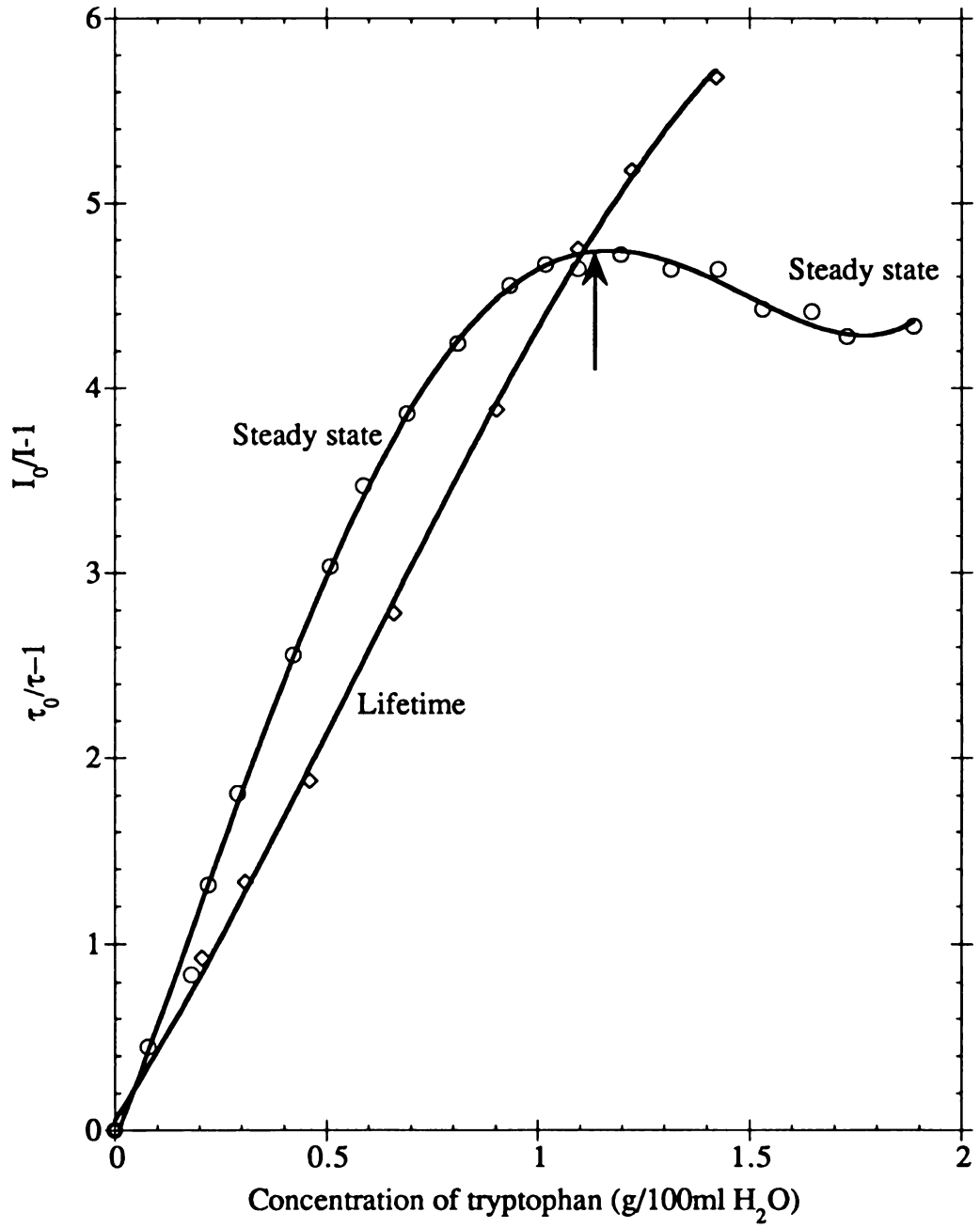

Figure 6.4 Lifetime and steady state quenching of pyranine fluorescence at 382nm by tryptophan in aqueous solutions at room temperature fit to Stern-Volmer Law. The arrow shows the solubility of tryptophan at 25^0C.

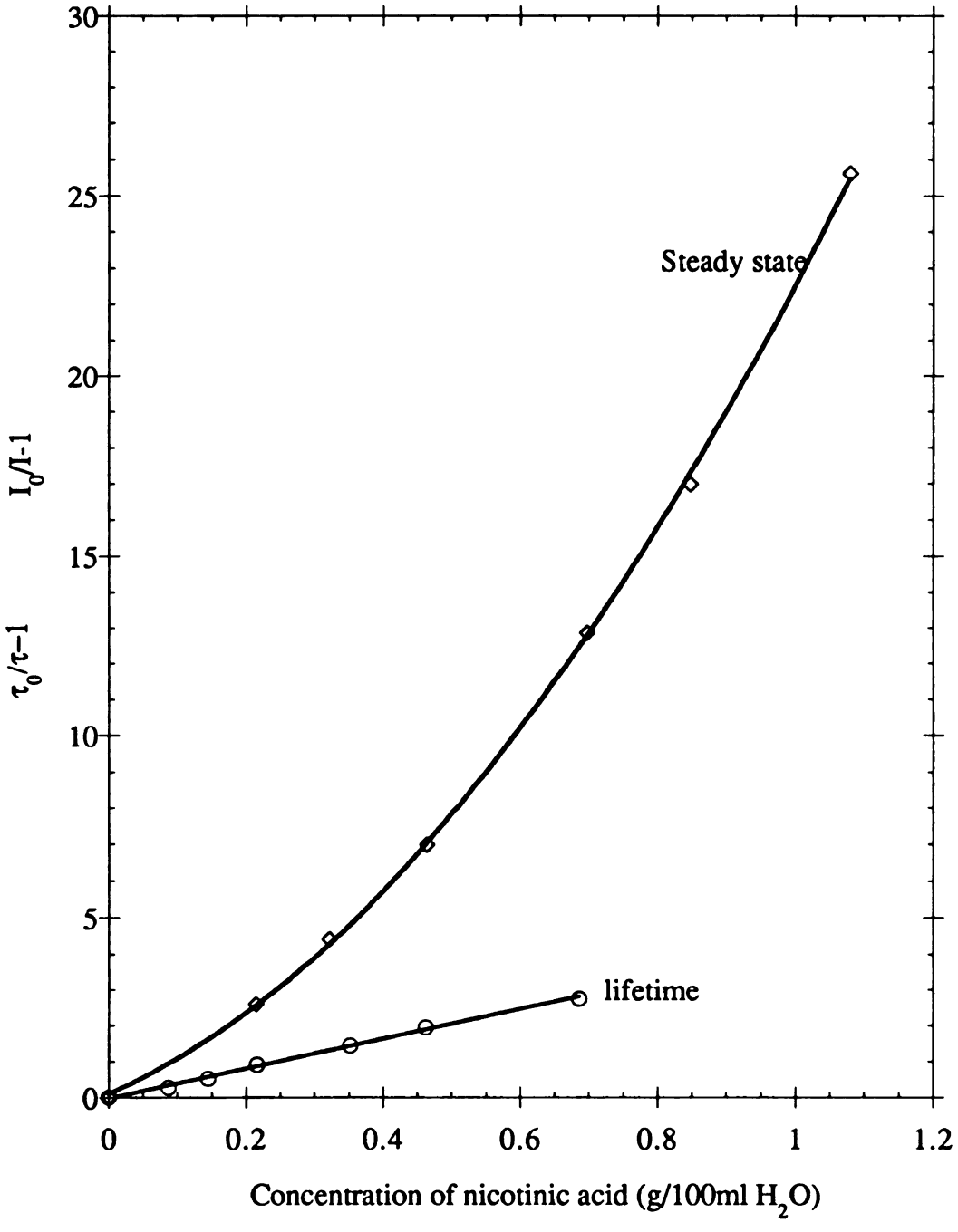

Figure 6.5 Lifetime and steady state quenching of pyranine fluorescence at 382nm by nicotinic acid in aqueous solutions at room temperature fit to Stern-Volmer law. The arrow shows solubility of nicotinic acid.

linear relationship with the concentration of nicotinic acid with the dynamic quenching constant 4.1 (100g H_2O/g nicotinic acid). Steady state quenching curves upward which shows the coexistence of dynamic quenching and static quenching.

The lifetime quenching plot of pyranine in phenylalanine solutions exhibits an uncommon shape (Figure 6.6). As previously discussed for quenching at 510nm, phenylalanine will only quench pyranine fluorescence statically by formation of a contact complex. The formation of a contact complex can protect pyranine from quenching by water. When the concentration of phenylalanine is not high, the protection is not quite complete. Water will quench the fluorescence of pyranine dynamically which will decrease the lifetime of pyranine. When the concentration of phenylalanine is higher, the quenching from water is stopped. The protection of quenching from water is much more effective at 510nm which the lifetime increase with the concentration of phenylalanine all the time. The reason is that the quenching of pyranine from water is by hydrogen transfer through a hydrogen bonding complex. The quenching of PyO^- at 510nm will be more effective than quenching at 382nm which is the emission of the PAH structure.

6.4 Conclusion

Time resolved fluorescence decay can help us understand steady state quenching better. Lifetime Stern-Volmer quenching plots of pyranine by tryptophan curve downward suggesting the formation of associates and aggregates at higher concentrations of tryptophan. Phenylalanine does not quench the fluorescence of pyranine dynamically at 510nm due to the increase of the lifetime with the increase of the phenylalanine concentration. Steady state studies show that phenylalanine will quench the fluorescence of pyranine. This behavior can be interpreted as the evidence of the formation of contact complex between phenylalanine and pyranine and this complex will protect the quenching from water by proton transfer through the hydrogen bond. Nicotinic acid will quench

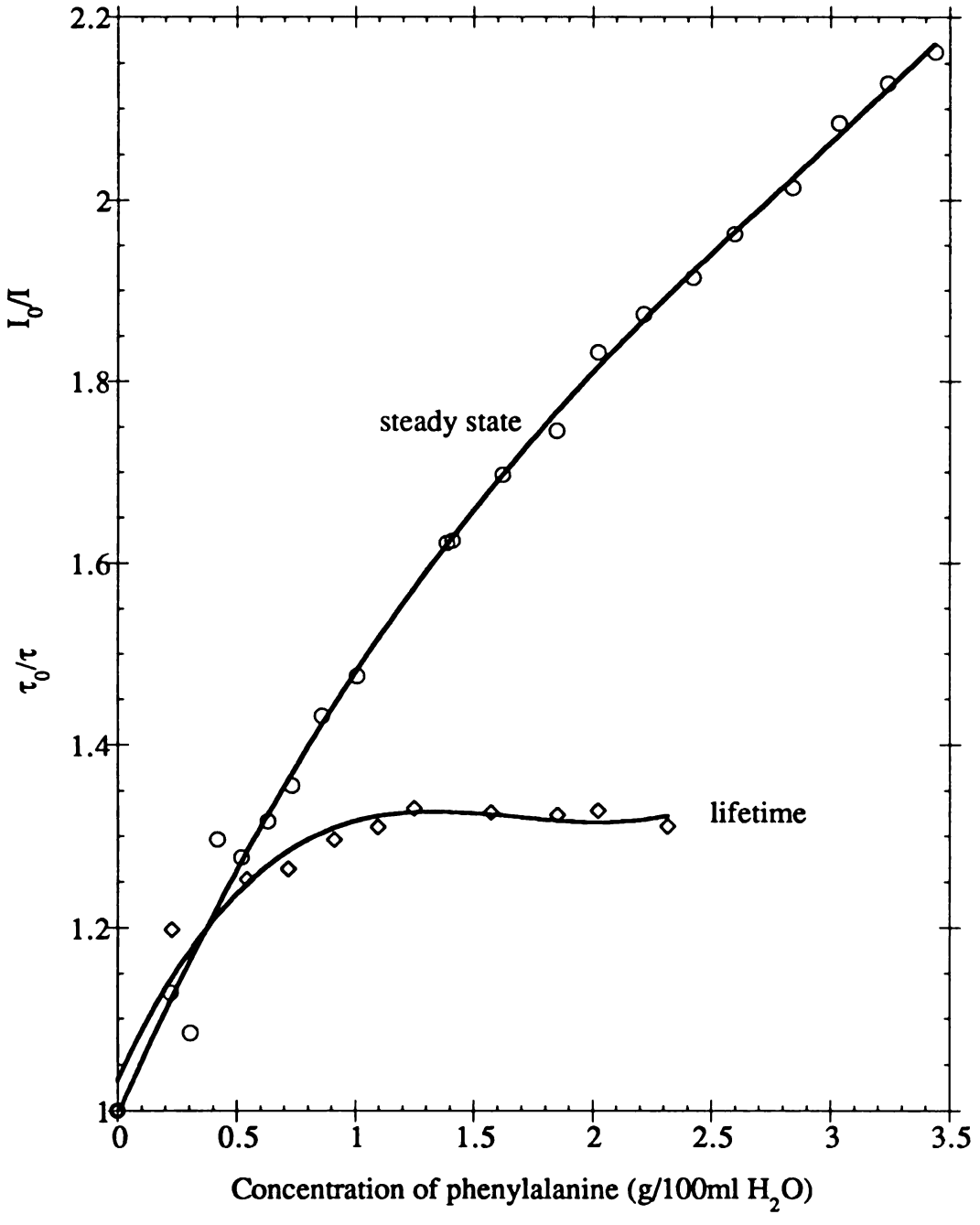

Figure 6.6 Lifetime and steady state quenching of pyranine fluorescence at 382nm by phenylalanine in aqueous solutions at room temperature fit to Stern-Volmer law

fluorescence of pyranine strongly dynamically and statically due to the small size, non-associates and strong hydrogen bonding with pyranine.

6.5 References

1. H. Kondo, I. Miwa, and J. Dunamoto, *J. Phys. Chem.*, **86**, 4826-31(1982)
2. E. Bardez, B. Goguillon, E. Keh, and B. Valeur, *J. Phys. Chem.*, **88**, 1909(1984)
3. G. D. Correll, R. N. Cheeser III, F. Mome, and J.H. Fendler, *J. Am. Chem. Soc.*, **100:4**, 1254-1262(1978)
4. J. N. Demas, *Excited State Lifetime Measurements*, Academic Press, New York (1983)
5. H. G. Marcelo, and F. C. De Schryver, *Chem. Rev.*, **93**, 199(1993)
6. F. S. Abrams, and E. London, *Biochemistry*, **31**, 5312(1992)
7. K. Kachel, E. Asuncion-Punzalan, and E. London, *Biochemistry*, **34**, 15475(1995)
8. C. Peviani, W. Hillen, N. Ettner, H. Lami, S. M. Doglia, E. Piemont, C. Ellouze, and M. Chabbert, *Biochemistry*, **34**, 13007(1995)
9. M. R. Eftink, and C. A. Ghiron, *Biochemistry*, **15**(3), 672-680(1976)
10. L. P. McMahon, W. J. Colucci, M. L. McLaughlin and M. D. Barkley *J. Am. Chem. Soc.*, **114**, 8442-8448(1992)
11. Yu Chen, Bo Liu, Hong-Tao Yu and Mary D. Barkley, *J. Am. Chem. Soc.*, **118**, 9271-9278(1996)

Chapter 7

THE DEPENDENCE OF EXCITATION WAVELENGTH OF TRYPTOPHAN FLUORESCENCE IN TRYPTOPHAN AQUEOUS SOLUTION

7.1 Introduction

The fluorescence of tryptophan has been investigated extensively due to the importance of the photophysics of tryptophan and the use of its fluorescence in the study of the structure and function of proteins and enzymes(1-6). Tryptophan is a very important intrinsic probe for the study of proteins and enzymes. The quenching study of tryptophan in proteins can provide us information about the folding of proteins and many other important information.

It had been reported that tryptophan fluorescence is very sensitive to environment. The emission maximum of tryptophan in protein changes in response to the different polarity and also maybe rigidity of the surrounding matrix from 308nm to 360nm (4). There are two excited states, ^1L_a and ^1L_b, for indole ring which have different dipoles where ^1L_a is more polar than the ^1L_b state (2,4). The fluorescence decay of tryptophan shows a double exponential decay at pH values where the zwitterion predominates with emission maxima at 350nm and 335nm. The two species were assigned to the non-interconverting relaxed ^1L_a and ^1L_b states (2). Szobo and Rayner interpreted the dual exponential decay of tryptophan fluorescence in terms of the presence of more than one tryptophan conformer in solution (1). Many people suggest the emission of tryptophan is comprised of two bands. However despite the extensive work regarding to fluorescence of

tryptophan, there are no reported studies on the excitation wavelength dependence of tryptophan fluorescence.

Fluorescence emission occurs from the zero-point vibrational level of the first excited singlet state, so a fluorescence emission spectrum is generally not dependent on the excitation wavelength. The fluorescence spectrum yields data about the vibrational level of the ground electronic state. When a fluorophore is in a polar and viscous environment where its mobility is restricted, the wavelength of maximum fluorescence will depend on the excitation wavelength. The maximum fluorescence emission will show a red-shift when excited with extreme red edge wavelength. This phenomenon is well known as red edge excitation shift (REES) (7,8). The origin of the REES phenomenon result from the reorientation process of solvent molecules around fluorophore when it is excited. The fluorophore in the solution will exist in the solvated state with solvent molecules around it. When the fluorophore is excited then the dipole of the fluorophore will change then the solvent molecules around fluorophore will reorient themselves to meet the minimum energy requirement This reorientation process or so-called solvent relaxation process is dependent on the viscosity of the solvent. If the viscosity is low the reorientation will be very fast around 10^{-12}s which is within the excited state lifetime 10^{-9}s. So when the viscosity is not very high the emission is not excitation wavelength dependence because emissions all occur from the solvent-relaxed state. That is the general situation for water, a very common solvent, which has no very high viscosity. But when the viscosity of the medium is very high, the solvent relaxation process will take longer time because the restriction of moving. When the solvent relaxation time is the same as or longer than the lifetime of fluorophore, the relaxation can not be done within the lifetime of fluorescence. So fluorescence will not happen from the lowest vibration state. In this case each excitation wavelength will excite selectively some special state fluorophores which have the similar solvent orientation in the excited state as solvent relaxed state. Fluorescence will occur from the special excited states and will be red shifted.

REES is rarely observed in aqueous solution. In this work we find that the emission spectra of tryptophan is excitation wavelength dependence in aqueous solution at all wavelengths which is not very common. The fluorescence of tryptophan is studied in this research. For comparison, the fluorescence of indole is studied at the same time.

7.2 Materials and Experiments

Tryptophan was purchased from Aldrich Chemical Company, Inc., Milwaukee, WI and used as received. Different concentrations of tryptophan solutions were prepared by dissolving the appropriate amount of tryptophan in 5ml HPLC water. Supersaturated solutions were prepared by heating the solution in the water bath until all the solute was dissolved and subsequent cooling to room temperature. The solutions were used as prepared without any degassing.

Fluorescence spectra of tryptophan in the aqueous solutions were collected within a couple hours of the preparation the solutions. All spectra were taken at room temperature with a Spex 1681 Fluorolog spectrometer equipped with a Xenon lamp source and a PMT detector. A quartz sample holder was used in all cases. Spectra were recorded at a 1.00mm increment and an integration time of 1.0 sec. Monochromator slits were at 0.5 mm for both excitation and emission spectra.

7.3 Results

7.3.1. The fluorescence spectra of tryptophan in aqueous solution

Fluorescence spectra of tryptophan in aqueous solution shown in Figure 7.1 show a broad peak with the maximum emission around 356nm when excited at 308nm. Figure 7.2 and Figure 7.3 show the maximum fluorescence intensity dependence on the concentration of tryptophan at different excitation wavelengths. When the excitation wavelength is lower than 310nm, the maximum emission intensity shows a parabolic plot regarding to the concentration of tryptophan (Figure 7.2). That is, when the concentration

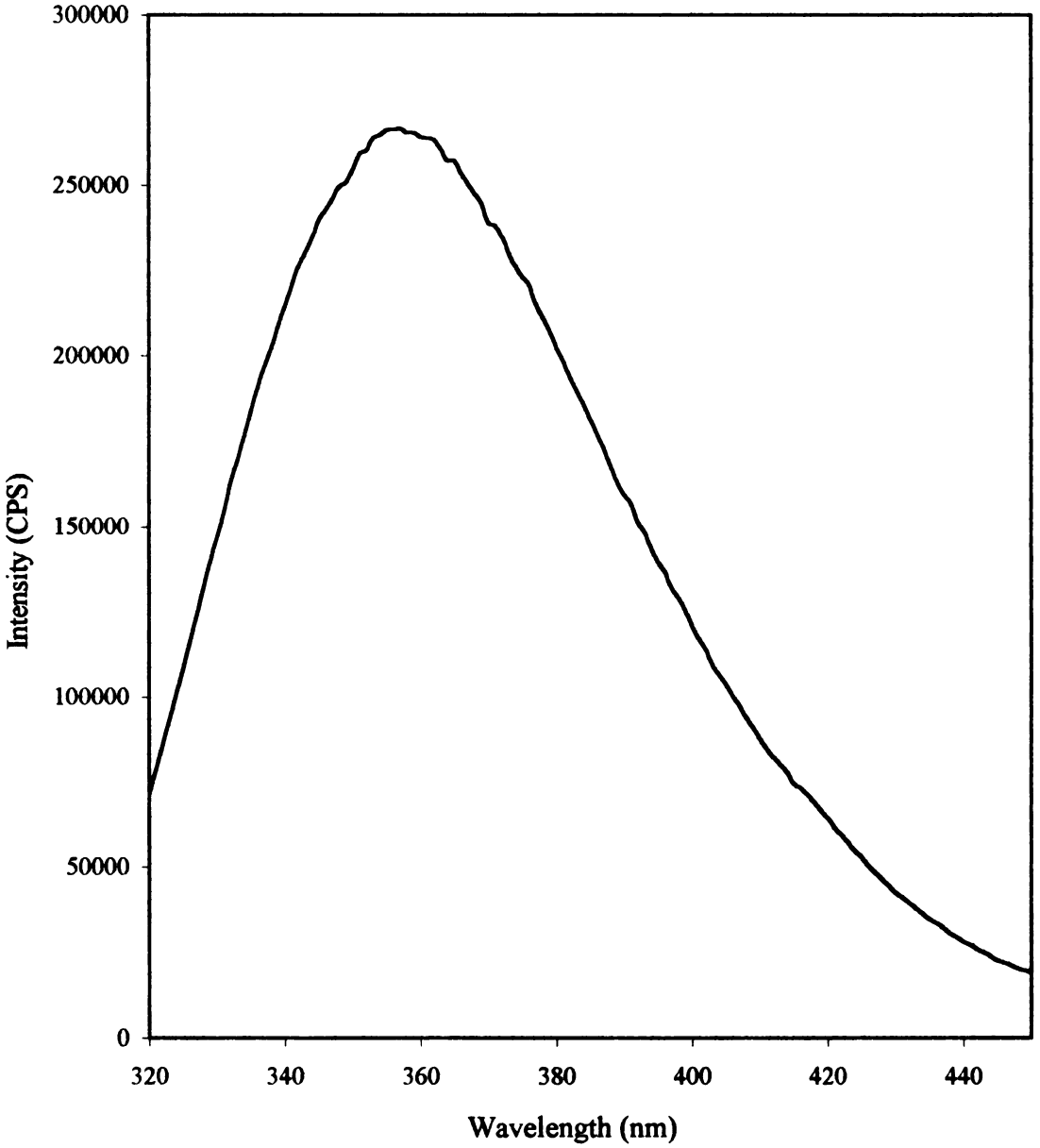

Figure 7.1 Fluorescence spectrum of tryptophan in aqueous solution excited at 308nm at room temperature

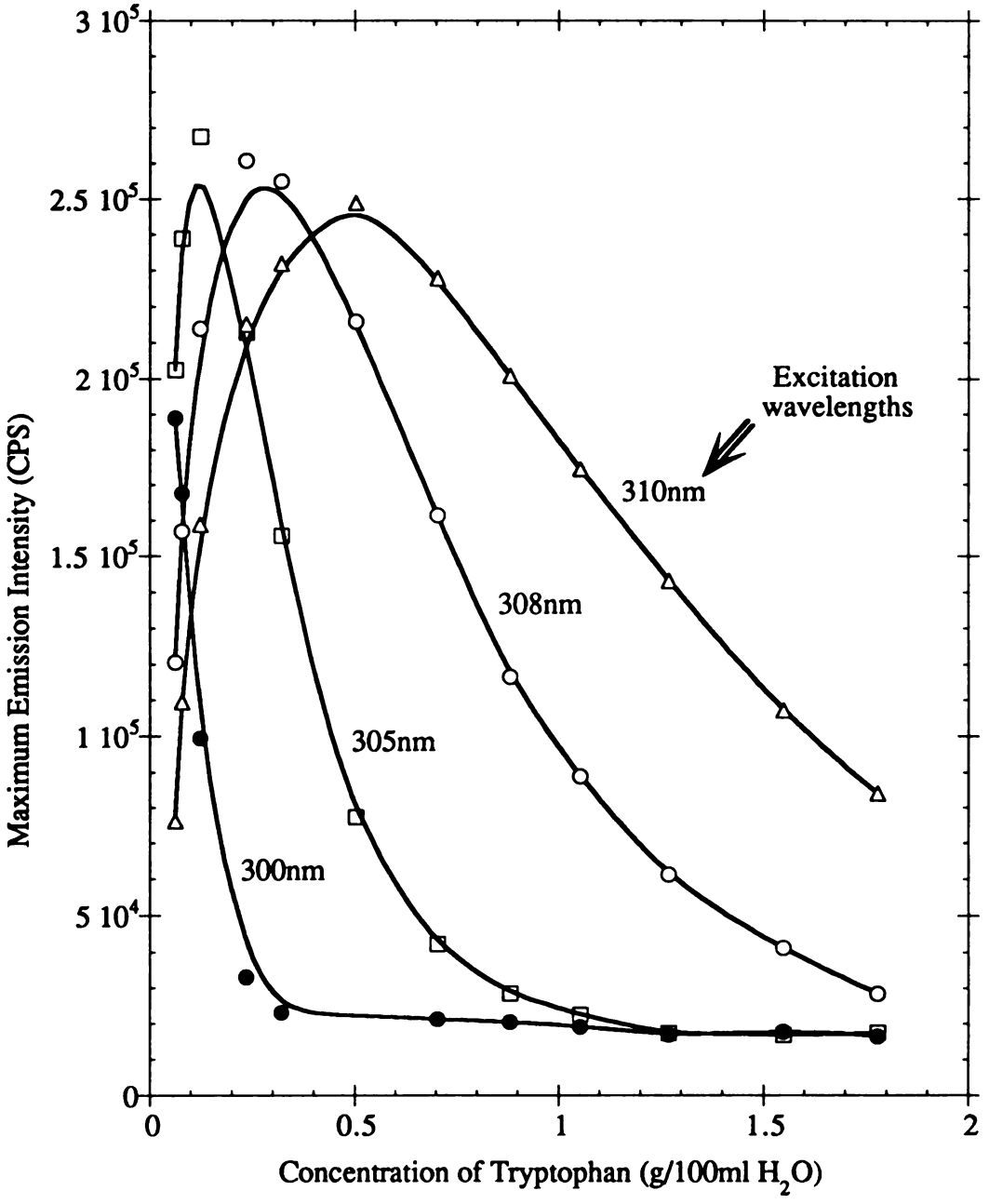

Figure 7.2 Maximum emission intensity dependence on the concentration of tryptophan at different excitation wavelengths which are smaller than 310nm at room temperature

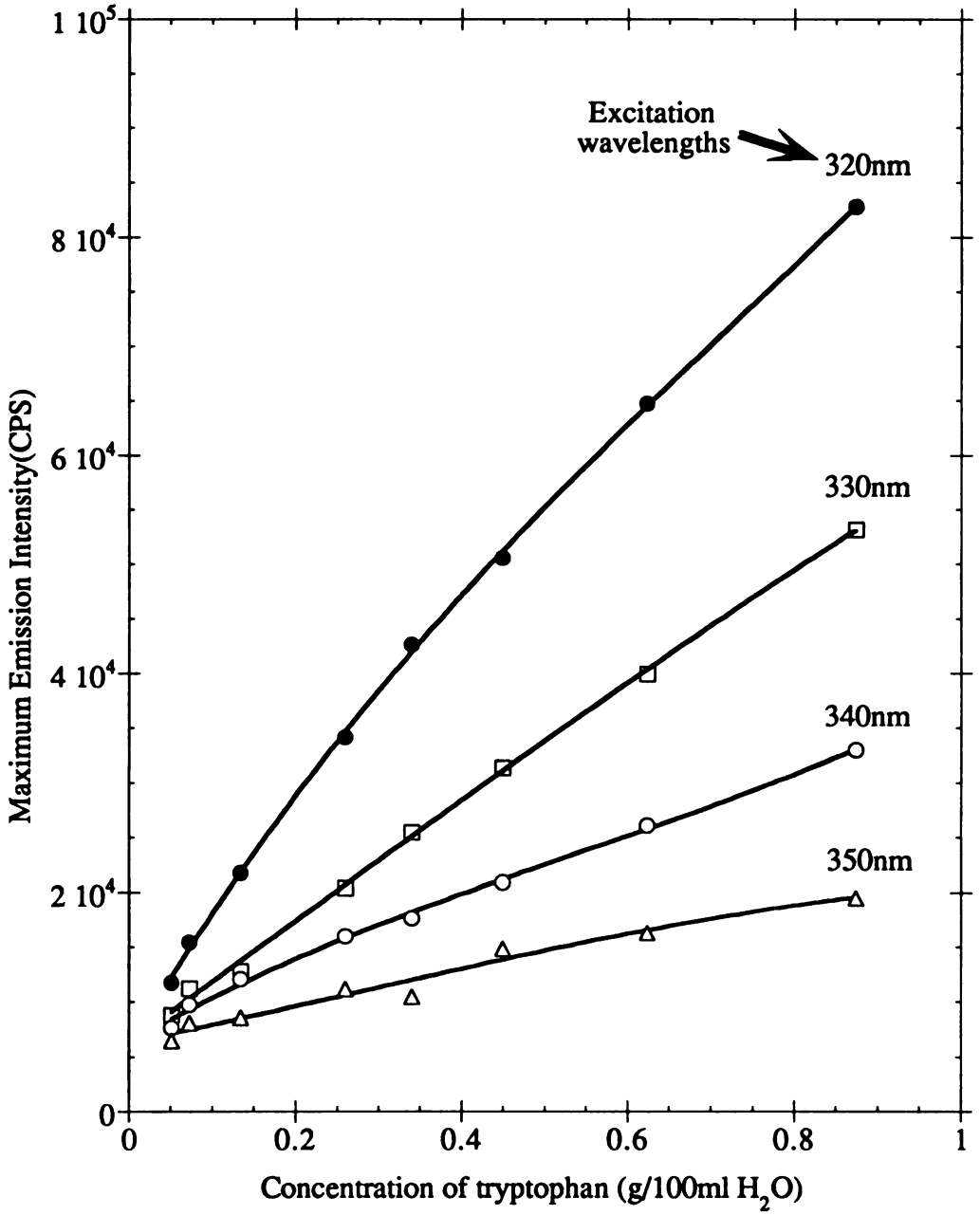

Figure 7.3 Maximum emission intensity dependence on the concentration of tryptophan at different excitation wavelengths which are higher than 320nm at room temperature.

of tryptophan is low, the intensity of tryptophan fluorescence will increase with the increase of the concentration of tryptophan. When the concentration of tryptophan is high, the fluorescence intensity of tryptophan will decrease with the increase of the concentration of tryptophan. Intensity changes with the concentration are sharper as shown in Figure 7.2. At different excitation wavelengths, the parabolic maximum occurs at different concentrations. When the excitation wavelength is greater than 320nm, the intensity of the maximum emission increased with the increase of concentration of tryptophan shown in Figure 7.3.

7.3.2. Excitation spectra versus concentration of tryptophan

The excitation spectra at different concentrations are shown in Figure 7.4. The emission wavelength is 420nm and the spectra were collected from 300nm to 400nm. The maximum of excitation wavelength shifts to red with the increase of concentration of tryptophan and the intensity of excitation spectra increased with the concentration. The excitation spectrum becomes broader with the increase of the concentration of tryptophan. With the increase of concentration of tryptophan the shoulder at longer wavelength becomes higher and higher.

7.3.3. Excitation wavelength dependence of maximum emission wavelength

Figure 7.5 shows the fluorescence spectra of tryptophan with the concentration of 1.632g tryptophan in 100ml H_2O which is supersaturated solution at different excitation wavelengths. The same solution excited with different excitation wavelengths shows different maximum emission and different emission intensity.

The maximum emission wavelength will depend on the excitation wavelength at all concentrations of tryptophan. The different tryptophan concentration is 0.37g/100ml H_2O which is much unsaturated, 1.108g/100ml H_2O which is saturated solution and 1.632g/100ml H_2O which is supersaturated solution. The plot of the maximum emission

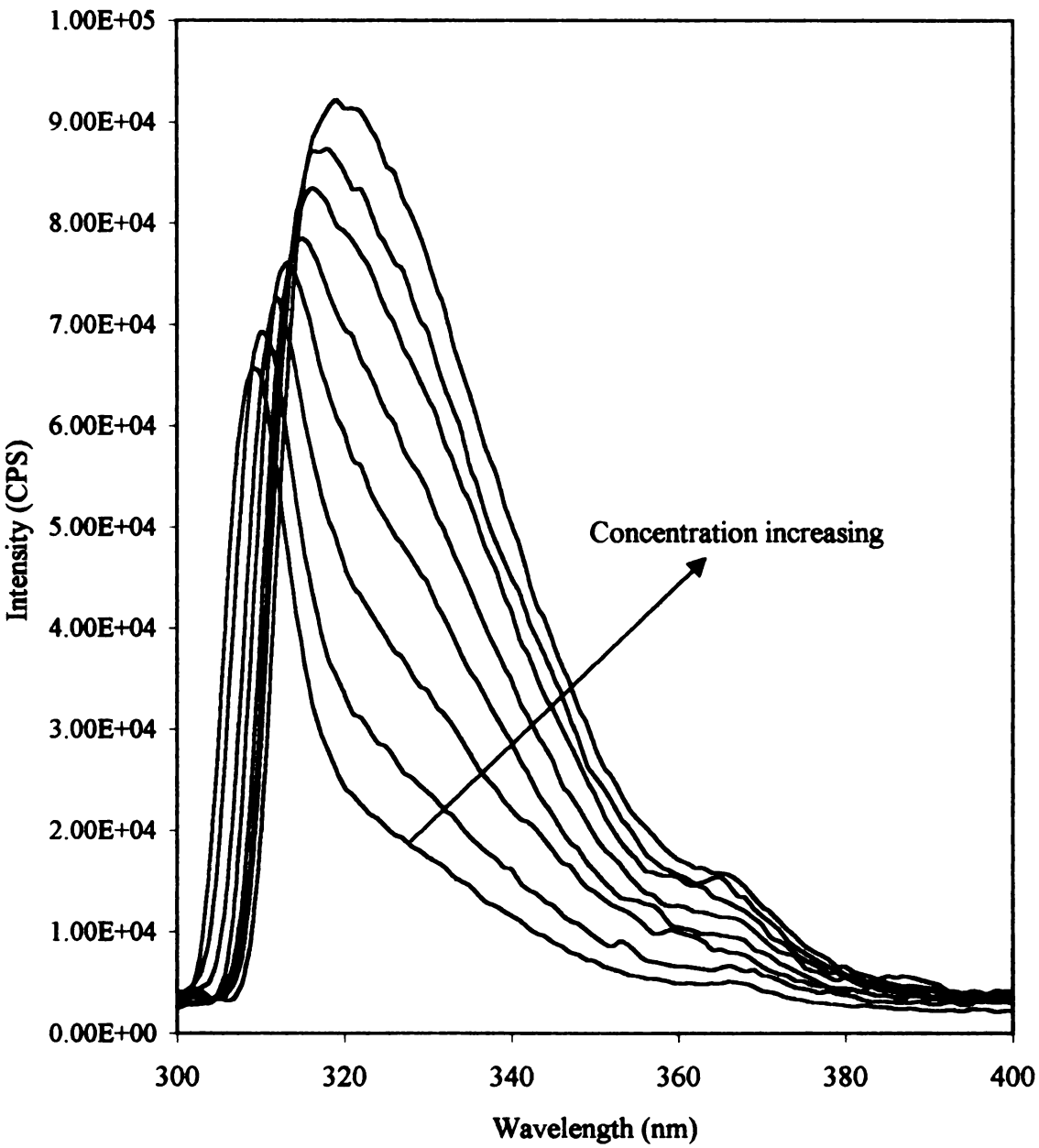

Figure 7.4 Excitation spectra of tryptophan at different tryptophan concentrations monitoring at 450nm emission wavelength

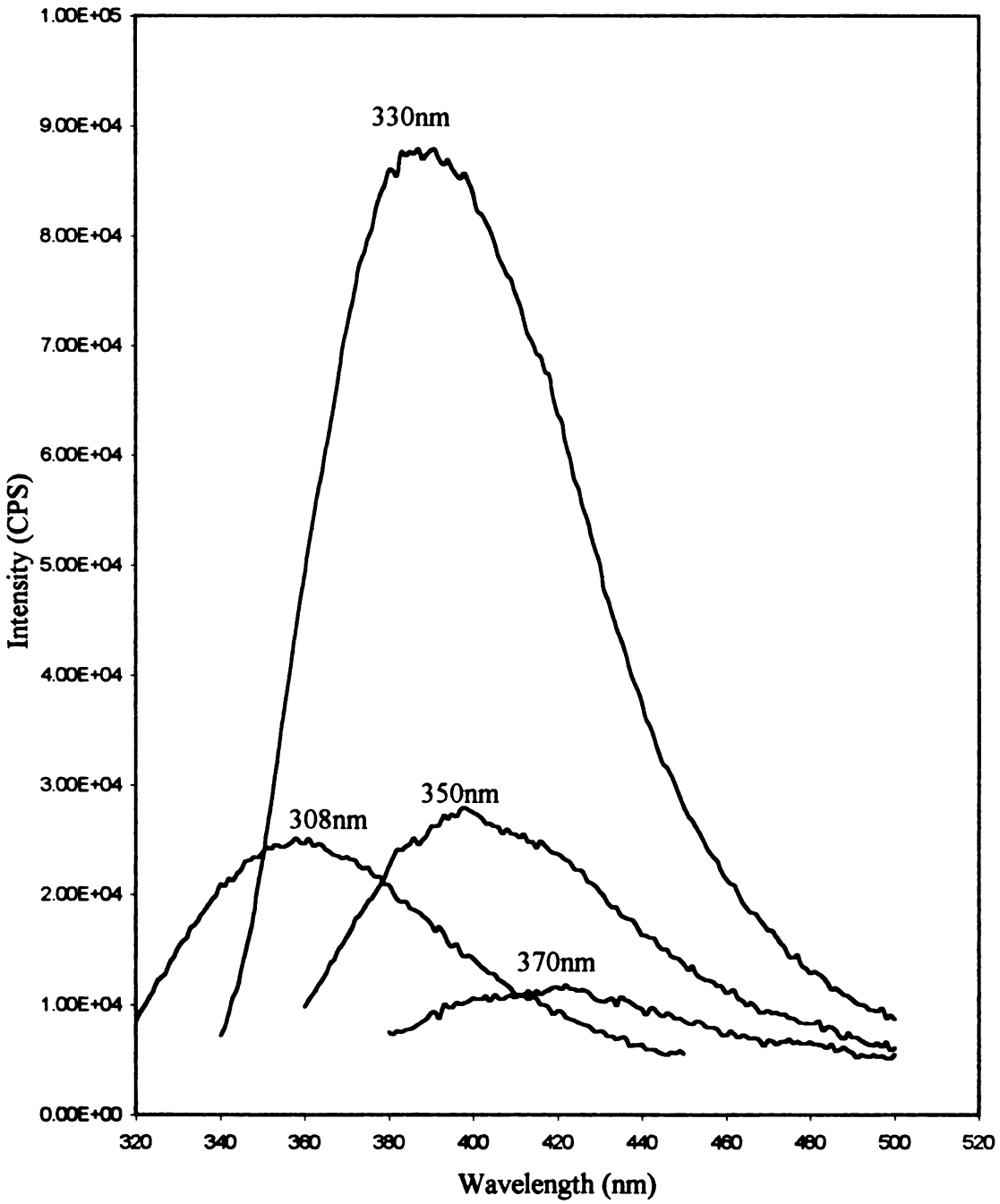

Figure 7.5 Fluorescence spectra of supersaturated tryptophan solution at different excitation wavelengths at room temperature

as a function of excitation wavelength for different concentrations is shown in Figure 7.6. From the plot of wavelength of excitation versus wavelength of maximum emission we can see the wavelength of maximum emission will increase with the increase of the wavelength of excitation for almost all excitation wavelengths. At lower excitation wavelengths, lower than 310nm, the emission wavelength does not change with the excitation wavelength and when the excitation wavelength is bigger than 310nm and lower than 330nm, the maximum emission wavelength increases sharply and nonlinearly with the excitation wavelength. When the excitation wavelength is larger than 350nm, the increase of the emission wavelength is linear with the increase of the excitation wavelength. When the excitation wavelength is between 330nm-350nm the relation between maximum emission and excitation is pretty complicated. It shows different changes with different concentrations. At low concentration, such as 0.37g tryptophan in 100ml H_2O, a sudden drop of fluorescence intensity occurs at 335nm, and at higher concentration, such as 1.108g tryptophan in 100ml H_2O, a sudden intensity drop occurs at 340nm. For a supersaturated solution, there is a curve down at wavelength 340nm but no sudden intensity drops. Three different solution concentrations have almost the same maximum emission versus excitation wavelength plot.

7.3.4 Lifetime of tryptophan in different solvents at different concentration

According to the literature tryptophan has a double-exponential decay at neutral pH. The major component has a life time of 3.1ns with emission max. at 350nm, and the minor component has a lifetime of 0.5ns with emission maximum at 335nm.

The decay curve of tryptophan also can be fitted by two exponentials with τ_1 around 2ns and τ_2 around 5ns at different solvents. The shorter lifetime will not change with the solvents, but the longer lifetime will change with the solvents. It almost becomes double

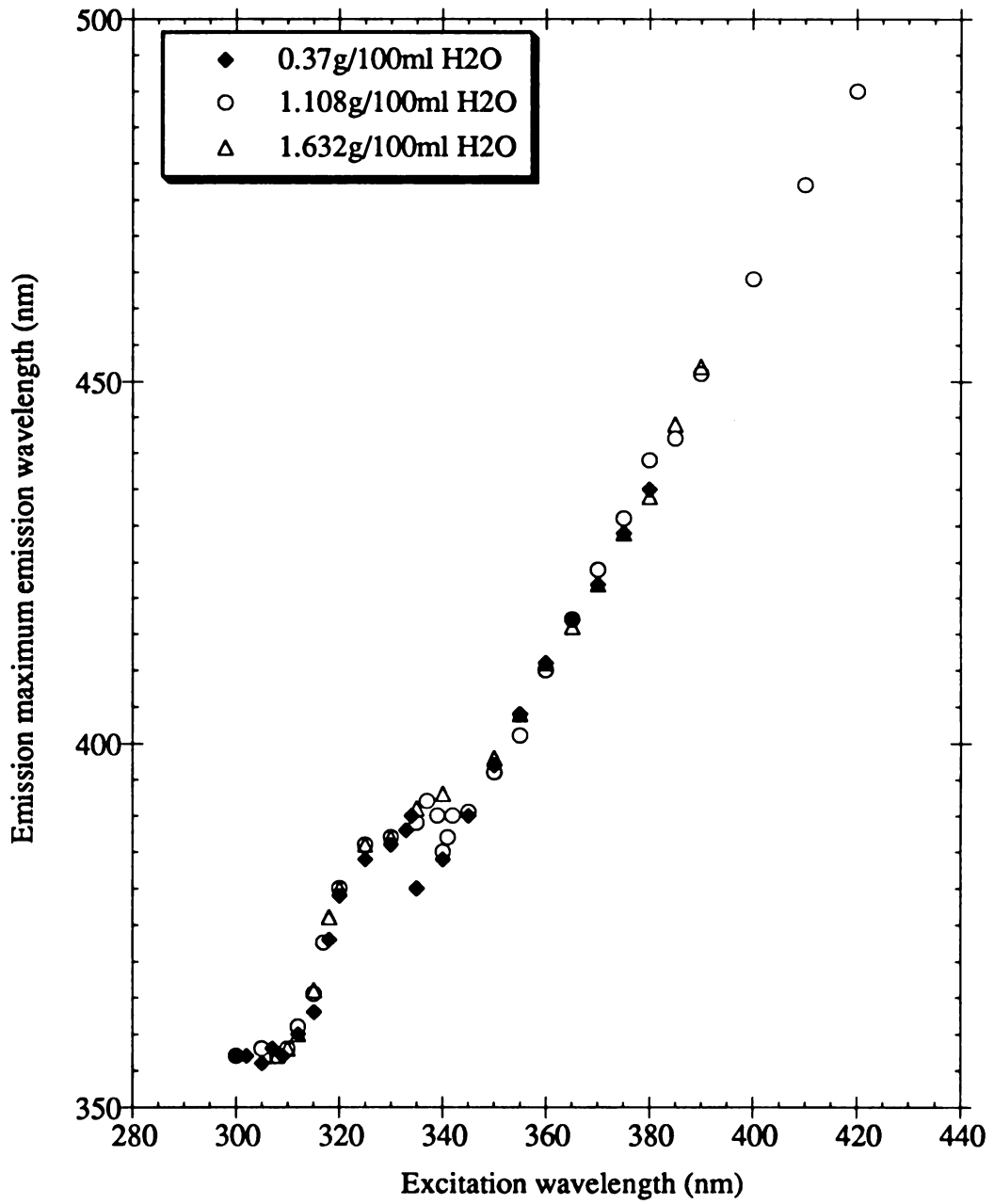

Figure 7.6 The dependence of the maximum emission wavelength on the excitation wavelength at different concentration of tryptophan solutions at room temperature

when the solvent is changed from water to the mixture of water and alcohol (1:1). The data is shown next:

H_20	τ_1=2.03ns	τ_2=3.168ns	x^2=0.658
EtOH+H_2O(1:1)	τ_1=2.34ns	τ_2=6.12ns	x^2=0.638
EtOH+H_2O+Propyl Acetate(2:2:1)	τ_1=1.920ns	τ_2=3.770ns	x^2=0.637

The lifetime of tryptophan will change with the concentration of tryptophan. In the mixture of water, ethanol and propyl acetate (2:2:1), the shorter lifetime of tryptophan just decreased slightly with the concentration of tryptophan and larger lifetime will have a large decrease with the tryptophan concentration increase (Figure 7.7). The lifetime of tryptophan in water will decrease with the concentration of tryptophan too. But the change is not as regularly as in mixture.

7.3.5 Comparison of indole fluorescence and tryptophan fluorescence

The fluorescence of tryptophan results from the indole ring. In order to support the hypothesis of the formation of associates due to the side chain of tryptophan in tryptophan solutions, the fluoresce of indole is studied as comparison. The excitation wavelength dependence of indole fluorescence is checked first. It turned out that the fluorescence of indole is not excitation wavelength dependence. The excitation spectra of tryptophan (0.116g/100ml water) and indole (0.051g/100ml water) are shown in Figure 7.8. Indole has a sharp peak at 299nm. The excitation spectrum of tryptophan is a sharp peak at 305nm but there is a tail followed this peak. The emission spectra of tryptophan and indole in water excited using the highest excitation intensity wavelength are shown in Figure 7.9. Tryptophan and indole have very similar emission spectra. Both are broad peaks. The maximum emission wavelength of indole will not change with the excitation wavelengths.

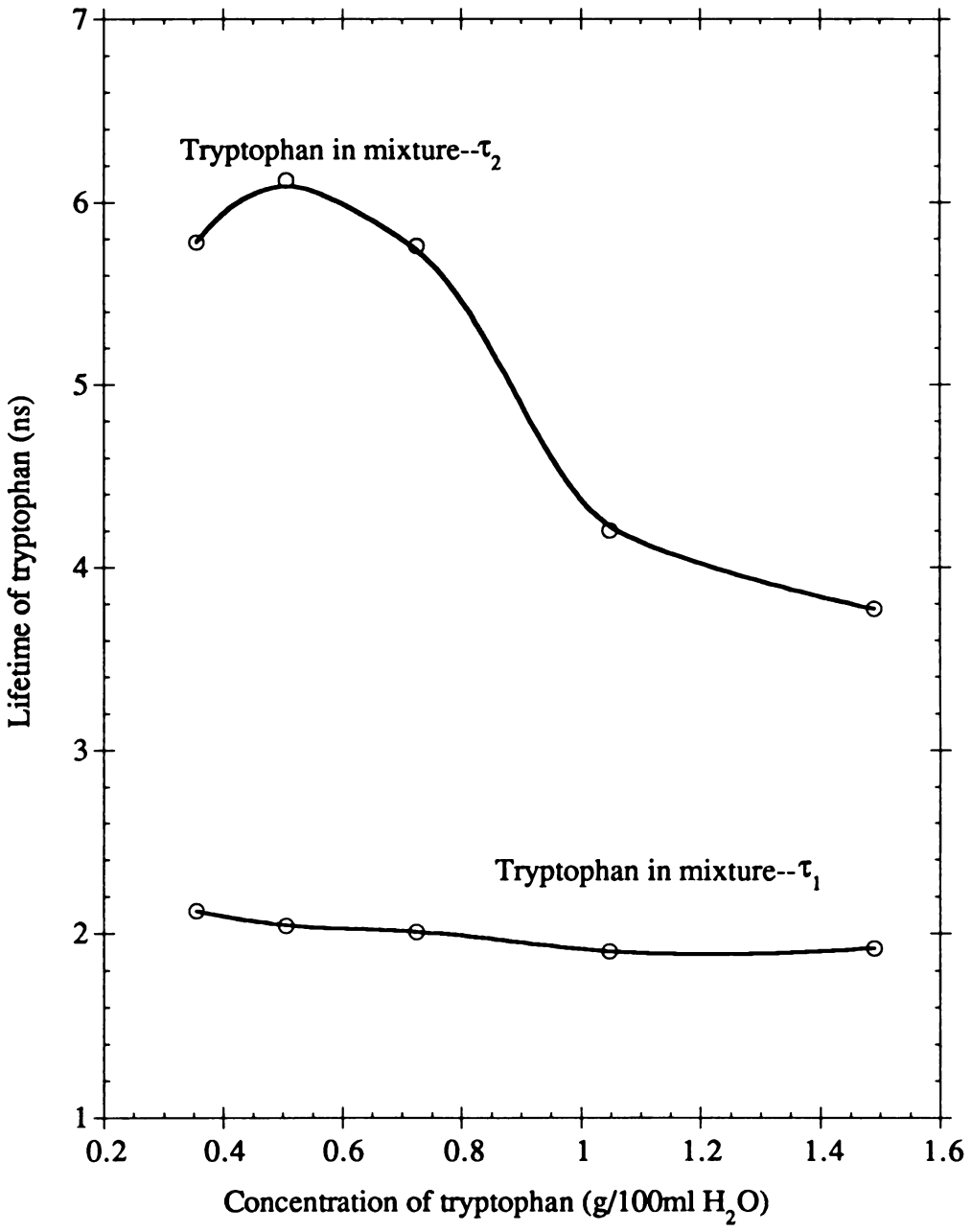

Figure 7.7 Lifetime of tryptophan in the mixture of water+ethenol+propyl acetate (2:2:1) at different concentrations of tryptophan at room temperature

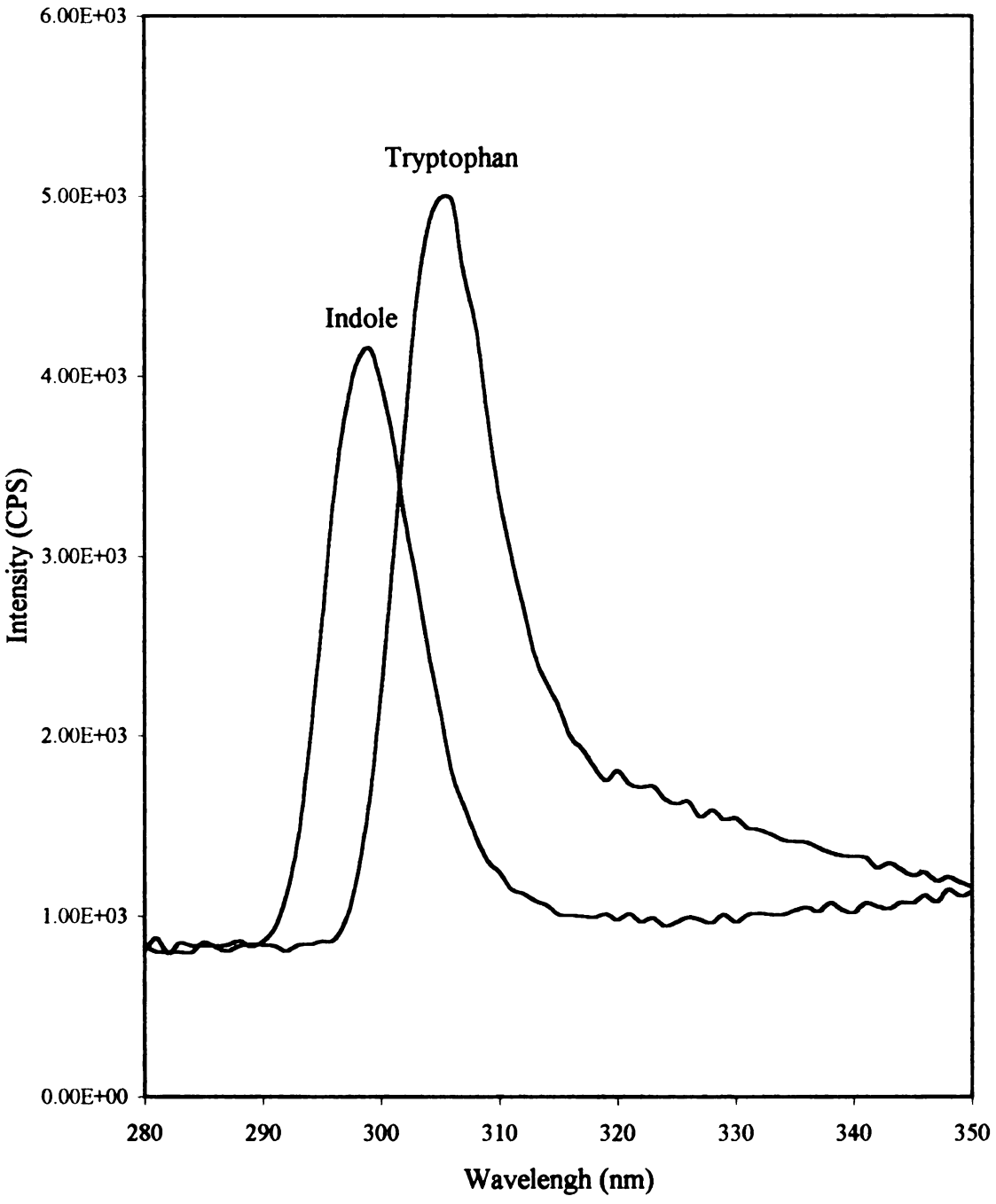

Figure 7.8 Excitation spectra of indole and tryptophan aqueous solutions at room temperature monitoring at 500nm emission wavelength

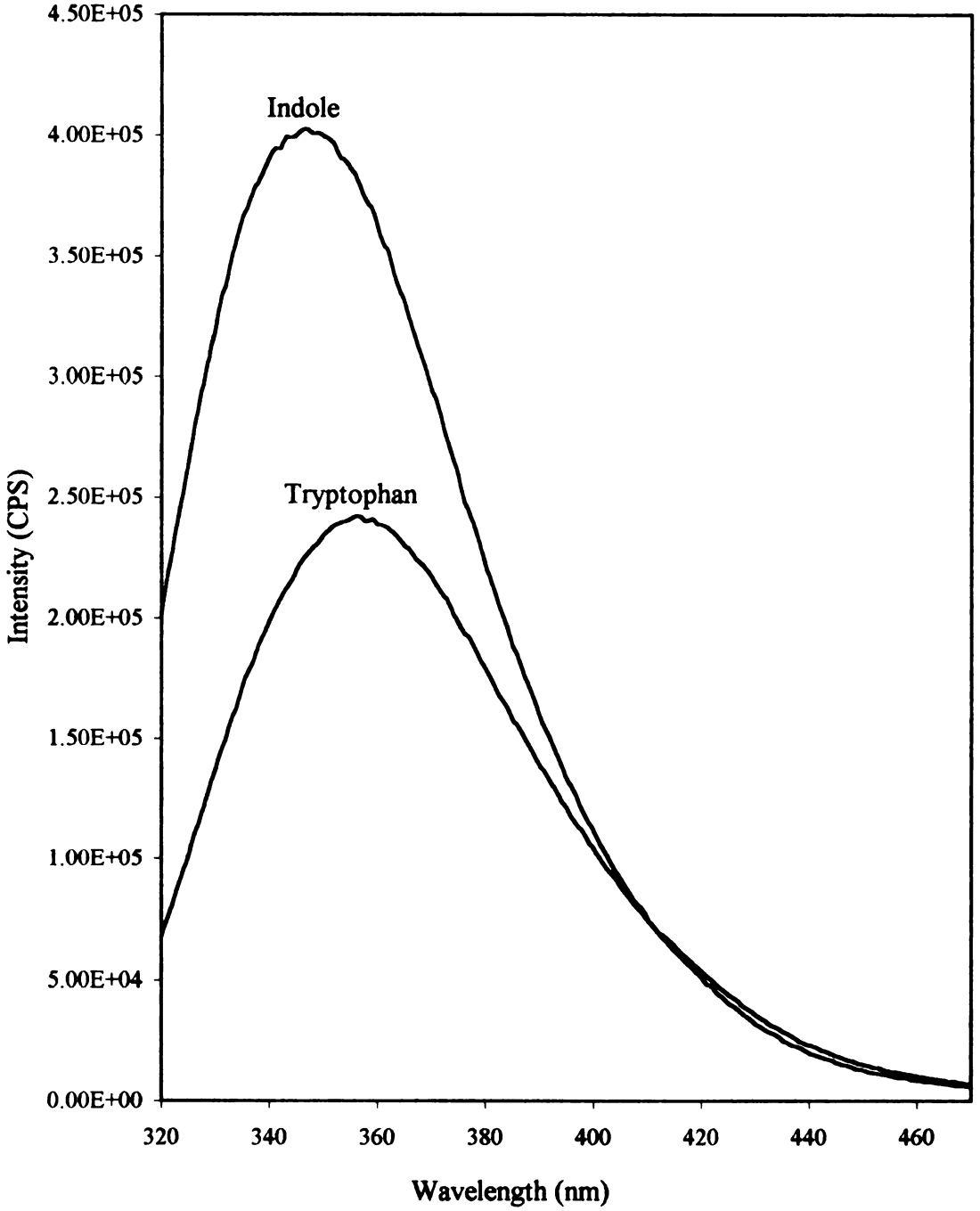

Figure 7.9 Fluorescence spectra of tryptophan and indole in water at room temperature

7.4 Discussion

Tryptophan in solution at a pH around 6.5 is a zwitterion. So two, three or more tryptophans may interact with each other to form dimers, trimmers or more complicated complexes, they can be two dimensional or three dimensional. These two or three dimensional structures produce different species of tryptophan in the solution which can be called associates. These associates will have different numbers of tryptophan molecules. Due to the co-bonding among rings or atoms, they will have different electronic structures, and different energy levels. The broad peak of tryptophan suggests many energy levels exist in the tryptophan solution. These different energy levels are close to each other, and they can not be distinguished so a broad emission band results.

In general, the larger the associate is, the lower the energy will be. Because many molecules together will share electrons which make the electricity cloud more spread, then lower energy level can be realized. Each associate will have a specific excitation which means each excitation wavelength will favor one specific associate which the energy difference between excited state and ground state is the same as the excitation energy. Different excitation wavelengths will excite selectively specific tryptophan associates in the solution. Different concentrations will result in different distributions of associate species and also different dominant associates. This explains why we get different excitation spectra at different concentrations. The red shift of the excitation wavelengths with the increase of the concentrations is the result of larger associates in higher concentrated solutions. The more molecules in the associate, the lower energy it will be. Then lower energy will be needed to excite the larger associate. The intensity of excitation spectra increase with the concentration is much easier to understand. More species will accumulate in the solution with the increase of concentration, so higher concentration solution will have higher intensity, and the same, broader peak at high concentration solutions will occur too.

The maximum emission intensity dependence on the concentration of tryptophan at different excitation wavelength is the result of the different population of species and each

species has specified excitation wavelength (Figure 7.2 and 7.3). When the excitation wavelength is lower than 320nm, a parabolic curve will appear regarding to the relation of maximum emission wavelength to concentration of tryptophan. Different excitation wavelengths will have different favor associates to excite which results in the different position of parabolic peak. Different concentrations of solution will have different populations of different species. This population difference results in the fluorescence changing with the concentration. When the excitation is lower than 310nm, due to the higher energy, many species can be excited resulting in the intensity dependence on the population of the species. The higher population, the higher the intensity. The larger the associates are, the lower the energy is. Longer excitation wavelength will tend to excite larger associates. So with the increase of the excitation wavelength, the parabolic peak will move toward higher concentration. When the excitation wavelength is longer than 320nm, those small species can not be excited at all due to the lower excitation energy. Only those larger associates can be excited and those large associates tend to exist only in high concentrated solutions and the population of those larger associates will increase with the increase concentration of tryptophan. So when the excitation wavelength is larger than 320nm, the intensity of maximum emission will increase with the concentration of tryptophan all the way.

The increase of emission wavelength with the excitation wavelength at longer wavelengths such as over 360nm can be interpreted as the REED phenomena detailed in the introduction. Due to the larger size of tryptophan associates, the relaxation process will not be very fast. Or we can say the larger size of tryptophan associates makes the energy of an associate much lower than a single solvated molecule. Low excitation energy will only excite selectively those larger associates. The size of the molecule makes the relaxation difficult, so the emission will not happen from lowest vibration level. The lower the excited energy is, the larger associates will be excited and the lower the emission energy will be, so the red shift will occur.

The same reason can be used to interpret the dependence of emission wavelength on the excitation wavelength at shorter wavelength range. We suppose there are many different tryptophan associates in the solution and each species will have definite excitation wavelength. When a definite excitation wavelength is used only specific species will be excited to its biggest degree and those excited species will emit at different wavelengths with the maximum emission intensity.

That the relation between maximum emission and excitation wavelength is not tryptophan concentration dependent supports specific species exist in the solution of tryptophan. At different concentrations the population of different species will be different, but not the types of species. Each type of species will have a definite emission maximum. A definite excitation wavelength will excite a definite species, then result in the dependence of maximum emission wavelength on excitation wavelength.

Exponential decay behavior of tryptophan fluorescence is dependent on excitation wavelength (1,9) The dependence is due to the associates in the solutions. As we know different excitation wavelengths will excite different species. It is very easy to understand different species will have different decay behaviors so dependence of decay on the excitation is the result. The decay of tryptophan is concentration dependent and solvent dependent. The different concentration will have different distribution of associates, in other words different concentration of excitation favor species.

It has been demonstrated that the fluorescence properties of some probes are sensitive to the hydrogen-bonding character of the solvent (10). The clearest manifestation of this effect is the drastic increase in the fluorescence lifetime in going from protic to polar approtic media. So the increase of the lifetime in the mixture of ethanol and water is due to the decrease of hydrogen bonding in the mixture than in pure water.

The fluorescence of tryptophan is due to the indole ring. The indole fluorescence is not excitation wavelength dependent. The only difference in indole and tryptophan is that tryptophan has side chain. The side chain of tryptophan is the reason for the formation of

associates. So the nondependence of indole emission on the excitation wavelength supports strongly our proposal of associates of tryptophan in the solution.

7.5 Conclusion

The maximum emission of tryptophan fluorescence in solution is excitation wavelength dependent. The dependence is the result of multiple molecule associates of tryptophan. These multiple molecule associates will have specific electronic structure and specific excitation energy. Different excitation wavelength will favor different specific species, resulting in different emission wavelengths.

The nondependence of emission on the excitation wavelength of indole fluorescence support strongly the assumption of associates in tryptophan solutions.

7.6 References

1. A. G. Szabo and D. M. Rayner, *J. Am. Chem. Soc.*, **102**, 554-563(1980)
2. David Creed, *Photochem. Photobio.*, **39**, 537(1984)
3. L. P. McMahon, W. J. Colucci, M. L. McLaughlin and M. D. Barkley *J. Am. Chem. Soc.*, **114**, 8442-8448(1992)
4. Hong-Tao Yu, W. J. Colucci, M. L. Mclaughlin and M. D. Barkley, *J. Am. Chem. Soc.*, **114**, 8449(1992)
5. Hong-Tao Yu, M. A. Vela, F. R. Fronczek, M. L. McLaughlin and M. D. Barkley, *J.Am. Chem. Soc.*, **117**, 348-357(1995)
6. Yu Chen, Bo Liu, Hong-Tao Yu and Mary D. Barkley, *J. Am. Chem. Soc.*, **118**, 9271-9278(1996)
7. S. Guha, S. S. Rawat, A. Chattopadhyay and B. Bhattacharyya, *Biochem.*, **35**,13426(1996)
8. J. R. Lakowicz, *Principles of Fluorescence Spectroscopy*, Plenum Press, New York and London(1983)

9. W. X. Balcavage and T. Alvager, *Mol. Photochem.*, **7**, 309 (1976)

10. Ramamurthy, V., *Photochemistry in Organized & Constrained Media*, VCH(1991)

Chapter 8

EXCITATION SPECTRA STUDY OF PYRANINE IN WATER AND DIFFERENT SOLUSITIONS WITH DIFFERENT CONCENTRATIONS

8.1 Introduction

The excitation spectrum is the dependence of emission intensity at a single wavelength upon the excitation wavelength (1). The excitation spectrum represents the relative quantum yield at each excitation wavelength. The excitation spectrum of a fluorophore is typically superimposable on its absorption spectrum, but excitation has advantage over adsorption on the sensitivity. Much higher sensitivity can be realized in the excitation spectra which means more information can be obtained. Excitation spectra reflect the vibrational levels of excited states. In general, the excited states and ground states will have the same vibrational structures so we can obtain the information of ground state vibrational structure by interpreting the data we obtained from excitation spectra.

The intensity of the excitation spectrum can be much higher than emission intensity for the same concentration solution. Therefore, the excitation spectrum can provide us information which would not show up in the emission spectra, such as the fine vibronic structure. It is a good supplement to the emission spectrum.

The majority of chemical or biological reactions occur in solutions. The interaction and behavior of solvent and solute in solutions has remained an interesting topic to many researchers for many years. It is clear that the properties of solute molecules will be

modified by solvents. Understanding the interaction is essential for the intrinsic properties of solutes to be understood better (2). Many crystallization processes occur from solutions; therefore, understanding the structure of solution, especially supersaturated solution structures, can help us to design and control crystallization better. Although such research has been conducted for decades, it is still not clear about what happens in solutions.

Excitation is seldom used as research method although Tucker (3) showed it a more convenient, fast and reliable for study of fluorescence quenching phenomena and less tedious and time consuming for the examination of spectra than simple emission (3).

In this research the excitation spectra of pyranine in water and in different concentrations of tryptophan, phenylalanine and nicotinic acid solutions at 510nm and 382nm emission wavelengths will be examined. The information about the interaction of solute molecules with pyranine will be described.

8.2 Materials and methods

Pyranine, also known as FDA D&C Green No. 8, was obtained from Lancaster, Windharn, NH and used as received. Aqueous solutions of pyranine were prepared by dissolution of 0.026 g in 5ml HPLC grade water. Three different concentrations of solutions were prepared by dissolving the appropriate amount of solutes in 5ml HPLC water. They are under saturated , saturated and supersaturated solutions. Supersaturated solutions were prepared by heating the solution in the water bath until all the solute was dissolved and subsequent cooling to room temperature. The solutions were used as prepared without any degassing.

Probe molecules were introduced by addition of five microliters of the pyranine solution to 5ml aqueous tryptophan, nicotinic acid and phenylalanine solutions resulting in a probe concentration of 10^{-5}M. All excitation spectra were collected at room temperature with a Spex 1681 Fluorolog spectrometer equipped with a Xenon lamp source and a PMT detector. A quartz sample holder was used in all cases. Spectra were recorded at 1.00mm

increment and an integration time of 1.0 sec. Emission wavelengths of 382nm and 510nm were used. The excitation spectra were recorded over a range from 260nm to 370nm for the 382nm emission wavelength and 280nm to 480nm for the 510nm emission wavelength. Monochromator slits were set at 0.5 mm for all spectra.

8.3 Results and discussions

8.3.1 Excitation spectra at 510nm emission wavelength

8.3.1.1. Excitation spectra at 510nm of pyranine in water and low concentration solutions

Excitation spectra of pyranine in water and low concentration of tryptophan, phenylalanine and nicotinic acid solutions at 510nm are shown in Figure 8.1. There are large differences between the excitation spectrum of pyranine is in water and excitation spectra of pyranine in tryptophan, phenylalanine and nicotinic acid solutions. There is a set of peaks around 460nm which are pretty strong when pyranine in water. Fine vibrational structure shows up in this set of peaks. There are some broad peaks from 360nm to 440nm. There is also a broad band which has two peaks at 290nm and 298nm respectively. The addition of solutes into the water alters the excitation spectrum of pyranine greatly even in trace amounts. With even trace amounts of phenylalanine and nicotinic acid in solution, the intensity of the band around 460nm decreases dramatically. The band at 402nm and 380nm shows up with the addition of solutes into water. The band around 460nm decreases a lot with the addition of tryptophan and phenylalanine and disappears with the addition of nicotinic acid. With the addition of phenylalanine the peak at 298nm disappears and the peak at 290nm increases. With the addition of tryptophan and nicotinic acid in solution, the band at lower wavelengths disappears. The band at lower wavelength can be assigned to the interaction of pyranine with water. The disappearance of the lower wavelength peaks can be interpreted as that the interaction between pyranine and solutes. The interaction between pyranine-nicotinic acid and pyranine-tryptophan are

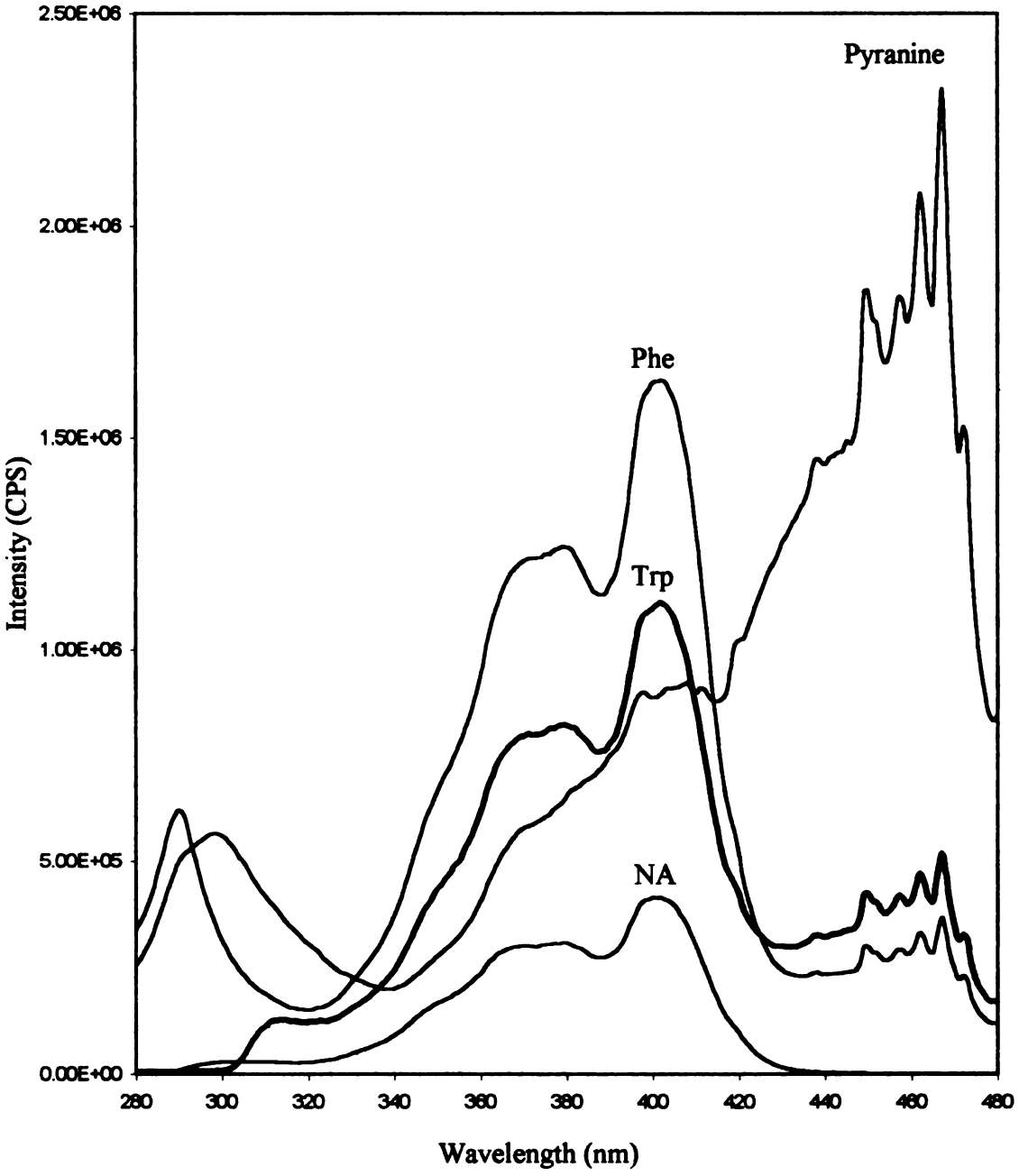

Figure 8.1 Excitation spectra of pyranine in water and in tryptophan(0.266g/100ml H_2O), phenylalanine(0.33g/100ml H_2O) and nicotinic acid(0.302g/100ml H_2O) aqueous solutions at 510nm emission wavelength at room temperature.

stronger which destroys the interaction between pyranine and water. The interaction of phenylalanine with pyranine is not as strong as nicotinic acid with pyranine but it is stronger than pyranine with water. Only one peak disappears. This results match quite well with the quenching results which is shown in chapter 5.

The excitation spectrum at emission wavelength 510nm and the emission spectrum with peak at 510nm of pyranine in water is shown in Figure 8.2. The spectra were obtained from the same solution at the same time. The intensity of the excitation is much higher than the emission spectra. In order to make them in the same scale, we decrease the slits to 0.25mm for the excitation spectra and the emission spectrum is at 0.5mm slit open. The emission spectrum shows a broad and single band with the peak at 510nm. The excitation spectrum shows the fine vibrational structure with five peaks around 460nm. They are at 450nm, 452nm, 457nm, 462nm, and 467nm respectively. The shape of this band is quite similar as the mirror of typical emission spectra of the polycyclic aromatic hydrocarbon (PAH). The typical emission spectrum of the PAH monomer will consist of five major vibronic bands which are generally labeled as I-V in progressive order, such as the 0-0 band is labeled I, etc.(4-9). If we ignore the fine structure in the excitation spectra, the emission spectra can be considered as a mirror image of the excitation image. The fluorescence spectrum of 1-aeabenz[a]anthracene in trifluoroethanol and in $HClO_4$-trifluoroethanol is reported to move from 360nm-405nm to 460nm-560nm with the protonation of the nitrogen lone electron pair by a hydrogen ion. At the same time the a broad, single band will replace the original fine vibrational structure bands (7). When pyranine is in high concentrations of weak acid solutions, two excited fluorescent states will exist and one in which the hydroxyl proton is associated with the molecule (PyOH) and one in which it is dissociated in pyranine (PyO^-) (10). The emission from PyOH* is at 440nm and the absorption at 405nm. PyO^-* will absorb at 445nm and emit at 510nm. The fluorescence of pyranine in water exhibits two bands one is from 370 to 430nm which contains three fine vibrational structure peaks and another is a broad band centered at

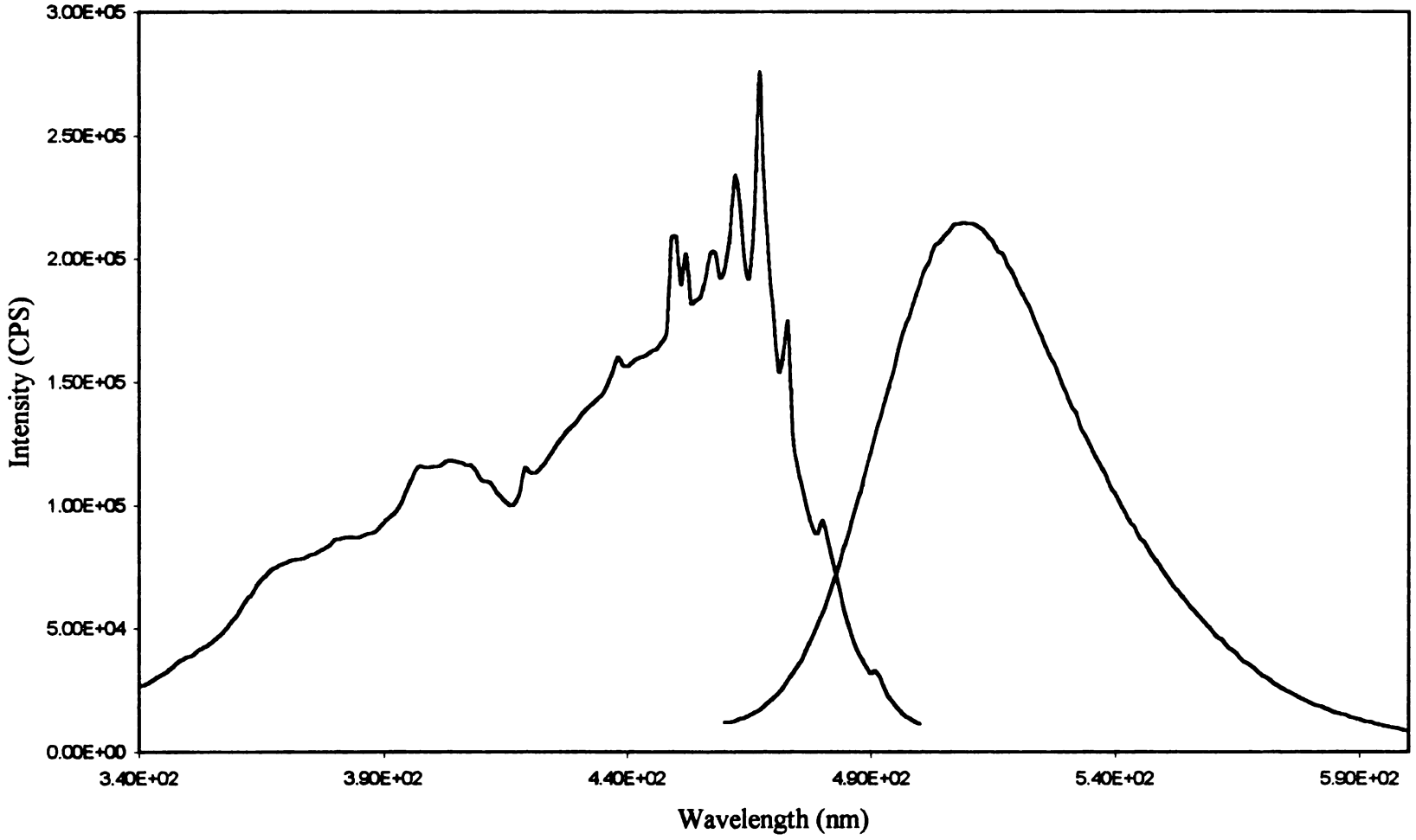

Figure 8.2 Emission spectrum of pyranine in water excited at 342nm and excitation spectrum of pyranine in water with emission wavelength 510nm at room temperature

510nm. The excitation from 370nm to 430nm will be discussed later. From the excitation spectrum we see a peak around 405nm which is assigned as the excitation of PyOH. The band with the fine vibrational structure around 460nm will be assigned to the excitation of PyO^-. The emission spectra will reflect the vibrational levels of the ground state and the excitation spectrum will reflect the vibrational levels of the excited states. The excited state has a higher dipole moment than ground state. PyO^{-*} will have a greater dipole moment than PyOH* because of the lack of the hydrogen ion which results in much larger energy spacing between the various vibrational levels. The fine vibronic structure can be detected in the excitation of PyO^-. In water, pyranine is surrounded by dipole orientated water molecules. In the inner layer water molecules will be bonded firmly with entirely dissociated sulfonate groups with a scheme shown in Figure 8.3. This is the reason that pyranine has such a high solubility in water. Peaks around 405nm and 460nm are the excitation of solvated PyOH (4.15×10^{-6}M) and PyO^- (5.85×10^{-6}M), respectively. The firmly bounded solvated pyranine PyO^- will show fine vibronic structures due to a higher dipole moment which is not hard to tell from the structure. We see almost continuous increasing in intensity of excitation spectrum from 340nm to 440nm which can be interpreted as at outer layer some non-orientated water molecules will bound with pyranine loosely. These loosely bounded water molecules at the outer layer will alter the energy of pyranine in some way. Because the bonding is really loose, and those loosely bonded water molecules move around in some region, the energy change is really small. The much higher intensity of the excitation than the emission is the result of quenching from water. Water will quench the fluorescence of pyranine but the excitation intensity will not be affected by quenchers that effectively.

The larger change in excitation spectra at 460nm with the addition of solutes into water is because all the solutes are acids. The addition of acid will favor PyOH in the equilibrium in solutions. The peak at 405nm, which is assigned as the excitation of PyOH,

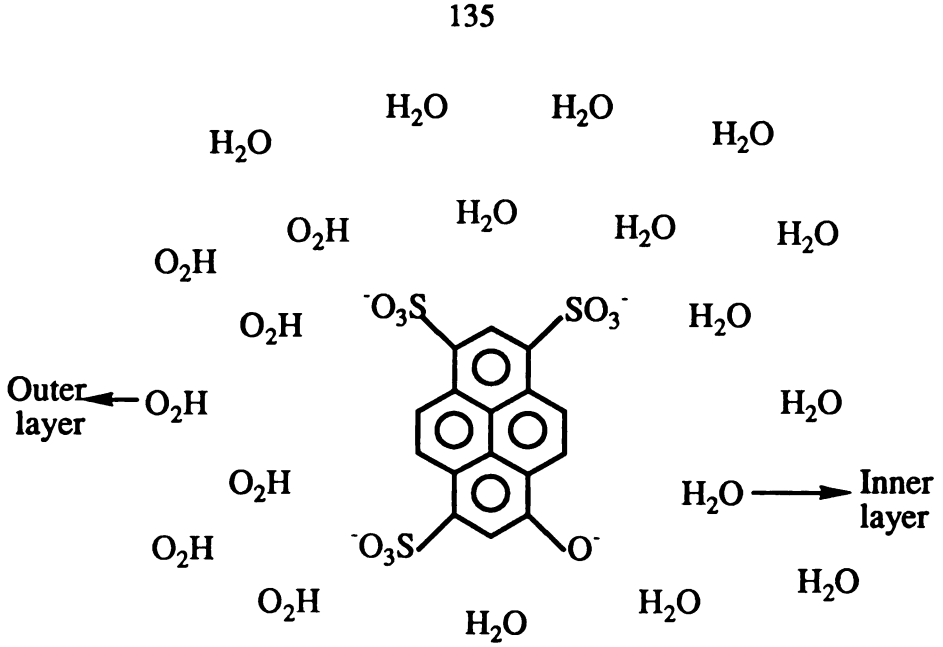

Solvated pyranine molecule in water

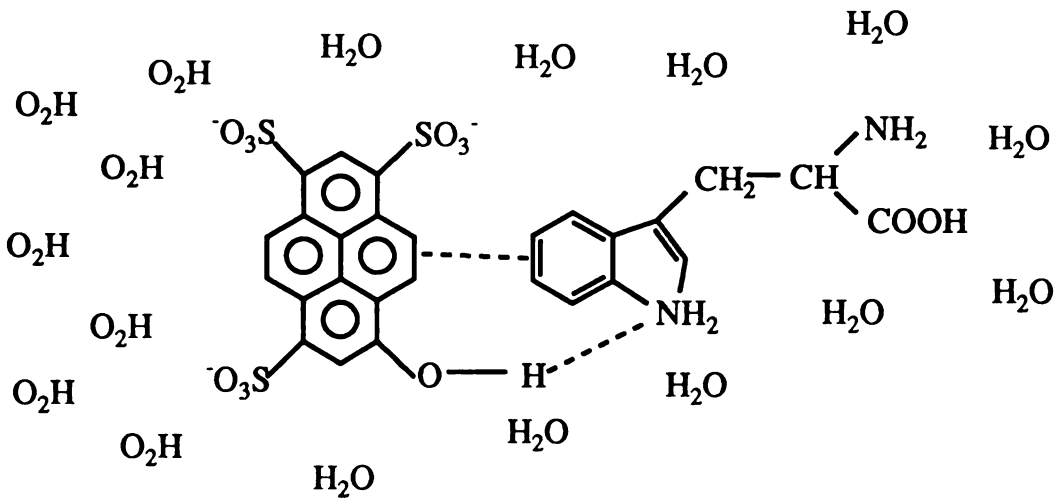

Solvated of complex between pyranine and tryptophan

Figure 8.3 Scheme of solvated structure of PyO- and the contact complex betweeen pyranine and tryptophan, phenylalanine and nicotinic acid

increases and the peak around 460nm, which is assigned as the excitation of $PyOH^-$, decreases. Especially, with the addition of nicotinic acid, the acidity of the solution has a larger increase, all pyranine will exist in the form of PyOH according to the calculation. The peak at 460nm disappears with the addition of nicotinic acid. However, the emission of pyranine in tryptophan, nicotinic acid and phenylalanine are all from PyO^{-*} due to the fast proton transfer reaction at excited states (refer to chapter 2 for details).

Even trace amounts of phenylalanine in solution, which does not change the pH of solution much, will decrease the intensity of the peak at 467nm significantly. We may conclude that the shift between PyOH and PyO- equilibrium may not be the only reason for the intensity change of two peaks. If the shift of the acid-base equilibrium between PyOH and PyO^- is the only reason for the peak change at 402nm and 467nm, the ratio of [PyO-]/[PyOH] should be equal to the ratio I_{467nm}/I_{402nm} at different pHs. Figure 8.4 shows the ratio of [PyO-]/[PyOH] and I_{467nm}/I_{402nm} at different pH values for phenylalanine and tryptophan solutions. The two ratios do not change the same way with the pH. The acidity of the solutions increases with the addition of phenylalanine and tryptophan to solution. The equilibrium between PyOH and PyO^- shifts from PyO^- to PyOH. The concentration of PyOH increases, so does the intensity at 402nm. The intensity increase is larger than the concentration increase which means some other factors will affect the intensity at 402nm. The other factor is the interaction of phenylalanine and tryptophan with pyranine. As we know from chapter 5, phenylalanine will quench fluorescence of pyranine slightly. If phenylalanine is far away from pyranine, the fluorescence of pyranine will be much more easily quenched by water around pyranine which is much smaller and will form hydrogen bonding complex with pyranine. The hydrogen bonding complex is the most effective quenching mechanism as evidenced by the stronger quenching of nicotinic acid and tryptophan. Pyranine can form a hydrogen bonding complex with water; therefore, water will quench the fluorescence of pyranine. Phenylalanine has a benzene ring structure. It is

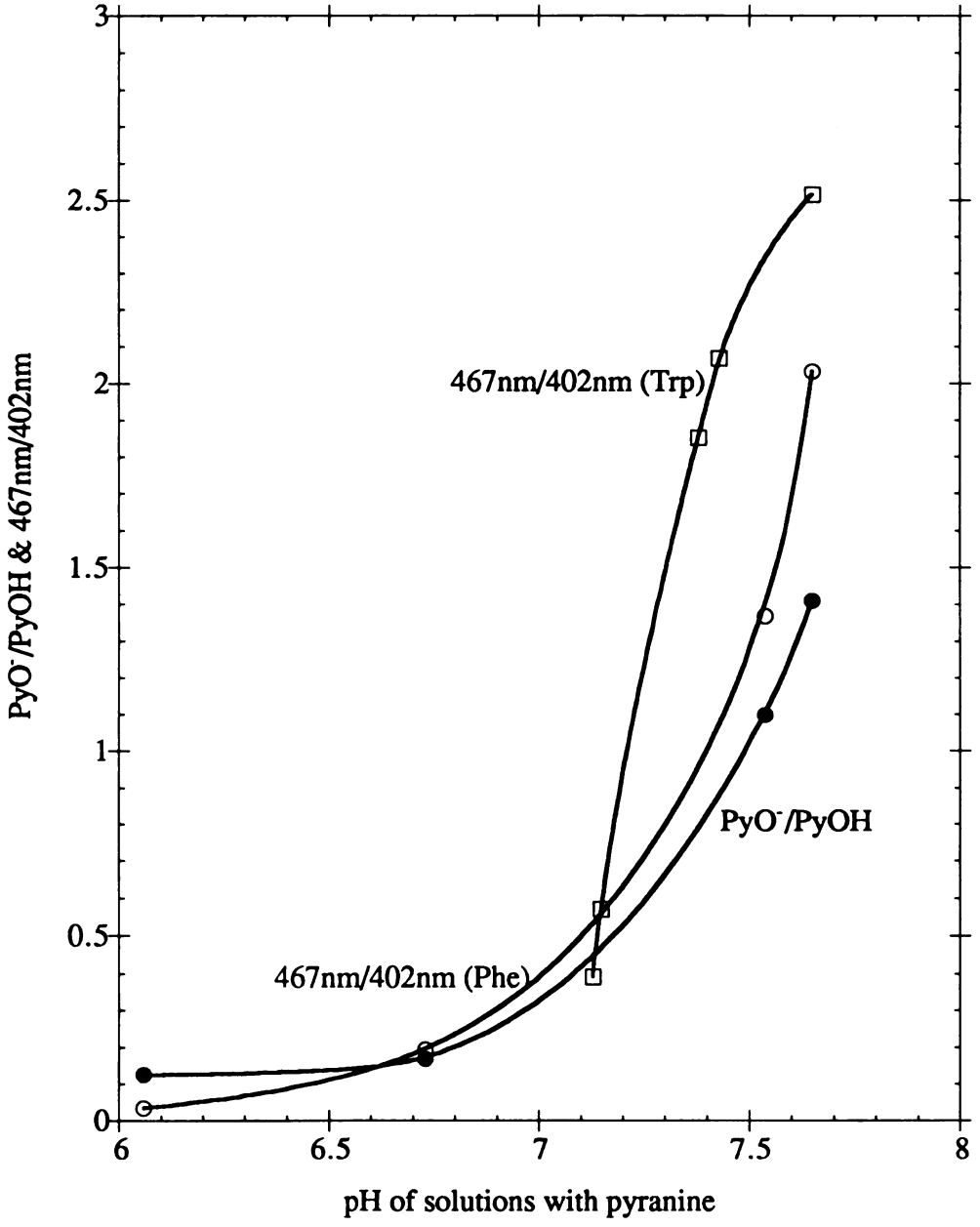

Figure 8.4 The concentration ratio of PyO^- and PyOH calculated based on pH and fluorescence intensity ratio of 467nm/402nm versus pH of solutions in tryptophan and phenylalanine solutions at room temperature.

very possible for pyranine and phenylalanine to be close to each other to form a kind of contact complex. It is feasible because phenylalanine will like pyranine better than water. When phenylalanine is added into water, it will try to find pyranine and to stay close to pyranine. When pyranine is excited, the distance of pyranine and phenylalanine becomes closer which is an exciplex. By formation of the exciplex, the fluorescence of pyranine is quenched. This contact complex will stabilize PyOH better because of the lower dipole moment of PyOH as compared to PyO^- and this contact complex can protect pyranine from quenching by water.

Tryptophan has two interactions with pyranine. Tryptophan will form a contact complex with pyranine similar to phenylalanine. The amine in the ring of tryptophan can form hydrogen bonding with the hydroxyl group in pyranine as shown in Figure 8.3. This function of tryptophan will pull the hydrogen ion from pyranine so it favors PyO^-. Trace amounts of tryptophan will not eliminate the peak at 467nm at all because the acid-base equilibrium will favor PyOH. These double functions of tryptophan results in the downward curve for the change with pH in tryptophan solution (Figure 8.4).

With the addition of nicotinic acid, the acidity of the solution will change significantly and the equilibrium between PyO^- and PyOH will all shift to PyOH. The shift will be the dominant factor.

The formation of a contact complex between pyranine-tryptophan and pyranine-phenylalanine will hinder the water accessibility of pyranine and limit the rotation of pyranine especially around hydroxyl group side (Figure 8.3). The addition of tryptophan and phenylalanine will increase the fluorescence intensity of pyranine at 510nm. Nicotinic acid has a strong quenching ability for pyranine and even trace amounts of nicotinic acid decrease the fluorescence intensity significantly.

8.3.1.2. Excitation spectra of pyranine in different concentration of solutions

The shape and maximum of the excitation spectra of pyranine does not change much with the increase of solute concentration except that the peak around 460nm disappears at higher concentration of phenylalanine. The intensity of the excitation spectra of pyranine decreases with the decrease of the concentration of tryptophan. The intensity changes a little with the concentration of phenylalanine. In nicotinic acid the intensity decreases dramatically with the increase of the concentration of nicotinic acid, but the shape and maximum remains unchanged. The intensity decrease results from the quenching of pyranine by solutes.

8.3.2 Excitation spectra at 382nm emission wavelength

8.3.2.1. Excitation spectra of pyranine in water and low concentration solutions

Figure 8.5 shows the excitation spectra of pyranine in water and in low concentrations of tryptophan, phenylalanine and nicotinic acid. There are four peaks in the excitation spectrum of pyranine in water and they are 270nm, 281nm, 448nm and 366nm and also a shoulder at 334nm. There is a peak at 308nm which is the excitation peak of tryptophan. With the addition of solutes in the water, the excitation intensity will drop. Nicotinic acid has the highest drop in intensity and tryptophan has an intermediate intensity drop and phenylalanine drops the least. The different decreases of the excitation intensity matches the different quenching abilities of the solute molecules to pyranine. As shown in chapter 5, nicotinic acid has the strongest quenching ability to pyranine and phenylalanine quench the fluorescence of pyranine only slightly.

With the addition of tryptophan and nicotinic acid into the water, the excitation peaks of pyranine at lower wavelengths disappears. Those peaks at low wavelengths can be assigned as the interaction between water and pyranine. The addition of tryptophan and nicotinic acid into water destroys the interaction between pyranine and water molecules

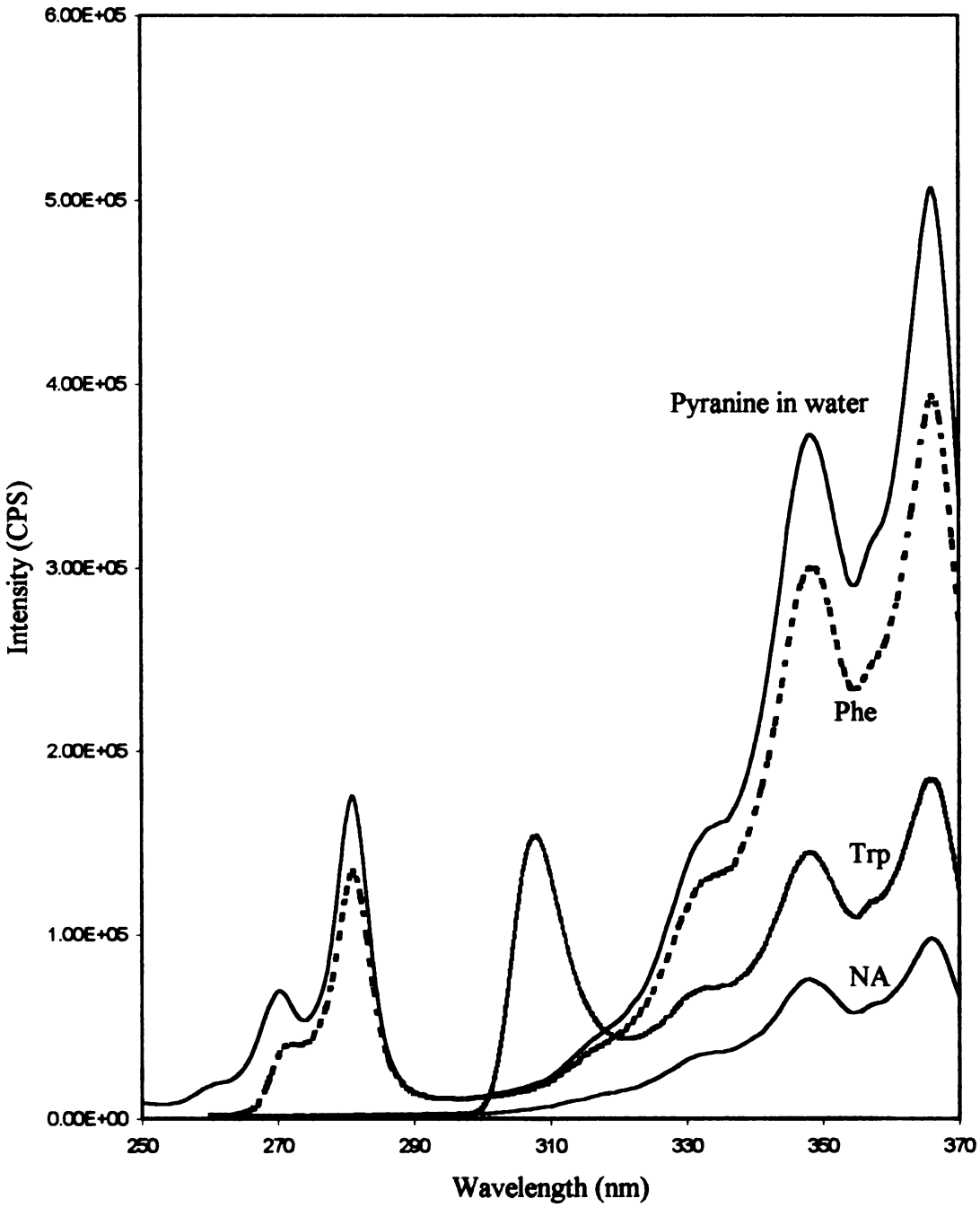

Figure 8.5 Excitation spectra of pyranine in water and in tryptophan(0.266g/100ml H_2O), phenylalanine(0.33g/100ml H_2O) and nicotinic acid(0.302g/100ml H_2O) aqueous solutions at 382nm emission wavelength at room temperature.

because of the stronger interaction of pyranine with tryptophan and nicotinic acid. Phenylalanine will have weaker interactions with pyranine compared with tryptophan and nicotinic acid, so the lower wavelength peak at 281nm remains in phenylalanine solutions, but the peak at 270nm is diminished.

The emission spectrum and excitation spectrum with 382nm emission wavelength of pyranine in water are shown in Figure 8.6. A good mirror image is observed.

8.3.2.2. Excitation spectra of pyranine in different concentration of solutions

The excitation spectra of pyranine in different concentrations of tryptophan are shown in Figure 8.7. The peak around between 300nm to 320nm is the excitation peak of tryptophan. As shown in chapter 7, the excitation spectra of tryptophan will shift to longer wavelengths with the increase of the concentration and the intensity will increase at the same time without pyranine in solution. With pyranine in solution, the red shift is the same, but the intensity decreases with the increase of the concentration. The pyranine excitation intensity at peak 348nm and 366nm decreases a lot with the increase of the concentration of tryptophan. Once again it matches with the quenching of tryptophan to pyranine.

Excitation spectra of pyranine in different concentrations of phenylalanine solutions are shown in Figure 8.8. The positions of the peaks are almost the same as pyranine in water. The peak intensity will decrease with the increase of concentration of phenylalanine. Because the unstability of supersaturated solutions of phenylalanine, we can not go to high supersaturations. As discussed in Figure 8.5, with the addition of phenylalanine, the peak at 270nm is eliminated, but with the increase of phenylalanine concentration, the peak at 270nm disappears. The disappearance of the peak can be interpreted as that the interaction of phenylalanine with pyranine is stronger than the interaction of water with pyranine although there is no hydrogen bonding between phenylalanine and pyranine. The contact

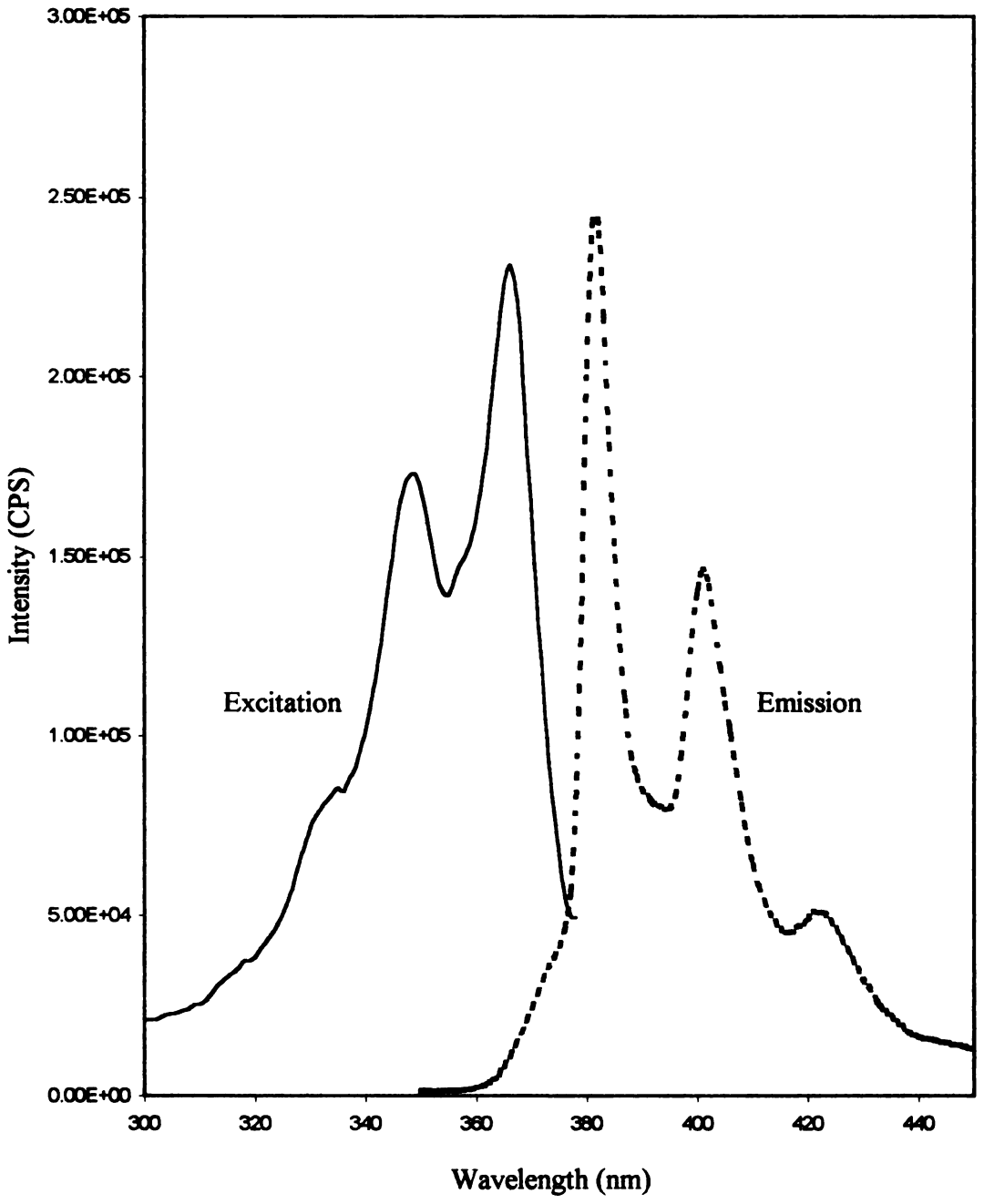

Figure 8.6 Emission spectrum of pyranine(10^{-5}M) in water excited at 342nm and excitation spectrum of pyranine(10^{-5}M) in water with emission wavelength at 382nm at room temperature

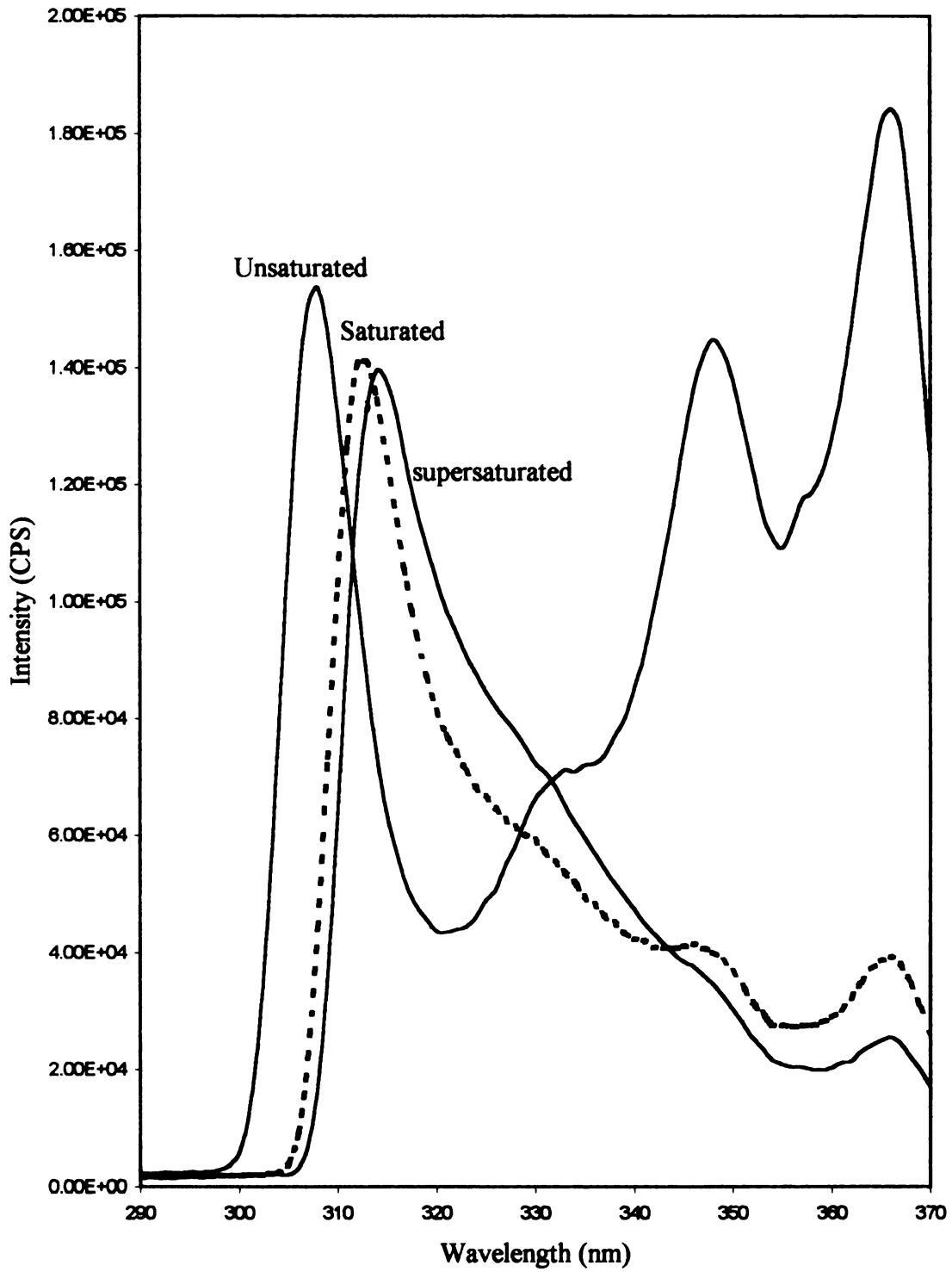

Figure 8.7 Excitation spectra of pyranine in different concentration of tryptophan aqueous solutions at 382nm emission wavelength at room temperature. Unsaturated: 0.266g, saturated: 1.112g, supersaturated: 1.574g in 100ml H_2O

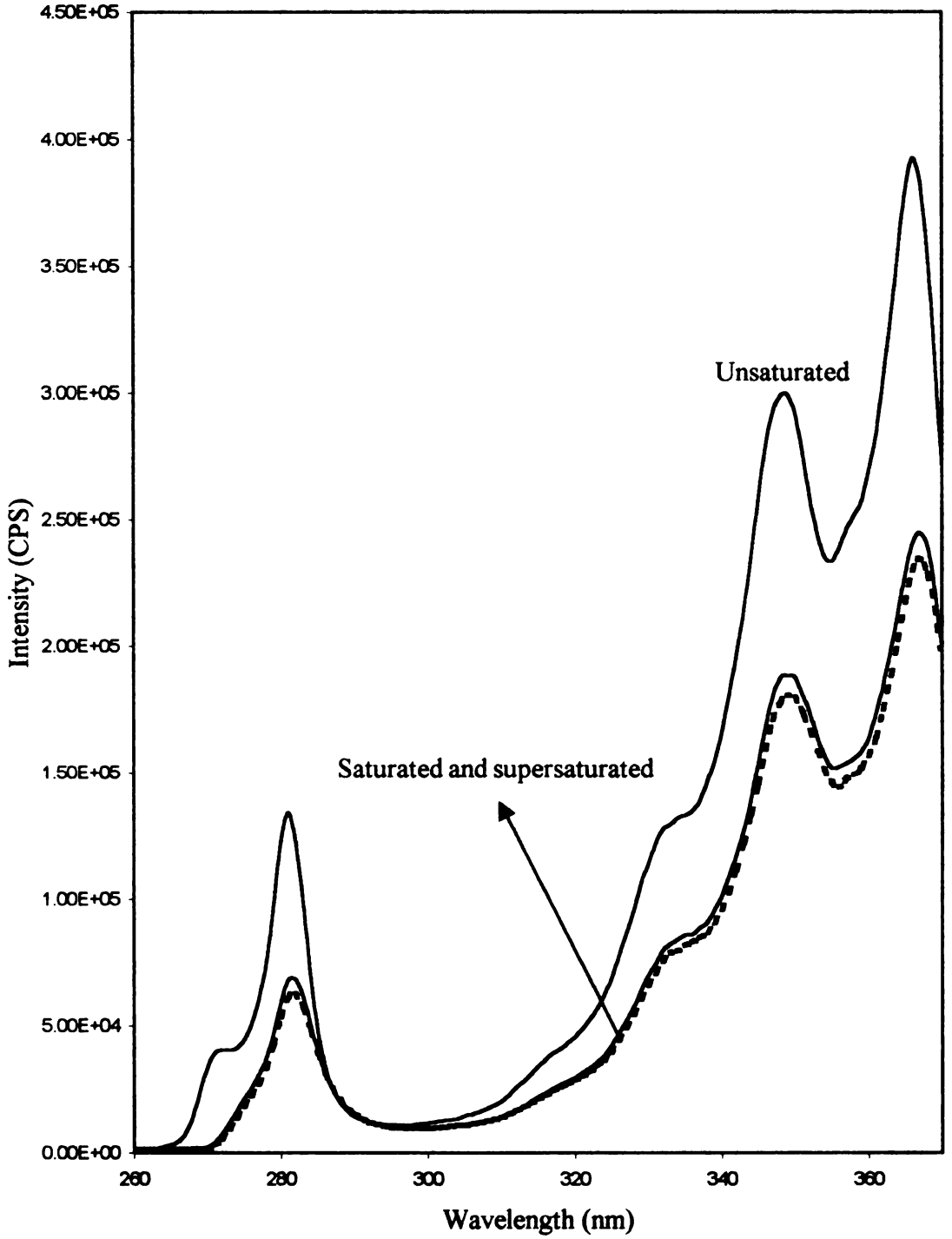

Figure 8.8 Excitation spectra of pyranine in different concentration of phenylalanine aqueous solutions at 382nm emission wavelength at room temperature. Undersaturated: 0.33g, saturated: 2.648g, supersaturated: 3.2g in 100ml H_2O

complex forms between pyranine and phenylalanine; therefore, with the addition of phenylalanine, the interaction between water and pyranine which has the peak at 270nm is destroyed by phenylalanine. With the increase of the concentration, the replacement of water by phenylalanine increases, thus the decrease of the peak at 270nm, and finally disappearance of peak 270nm.

Excitation spectra of pyranine in different concentration of nicotinic acid solutions show a large decrease in the excitation intensity with the increase of the nicotinic acid concentration This sharp decrease is the result of the strong quenching ability of nicotinic acid.

8.4 Conclusion

The excitation spectra of pyranine change dramatically with the addition of solutes in even trace amounts. For the excitation spectra at 510nm, a large decrease at 460nm and increase at 402nm is the results of the acid-base shift between PyO^- and PyOH and contact complex formation between pyranine and solute molecules. The disappearance of peaks at lower wavelengths of excitation with the addition of solutes into water was taken as the evidence of the formation of the complex which destroys the interaction of pyranine with water.

8.5 Reference

1. J. R. Lakowicz, *Principles of Fluorescence Spectroscopy*, Plenum Press, New York and London(1983)

2. J. F. Coetzee, C. D. Ritchie, *Solute-solvent interactions*, Marcel Dekker, New York and London(1969)

3. S. A. Tucker, W. E. Acree, JR., *Applied Spectroscopy*, **46**(9), 1388(1992)

4 Jan Stahlberg and Mats Almgren, *Anal. Chem.*, **57**, 817-821(1995)

5 W. E. Acree, JR., S. A. Tucker, A. I. Zvaigzne, Hans-FR. Grutzmacher,

Applied Spectroscopy, **44**(3), 477(1990)

6 S. A. Tucker, W. E. Acree, JR., and M. J. Tanga,
Applied Spectroscopy, **45**(1), 57(1991)

7 S. A. Tucker, W. E. Acree, JR., and M. J. Tanga, M. Zander, J. C. Fetzer, S. Tokita, K. Hiruta, K. Kitahara and H. Nishi,
Applied Spectroscopy, **45**(7), 1188(1991)

8 S. A. Tucker, W. E. Acree, JR., and M. J. Tanga, S. Tokita, K. Hiruta, and H. Langhals, *Applied Spectroscopy*, **46**(2), 229(1992)

9 M. U. Kumke, H. G. Lohmannsroben and Th. Roch, *Analyst*, **119**, 997(1194)

10. H. Kondo, I. Miwa, and J. Dunamoto, *J. Phys. Chem.*, **86**, 4826-31(1982)

Chapter 9

SUMMARY OF THE WORK AND PROPOSED FUTURE WORK

9.1. Summary of the work

In this research pyranine, PBA and CA were investigated as potential fluorescence probes to measure the supersaturation of low solubility aqueous systems, such as tryptophan. nicotinic acid, phenylalanine and benzoic acid. The measurement of supersaturation is realized by measuring the concentration of solution. Any physical properties which change with the concentration can serve as the calibration curves to measure the supersaturation. Fluorescence was shown to be a very useful technique to measure the supersaturation of low solubility systems due to the change of PIR (Peak Intensity Ratio) of fluorescence with concentration. Monitoring the PIR during the crystallization, we can know the supersaturation. By changing the outside conditions, we can control the supersaturation resulting in control of the crystallization for desired crystal size distributions (CSD).

Pyranine was shown as a very promising probe for use as the sensor to monitor crystallization in the solution due to the smooth and nonlinear calibration curves which show a higher signal response at supersaturated region. Additionally, pyranine will not enter the crystal lattice of the crystalline products. Pyranine is not listed as a food additive by FDA, so it can not be added directly into food and pharmaceutical production process. Carminic acid (CA), one of approved food additives by FDA, was investigated as a potential probe to measure the supersaturation. CA was shown to be a good sensor for phenylalanine by following the intensity change with the concentration of phenylalanine.

Another way to avoid adding the probe into the system directly is to immobilize the probe molecule. Due to the good behavior of pyranine in water solution as a probe sensor, pyranine was immobilized onto an ion-exchange membrane to prevent it from possibly contaminating the crystal products. The PIR (Peak Intensity Ratio) changes linearly with the concentration of solutes for immobilized probe.

Fluorescence quenching requires the contact of fluorophores and quenchers, so the interaction of fluorophore and quenchers can provide information about the organization of solutes in solutions. All quenching curves show discontinuities in supersaturated region which indicates the different solution structure of supersaturated solutions and unsaturated solution. This discontinuity was taken as the evidence of the formation of aggregates of the solutes in supersaturated solutions. Different molecules such as tryptophan, nicotinic acid and phenylalanine show totally different quenching behaviors relate to pyranine in solution or to immobilized pyranine. The different quenching behaviors are the results of the different interactions of pyranine with solute molecules. The contact complex was suggested as the mechanism of the interactions between pyranine and solute molecules. The stronger quenching abilities of tryptophan and nicotinic acid are the results of formation of hydrogen bonding complex with pyranine due to the presence of the amine in the rings. The different steady state quenching and lifetime quenching behavior of phenylalanine support strongly the contact complex assumption. The excitation spectra of pyranine changes significantly even with the addition of trace amount of solutes into water and the different dependence of concentration ratio and intensity ratio on pH of solutions also support the formation of contact complex assumptions. The associates were suggested in tryptophan solutions and phenylalanine due to the downward curvatures of quenching plots of phenylalanine for pyranine and tryptophan for carminic acid. It was shown only 73% of phenylalanine and tryptophan are accessible to the fluorophore to quench the fluorescence. The excitation wavelength dependence of the tryptophan maximum emission wavelength support the exists of the associates in tryptophan solutions.

9.2 Future work

9.2.1 Structure study of supersaturated solutions

Due to the importance of the supersaturation to crystallization , the structure of supersaturated solutions is always an important subject. The fluorescence quenching technique is shown as a powerful tool for system study. So much useful information can be obtained from such a simple technique. The fluorescence quenching technique should be paid much attention due to its high sensitivity to the interaction. Some systematic research can be conducted to investigate the reason for such different quenching behaviors by different molecules. By choosing different structures of molecules, such as some molecules with the similar structure as tryptophan. nicotinic acid and phenylalanine, we can tell what is the main reason for the different quenching behavior, then the different interactions will be interpreted. Suggested molecules are shown in Figure 9.1 which have similar structure as tryptophan or phenylalanine. Using these molecules as target molecules to study the different quenching then to obtain the information about interactions.

The interaction of molecules will change the properties of the molecule somehow. So any techniques which can detect the change due to the interaction can be employed as tools to study the structure of solutions. Due to the improvement of the sensitivity of old techniques, such as Raman, FTIR and UV-Vis, they may be utilized as the analytical techniques to detect the interactions in solutions because the interaction may change the vibration frequency. The change of the vibration frequency can be used as the evidence to interpret the interaction of molecules. The same material in solid and solution phase will have different Raman shifts which may be provide some information about the structure. New method may be developed for this purpose.

Time resolved fluorescence is always a very powerful technique to study the interaction of molecules. Measurements of the rotational transport properties of the

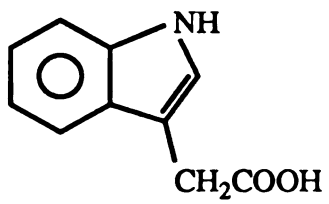

indoleacetic acid

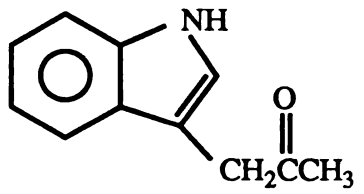

3-indolylacetone

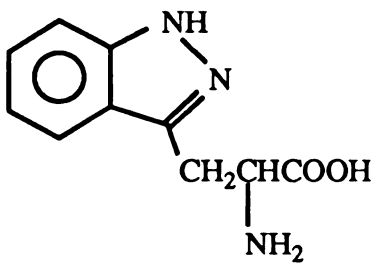

tryptazan

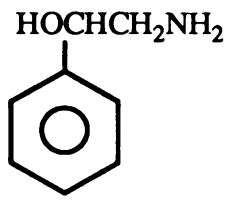

phenylethanolamine

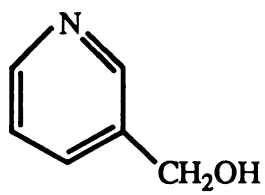

nicotinyl alcohol

Figure 9.1. Suggested molecules can be used to study fluorescence quenching systemically as compared to tryptophan, phenylalanine and nicotinic acid

fluorophores, obtained from fluorescence depolarization techniques, are highly sensitive to molecular scale interactions (1,2). The time dependent anisotropy measurements result in the direct quantization of rotational correlation times (1). The use of time resolved fluorescence methods to investigate the microscopic interactions between the solvent and solute and the supersaturated solution behavior should result in a more directed and rational approach to understand and control the crystallization. So more researches should be conducted by using time resolved fluorescence technique. The contact complex model can be invested by anisotropy measurements because the contact complex will slow the rotation rate of probe.

9.2.2. Flow Injection Analysis (FIA)

The automation of chemical methods is necessary for cost. safety and reliability. Conventional batch operations are not cost effective. In general, batch methods require highly skilled chemists to carry out the individual tasks and the reproducibility for batch operation is low (3). Batch analysis always involve multiple stages of careful operation, with frequent transfers of solutions from one vessel to another, and thus exposing the sample to serious contamination risks. Also during the transfer it is very easy to cause some changes, which makes the result different from the true situation (4).

Despite the obvious drawbacks of the manual batch procedure, little has been attempted for its automation, presumably owing to difficulties in designing efficient automated procedures. The difficulties in on-line continuous manipulation of a heterogeneous system come from potentially serious blockage problems.

The inception of FIA (flow injection analysis) is the result of a long search for better laboratory techniques in solution manipulation which could match the efficiency of the computer age. FIA was found to be powerful technique, not only for performing serial analysis, but also for separation operations. FIA is a non-chromatographic flow analysis technique for quantitative analysis, performed by reproducibly manipulating sample and

reagent zones in a flow under thermodynamically non-equilibrated conditions. Two basic features of FIA are: 1) reproducible manipulation of sample and reagent zones through precise timing; 2) quantitative evaluation of analyte concentration under thermodynamically nonequilibrated conditions (4). FIA methods exhibit extremely favorable features over batch analysis. They are high sample throughput, high enrichment efficiencies for preconcentration systems, low sample consumption, low reagent consumption, low contamination risks owing to closed and inert separation system, and high reproducibility. The most important is that simple automated operation which allows implementation with continues monitoring systems and use in process control (4)

A schematic diagram of basic FIA system showing the various components are shown in Figure 9.2. In this traditional FIA system the sample is added by pulses and reagent is continuously pumped. In our system the amount of sample available is large, so the design of such a system is a little different from the traditional way (3). In our system the reverse flow injection analysis (rFIA) is utilized. The main difference between FIA and rFIA is that in rFIA the samples are continuously pumped and the reagent which is probe in our case is injected(The schematic diagram of our system is shown next). The other differences of our system from conventional FIA:

1) Size of sample--sizes of sample are large in our system

2) Not filtered--no filtration is needed for our system

4) Recycle--after the analysis the solution can go back to crystallizer so there is no waste.

5) Slurry scattering--may be useful for measuring the amount of crystals

The advantage of using FIA for fluorescence based measurements is that the performance of fluorimetric detectors can be enhanced significantly. FIA stabilizes the solution conditions thereby increasing precision. The reproducibility of fluorescence measurements are reportedly improved by better control of the reaction conditions in the FIA systems, and selectivity may be enhanced by on-line removal of potential quenching interference using FIA separation techniques (3,4).

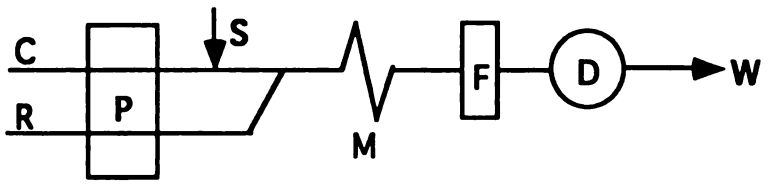

P: pump; C: carrier; R: reagent; S: sample injector; F: Filter
M: mixing(reaction) coil; D: flow through detector; W: Waste.

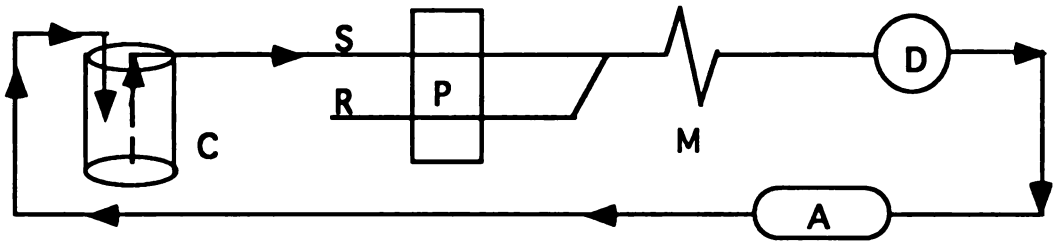

C: crystallizer; P: pump; S: crystallization slurry; R: probe solution;
M: mixing coil; D: fluorometer; A: remove probe;

Figure 9.2 A schematic diagram of basic flow injection analysis (FIA) system and reverse flow injection analysis (rFIA) showing the various components

In experiments crystallization solution is pumped through the tube and mixes with probe solution, the mixture flows through fluorolog spectrometer to measure the PIR, therefore supersaturation can be obtained. A crystallizer condition, such as temperature, can be changed to control the supersaturation as low as possible in order to obtain the desired CSD. The process is flowing all the time, and the supersaturation can be measured *in-situ* in real time. Using FIA, *in-situ* monitoring the crystallization can be realized.

9.3. References

1. V. R. Kaufman, D. Anvir, D. Pines-Rojanski, and D. Huppert, *J. Non-crystalline Solids*, **99**, 379-386 (1988)
2. J. C. Pouxviel, B. Dunn, and J. I. Zink, *J. Phys Chem.*, **93**, 2134-2139 (1989)
3. B. Karlberg, and G. E. Pacey, *Flow Injection Analysis-a Practical Guide*, Elsevier(1989)
4. Z. L. Fang, *Flow Injection Separation and Preconcentration*, VCH(1993)

Appendix

Appendix

Table A1 Raw data for Figure 2.4

Concentration of tryptophan (g/100ml H_2O)	**Peak Intensity Ratio (PIR) of 382/510**	**Peak Intensity Ratio (PIR) of 401/510**
0.510	0.290	0.194
0.588	0.285	0.200
0.692	0.286	0.208
0.812	0.302	0.233
0.934	0.320	0.254
1.02	0.342	0.283
1.10	0.369	0.308
1.20	0.388	0.337
1.32	0.432	0.388
1.43	0.474	0.433
1.53	0.530	0.491
1.65	0.575	0.543
1.73	0.630	0.595
1.89	0.716	0.696

Table A2 Raw data for Figure 2.5

Concentration of nicotinic acid (g/100ml H_2O)	Peak Intensity Ratio (PIR) (428/510)
0.00	0.101
0.320	0.145
0.836	0.232
1.04	0.274
1.38	0.358
1.74	0.465
1.91	0.561
2.24	0.653
2.46	0.705
2.71	0.839

Table A3 Raw data for Figure 2.6

Concentration of bezoic acid (g/100ml H_2O)	Peak Intensity Ratio (PIR) (382/509)
0.000	0.612
0.056	0.454
0.121	0.499
0.248	0.553
0.320	0.601
0.412	0.659
0.462	0.732
0.556	0.803

Table A4 Raw data for Figure 3.3

Trp	PIR	Phe	PIR	NA	PIR
0.634	0.307	0.766	0.196	0.460	0.501
0.820	0.332	1.088	0.201	0.694	0.547
0.986	0.348	1.636	0.204	0.844	0.556
1.129	0.369	2.156	0.214	1.058	0.563
1.368	0.411	2.452	0.217	1.322	0.594
1.624	0.476	2.704	0.212	1.520	0.621
1.784	0.471	2.874	0.207	1.790	0.625
1.880	0.513	3.168	0.207	2.052	0.636
		3.260	0.214	2.234	0.658
		3.456	0.217	2.652	0.683
		3.690	0.219		

Table A5 Raw data for Figure 3.4

Reproducibility of immobilized pyranine in tryptophan solutions

Concentration of tryptophan (11/12)	PIR	Conecntration of tryptophan (11/18)	PIR
0.00	0.1840	0.634	0.3074
0.214	0.2295	0.820	0.3321
0.394	0.2526	0.986	0.3479
0.640	0.2636	1.128	0.3696
0.832	0.2957	1.368	0.4113
1.004	0.3717	1.624	0.4757
1.128	0.3522	1.784	0.4706
1.308	0.3899	1.880	0.5131
1.400	0.4185		
1.892	0.5259		

Reproducibility of immobilized pyranine in nicotinic acid solutions

Concentration of nicotinic acid (01/20)	PIR	Concentration of nicotinic acid (01/28)	PIR
0.00	0.2228	0.000	0.2016
0.460	0.5012	0.666	0.5311
0.694	0.5472	0.910	0.5686
0.844	0.5556	1.124	0.5748
1.058	0.5632	1.286	0.6003
1.322	0.5933	1.524	0.6102
1.520	0.6210	1.774	0.6413
1.790	0.6249	1.938	0.6554
2.052	0.6365	2.142	0.6773
2.234	0.6576	2.348	0.6699
2.652	0.6831		

Table A6 Raw data for Figure 4.3

Concentration of tryptophan (g/100ml H_2O)	Intensity at 375nm	Intensity at 395nm
0.068	4.7900e+05	3.0300e+05
0.137	3.2000e+05	2.0600e+05
0.216	2.2700e+05	1.5000e+05
0.296	1.8300e+05	1.2500e+05
0.390	1.4800e+05	1.0700e+05
0.522	1.2600e+05	97027
0.588	1.2500e+05	98512
0.710	1.1600e+05	96381
0.818	1.1400e+05	98811
0.906	1.1200e+05	1.0000e+05
1.020	1.1400e+05	1.0500e+05
1.112	1.1300e+05	1.0800e+05
1.222	1.1600e+05	1.1200e+05
1.428	1.2400e+05	1.2000e+05
1.528	1.2400e+05	1.2300e+05
1.612	1.2600e+05	1.2800e+05
1.700	1.2400e+05	1.2700e+05
1.828	1.3100e+05	1.3400e+05

Table A7 Raw data for Figure 4.4

Concentration of tryptophan (g/100ml H_2O)	PIR (395/375)
0.068	0.631
0.1367	0.645
0.216	0.661
0.296	0.685
0.390	0.724
0.522	0.768
0.588	0.787
0.710	0.829
0.818	0.867
0.906	0.895
1.020	0.922
1.112	0.950
1.222	0.966
1.428	0.991
1.528	1.017
1.612	1.024
1.700	1.024
1.828	1.039

Table A8 Raw data of Figure 4.6

Concentration of phenylalanine (g/100ml H_2O)	Fluorescence intensity at 595nm
0.212	3.2531e+05
0.228	3.5235e+05
0.276	4.2897e+05
0.652	6.4569e+05
0.940	6.5931e+05
1.420	9.0312e+05
1.967	1.2616e+06
2.400	1.3453e+06
2.950	1.4850e+06
3.585	1.6983e+06
4.217	1.9785e+06

Table A9 Raw data of Figure 4.7

Concentration of tryptophan (g/100ml H_2O)	Fluorescence intensity at 595nm
0.243	3.5910e+05
0.420	2.5895e+05
0.616	2.3754e+05
0.852	2.1484e+05
1.166	1.9538e+05
1.266	1.9151e+05
1.434	1.8342e+05
1.660	1.7880e+05
1.890	1.7131e+05

Table A10 Raw data for Figure 4.8

Concentration of tryptophan (g/100ml H_2O)	S-V at 375nm	S-V at 395nm
0.000	0.000	0.000
0.068	1.128	1.116
0.137	2.190	2.104
0.216	3.489	3.264
0.296	4.577	4.108
0.390	5.911	4.993
0.522	7.070	5.596
0.588	7.147	5.497
0.710	7.770	5.640
0.818	7.951	5.477
0.906	8.115	5.394
1.020	7.971	5.107
1.112	8.011	4.954
1.222	7.778	4.699
1.340	7.199	4.325
1.428	7.252	4.225
1.528	7.128	4.016
1.612	7.246	4.051
1.700	6.774	3.766
1.828	6.522	3.542

Table A11 Raw data for Figure 4.9

Concentration of tryptophan (g/100ml H_2O)	Reciprocal intensity at 595nm
0.243	2.785e-06
0.420	3.862e-06
0.616	4.210e-06
0.852	4.655e-06
1.166	5.118e-06
1.266	5.222e-06
1.434	5.452e-06
1.660	5.593e-06
1.890	5.837e-06

Table A12 Raw data for Figure 4.10

Reciprocal concentration of tryptophan	S-V-II at 595nm
2.380	4.089
1.624	3.257
1.174	2.679
0.858	2.325
0.790	2.266
0.698	2.151
0.602	2.090
0.529	1.999

Table A13 Raw data for Figure 5.1

Concentration of tryptophan (g/100ml H_2O)	S-V at 382nm
0.000	0.000
0.079	0.448
0.180	0.839
0.220	1.316
0.290	1.807
0.422	2.558
0.510	3.034
0.588	3.470
0.692	3.863
0.812	4.243
0.934	4.552
1.020	4.664
1.096	4.640
1.196	4.717
1.316	4.638
1.426	4.637
1.532	4.424
1.648	4.411
1.730	4.277

Table A14 Raw data for Figure 5.2

Concentration of tryptophan (g/100ml H_2O)	Reciprocal intensity at 510nm
0.079	2.688e-06
0.180	2.703e-06
0.220	2.890e-06
0.290	3.086e-06
0.422	3.584e-06
0.510	3.876e-06
0.588	4.219e-06
0.692	4.608e-06
0.812	5.236e-06
0.934	5.882e-06
1.020	6.410e-06
1.096	6.897e-06
1.196	7.353e-06
1.316	8.065e-06
1.426	8.850e-06
1.532	9.524e-06
1.648	1.031e-05
1.730	1.101e-05
1.888	1.264e-05

Table A15 Raw data for Figure 5.3

Concentration of phenylalanine (g/100ml H_2O)	S-V at 382nm
0.000	1.000
0.224	1.128
0.306	1.084
0.420	1.296
0.522	1.275
0.632	1.316
0.732	1.355
0.860	1.431
1.008	1.475
1.388	1.622
1.410	1.624
1.622	1.697
1.852	1.745
2.024	1.831
2.216	1.873
2.424	1.913
2.598	1.962
2.842	2.013
3.036	2.084
3.240	2.127
3.440	2.162

Table A16 Raw data for Figure 5.4

Reciprocal Concentration of phenylalanine	S-V III at 382nm
1.916	4.631
1.582	4.166
1.366	3.817
1.163	3.320
0.992	3.104
0.720	2.609
0.709	2.601
0.617	2.435
0.540	2.343
0.494	2.203
0.451	2.145
0.413	2.095
0.385	2.040
0.352	1.987
0.329	1.923
0.309	1.887
0.291	1.861

Table A17 Raw data for Figure 5.5

Concentration of nicotinic acid	S-V at 382nm
0.000	0.000
0.214	2.584
0.322	4.409
0.464	6.995
0.698	12.87
0.848	16.99
1.080	25.62
1.334	33.97
1.494	41.06
1.796	51.58
1.960	58.48
2.272	67.35
2.420	75.73

Table A18 Raw data for Figure 5.6

Concentration of Nicotinic acid	S-V I at 382nm
0.320	14.09
0.836	22.78
1.040	26.00
1.384	31.19
1.744	35.67
1.910	38.52
2.244	39.55
2.456	39.81
2.708	39.54

Table A19 Raw data for Figure 5.7

Concentration of nicotinic acid	S-V II at 382nm
0.000	1.000
0.214	3.255
0.322	4.679
0.464	6.488
0.698	10.13
0.848	12.28
1.080	16.38
1.334	19.18
1.494	21.47
1.796	23.43
1.960	24.62
2.272	24.59
2.420	25.82

Table A20 Raw data for Figure 5.8

Concentration of nicotinic acid (g/100ml H_2O)	S-V at 510nm 342nmEx	S-V at 510nm 360nmEx
0.000	0.000	0.000
0.214	1.430	1.421
0.322	2.815	2.735
0.464	5.110	4.974
0.698	10.87	10.39
0.848	16.37	15.52
1.080	26.06	25.48
1.334	40.69	39.49
1.494	50.91	49.62
1.796	78.19	74.52
1.960	93.64	91.23
2.160	105.6	112.3
2.272	117.1	125.0
2.420	140.4	142.0

Table A21 Raw data for Figure 6.2

Concentration of tryptophan	Lifetime S-V at 510nm
0.000	1.000
0.151	1.085
0.232	1.132
0.454	1.238
0.638	1.295
0.820	1.365
0.956	1.418
1.030	1.429
1.268	1.502
1.396	1.518
1.592	1.564
1.810	1.602

Table A22 Raw data for Figure 6.2

Concentration of nicotinic acid	Lifetime S-V at 510nm
0.000	1.000
0.210	1.836
0.354	2.253
0.616	2.977
0.786	3.463
0.964	4.083
1.102	4.517
1.318	5.428
1.632	6.441
1.894	7.638

Table A 23 Raw data of Figure 6.3

Concentration of phenylalanine (g/100ml H_2O)	S-V at 510nm	Concentration of phenylalanine (g/100ml H_2O)	Lifetime S-V at 510nm
0.000	1.000	0.000	1.000
0.462	1.033	0.290	0.998
0.758	1.040	0.492	0.999
1.132	1.010	0.720	0.984
1.592	1.066	0.944	0.984
1.946	1.079	1.144	0.980
2.234	1.062	1.300	0.974
2.404	1.132	1.550	0.980
2.524	1.105	1.694	0.976
2.622	1.125	1.956	0.971
2.720	1.113	2.196	0.975
2.806	1.122	2.414	0.962
2.896	1.125	2.596	0.970
3.022	1.141	3.060	0.963
3.142	1.125	3.234	0.964
3.400	1.185		
3.602	1.146		

Table A 24 Raw data of Figure 6.4

Concentration of tryptophan (g/100ml H_2O)	S-V at 382nm	Concentration of tryptophan (g/100ml H_2O)	Lifetime S-V at 382nm
0.000	0.000	0.000	0.000
0.079	0.448	0.206	0.927
0.180	0.839	0.308	1.332
0.220	1.316	0.460	1.879
0.290	1.807	0.660	2.784
0.422	2.558	0.904	3.885
0.510	3.034	1.096	4.751
0.588	3.470	1.224	5.176
0.692	3.863	1.422	5.682
0.812	4.243		
0.934	4.552		
1.020	4.664		
1.096	4.640		
1.196	4.717		
1.316	4.638		
1.426	4.637		
1.532	4.424		
1.648	4.411		
1.730	4.277		
1.888	4.334		

Table A 25 Raw data of Figure 6.5

Concentration of nicotinic acid (g/100ml H_2O)	S-V at 382nm	Concentration of nicotinic acid (g/100ml H_2O)	Lifetime S-V at 382nm
0.000	0.000	0.000	0.000
0.214	2.584	0.087	0.261
0.322	4.409	0.145	0.522
0.464	6.995	0.216	0.904
0.698	12.87	0.352	1.450
0.848	16.99	0.462	1.929
1.080	25.62	0.686	2.749
1.334	33.97		
1.494	41.06		
1.796	51.58		
1.960	58.48		
2.160	60.09		
2.272	67.35		
2.420	75.73		

Table A 26 Raw data of Figure 6.6

Concentration of phenylalanine (g/100ml H_2O)	S-V at 382nm	Concentration of phenylalanine (g/100ml H_2O)	Lifetime at 382nm
0.000	0.000	0.000	0.000
0.310	0.293	0.228	0.198
0.462	0.312	0.544	0.252
0.758	0.496	0.718	0.264
1.132	0.664	0.912	0.295
1.592	0.827	1.096	0.309
1.946	0.941	1.248	0.330
2.234	1.010	1.574	0.326
2.404	1.159	1.854	0.323
2.524	1.139	2.024	0.328
2.622	1.183	2.316	0.310
2.720	1.142		
2.806	1.192		
2.896	1.174		
3.022	1.269		
3.142	1.225		
3.400	1.382		
3.602	1.346		

Table A27 Raw data of Figure 7.2

Concentration of tryptophan	300nm Ex	305nm Ex	308nm Ex	310nm Ex
0.062	1.8886e+05	2.0247e+05	1.2050e+05	76216
0.0787	1.6750e+05	2.3890e+05	1.5689e+05	1.0960e+05
0.124	99470	2.6750e+05	2.1390e+05	1.5880e+05
0.236	32924	2.1293e+05	2.6068e+05	2.1527e+05
0.322	23159	1.5571e+05	2.5484e+05	2.3180e+05
0.504		77477	2.1596e+05	2.4894e+05
0.704	21253	42269	1.6130e+05	2.2780e+05
0.882	20464	28521	1.1661e+05	2.0090e+05
1.054	19050	22627	88747	1.7453e+05
1.270	16909	17316	61175	1.4330e+05
1.550	17741	16885	41082	1.0720e+05
1.780	16444	17500	28469	83971

Table A28 Raw data of Figure 7.3

Concentration of tryptophan	320nm Ex	330nm Ex	340nm Ex	350nm Ex
0.062	13067	20111	19430	15639
0.0787	32244	29733	16479	16226
0.124	41225	35099	31437	29154
0.236	47020	34134	27937	23398
0.322	51897	38014	30003	24844
0.504	65829	45257	35113	27058
0.704	81749	56484	39646	29363
0.882	91910	63039	43695	29459
1.054	1.0122e+05	69543	46903	32522
1.270	1.1370e+05	79225	52504	32417
1.550	1.2582e+05	88773	57678	36315
1.780	1.3195e+05	94932	62964	36918

Table A29 Raw data of Figure 7.6

Excitation wavelength at unsaturated concentration of tryptophan	Emission wavelength at unsaturated concentration of tryptophan	Excitation wavelength at supersaturateconce ntration of tryptophan	Emission wavelength at supersaturated concentration of tryptophan
300.00	357.00	308.00	357.00
302.00	357.00	310.00	358.00
305.00	356.00	312.00	360.00
307.00	358.00	315.00	366.00
309.00	357.00	318.00	376.00
312.00	360.00	320.00	380.00
315.00	363.00	325.00	386.00
318.00	373.00	330.00	387.00
320.00	379.00	335.00	391.00
325.00	384.00	340.00	393.00
330.00	386.00	350.00	398.00
333.00	388.00	355.00	404.00
334.00	390.00	360.00	411.00
335.00	380.00	365.00	416.00
340.00	384.00	370.00	422.00
345.00	390.00	375.00	429.00
350.00	397.00	380.00	434.00
355.00	404.00	385.00	444.00
360.00	411.00	390.00	452.00
365.00	417.00		
370.00	422.00		
375.00	429.00		
380.00	435.00		

Continue of Table A 29

Excitation wavelength at saturated concentration of tryptophan	Emission wavelength at saturated concentration of tryptophan
300.00	357.00
305.00	358.00
308.00	357.00
310.00	358.00
312.00	361.00
315.00	365.50
317.00	372.50
320.00	380.00
325.00	386.00
330.00	387.00
335.00	389.00
337.00	392.00
339.00	390.00
340.00	385.00
341.00	387.00
342.00	390.00
345.00	390.50
350.00	396.00
355.00	401.00
360.00	410.00
365.00	417.00
370.00	424.00
375.00	431.00
380.00	439.00
385.00	442.00
390.00	451.00
400.00	464.00
410.00	477.00
420.00	490.00

Table A30 Raw data of Figure 7.7

Concentration of tryptophan (g/100ml H_2O)	Lifetime in mixture solvent (ns)	Lifetime in mixture solvent (ns)
0.356	2.12	5.78
0.506	2.04	6.12
0.724	2.01	5.76
1.048	1.90	4.20
1.490	1.92	3.77

Table A31 Raw data of Figure 8.4

pH of tryptophan solutions	PyO^- /PyOH in tryptophan solutions	467nm/402 nm in tryptophan solutions	pH of phenylalanine solutions	PyO^-/PyOH in phenylalanine solutions	467nm/402nm phenylalanine solutions
7.13	0.427	0.391	6.06	0.126	0.0337
7.15	0.447	0.571	6.73	0.170	0.1934
7.38	0.757	1.852	7.54	1.10	1.368
7.43	0.852	2.069	7.65	1.41	2.033
7.65	1.41	2.517			